Monitoring of the single-cell morphology for the evaluation of microbial eukaryotic bioprocesses

vorgelegt von

M. Sc.

Anna-Maria Marbà-Ardébol

geb. in Vilanova de Bellpuig

von der Fakultät III-Prozesswissenschaften

der Technischen Universität Berlin

zur Erlangung des akademischen Grades

Doktorin der Ingenieurwissenschaften

-Dr.-Ing.-

genehmigte Dissertation

Promotionsausschuss:

Vorsitzender: Prof. Dr. Roland Lauster

Gutachter: Prof. Dr. Peter Neubauer

Gutachter: Prof. Dr. Ir. Frank Delvigne

Gutachter: Dr. Erik Pollmann

Tag der wissenschaftlichen Aussprache: 19. März 2018

Berlin 2018

Abstract

Cell morphology is not only influenced by the cell cycle, the aging or individual properties, but also by environmental impacts such as those occurring on a large-scale. Cell morphology can be a suitable parameter for *in situ* measurements as it changes dynamically and is often related to cell physiology. In order to be able to identify relationships between cell physiology and morphology, statistically representative amounts of data have to be measured. It should be considered that the behaviour of cells is not only dynamic, but also very sensitive to environmental changes. Therefore, *off line* measurements may not be suitable for detecting small changes in the morphological properties. Sampling and sample preparation would conceal this, apart from an often insufficient number of data or an unreasonable amount of time and effort.

Among the techniques that are able to capture the morphological characteristics of cells in real-time, automated imaging technologies are promising, because they provide additional information about cellular structures, shape and cell aggregation beyond size. Photo-optical *in situ* microscopy (ISM) and three-dimensional holographic microscopy (DHM) were used in this study to measure the morphological dynamics in eukaryotic cultures on a single-cell basis, using heterotrophic algae and yeast as examples.

The intracellular concentration of the polyunsaturated fatty acid docosahexaenoic acid (DHA) in the heterotrophic algae *Cryptecodinium cohnii* was monitored. A second order correlation between the DHA content as measured *off line* chromatographically and the prediction using the average Sauter diameter was found. A different media composition did not only influence the cell size, but also the circularity and phase homogeneity of the algae cells. Consequently, different chloride ion substitutes were tested with respect to the cell growth and lipid accumulation in *C. cohnii*.

Multi-compartment reactors were used to investigate the influence of gradients, as they occur in a large-scale, on the morphological heterogeneity in *Saccharomyces cerevisiae* cultures. Contrary to expectations, the sterol synthesis was positively influenced by oscillatory oxygen availability (ergosterol ester concentrations increased by 75 %), although microbial growth was decreased (the biomass concentration was reduced by 20 %).

Budding of yeast was monitored in batch cultivation using ISM. A narrow size distribution was measured during the growth phase while the population homogeneity increased. If glucose was depleted, the percentage of non-budding cells remained almost constant due to a significant reduction in growth activity. The ratio of budding and total cells was successfully applied to differentiate between the different growth stages.

The methods proved to be suitable for monitoring morphological properties over a relevant concentration range. Faster particle identification, including overlapping particles, and further investigations to better understand the relations between the shape and state of a cell will allow the technology to be used to control a variety of bioprocesses.

Zusammenfassung

Die Zellmorphologie wird nicht nur durch den Zellzyklus, die Alterungs- oder individuelle Eigenschaften beeinflusst, sondern auch durch Umweltbelastungen, wie sie z.B. im großen Maßstab auftreten. Die Zellmorphologie kann ein geeignete Parameter für eine *in situ* Messung sein, da sie sich dynamisch verändert und dabei oft mit der Zellphysiologie zusammenhängt. Um Beziehungen zwischen der Zellphysiologie und Morphologie identifizieren zu können, müssen statistisch repräsentative Datenmengen gemessen werden. Zu Berücksichtigen ist, dass das Verhalten der Zellen dabei nicht nur extrem dynamisch ist, sondern auch sehr sensibel gegenüber Umweltveränderungen. Daher können *off line* Messungen ungeeignet sein, kleinere Änderungen in den morphologischen Eigenschaften zu detektieren. Die Probenahme und in der Regel die Probenvorbereitung würde diese überdecken, abgesehen von einer oft nicht ausreichenden Anzahl von Daten oder eines nicht vertretbaren Aufwandes.

Unter den Techniken, die in der Lage sind, morphologische Merkmale von Zellen zeitnah zu erfassen, sind automatisierte Bildgebungstechnologien vielversprechend, da sie über die Größe hinaus weitere Informationen über zelluläre Strukturen, Form und Zellaggregation liefern. Die photo-optische *in situ* Mikroskopie (ISM) und die drei-dimensionale holographische Mikroskopie (DHM) wurden in dieser Studie zur Messung der morphologischen Dynamik in eukaryontischen Kulturen auf Einzelzellbasis eingesetzt, die exemplarisch an heterotrophen Algen und Hefe untersucht wurde.

Die intrazelluläre Konzentration der mehrfach ungesättigten Fettsäure Docosahexaensäure (DHA) in der heterotrophen Alge *Cryptecodinium cohnii* wurde überwacht. Eine Korrelation zweiter Ordnung zwischen dem DHA-Gehalt, wie er *off line* chromatographisch gemessen wurde, und der Vorhersage unter Verwendung des Durchschnitts des Sauter-Durchmessers konnte gefunden werden. Eine unterschiedliche Medienzusammensetzung beeinflusste nicht nur die Zellgröße, sondern auch die Zirkularität und Phasenhomogenität der Algenzellen. Folglich wurden verschiedene Chloridionenersatzstoffe hinsichtlich des Zellwachstums und der Lipidakkumulation in *C. cohnii* getestet.

Mehrkompartimenten-Reaktoren wurden eingesetzt, um den Einfluss von Gradienten, wie sie im großen Maßstab auftreten, auf die morphologische Heterogenität innerhalb von *Saccharomyces cerevisiae* Kulturen zu untersuchen. Insbesondere wurden die Auswirkungen von

Sauerstofflimitierungen auf die Zellheterogenität untersucht. Entgegen den Erwartungen wurde die Sterolsynthese durch die oszillatorische Sauerstoffverfügbarkeit positiv beeinflusst (die Ergosterolesterkonzentrationen stiegen um 75 %), obwohl sich das mikrobielle Wachstum verlangsamte (die Biomassekonzentration war um 20 % erniedrigt).

Darüber hinaus wurde die Knospung der Hefe mit Hilfe der ISM auf Einzelzellebene in Batchkultivierungen überwacht. Die Größenverteilung wurde während der Wachstumsphase enger, so dass die Populationshomogenität zunahm. War die Glukose verbraucht, blieb der Prozentsatz der Nicht-knospenden Zellen aufgrund einer stark verminderten Wachstumsaktivität nahezu konstant. Anhand des Anteils knospender Zellen konnte zwischen den verschiedenen Kultivierungsstadien unterschieden werden.

Die gezeigten Methoden erwiesen sich als geeignet zur Überwachung morphologischer Eigenschaften über einen relevanten Konzentrationsbereich hinweg. Eine schnellere Partikelidentifizierung, auch von überlappenden Partikeln, und weitere Untersuchungen zu einem besseren Verständnis der Zusammenhänge zwischen Form und Zustand einer Zelle wird den Einsatz der Technologie zur Kontrolle einer Vielzahl an Bioprozessen erlauben.

Acknowledgements

I am very grateful to Stefan Junne for believing in me already during my MSc. thesis project and by offering me the opportunity, as the group leader of the bioprocess group, to return to TU Berlin for the PhD project. I would like to thank him for his constant support in the preparation of experiments, manuscripts and also the present thesis.

I would like to thank Peter Neubauer, who gave me the opportunity to work in his lab and gain knowledge in bioprocesses. I appreciate his enthusiasm, as well as all the suggestions and fruitful discussions regarding my work.

Besides, I would like to thank the rest of my thesis committee: Prof. Frank Delvigne and Dr. Erik Pollmann, as well as Dr. Michael Quanz for taking my work into consideration.

My gratitude goes to the SOPAT GmbH employees. A special mention to Jörn Emmerich, who adapt the sensor's hardware to monitor algae and yeast cells. He was always open for discussion and arranged all the logistics for the measurements. Also thanks to Michael Muthig for his work regarding the automatic cell recognition. I thank Ovizio Imaging Systems NV/SA for their kind support in adjusting the algorithms for the automated algae detection.

Many thanks for the support of the students Ewelina Buziuk, Paula Ferré, Juan Fusté, Miriam Garcia, Rosine Mezatio, Daniel Wirrkowski, Hüseyin Yassi and Olivia D. Zakrzewski for the work connected to this thesis and to other projects. Furthermore, I would like to thank Brigitte Burckhardt, Irmgard Maue-Mohn and Thomas Högl for the support regarding the practical work. And thanks to all colleagues from the chair of bioprocess engineering especially Anja, it was fantastic having you inside and outside the laboratory, I have really missed you the last months. I would like to thank also Klaus, you were always prepared to lend a hand; Anika, for the perfect organization at every event and for your work in relation to the scale-down experiments; Howard, for cheering up the atmosphere every time you visit us.

Last but not the least, I thank my parents, they were always there encouraging me and believing in me. My both families (Catalan and German) and friends for their unconditional support. I thank specially Sarah and Mireia for giving me advice on English grammar. An enormous thank you to you Andi for always being by my side.

Funding: The work was partially supported by the German Federal Ministry of Food and Agriculture within the innovation program coordinated by the federal office for agriculture and food (project: FENA – fishmeal and oil feed substitutes for a sustainable aquaculture, project no.: 511-06.01-28-1-73.026-10), as well as by the German Federal Ministry of Economics and Energy within the framework program ZIM-Koop, project "Smart Process Inspection", grant no. ZF 4184201CR5.

Contents

1. Introduction

1.1. Background

The structure, composition and intracellular metabolite concentrations of a cultivation is usually assumed to be synchronized in industrial bioprocesses. As consequence, a control of macroscopic variables would be sufficient to achieve optimal yields. However, in bioprocesses, as well as in nature, each cell has certain different features, populations are not homogeneous (Delvigne and Goffin, 2014). Therefore, the assumption of a homogeneous culture may lead to wrong conclusions. Nevertheless, the feasibility to measure heterogeneity in industrial bioprocesses is limited until now. The understanding and consideration of this cell variability can have a huge impact on the process yields and quality of products. Cell heterogeneity can be used to predict the suitability of cultivation conditions and strain engineering.

Despite of the huge impact on the process performance, the physiology of cultures is usually still observed by *off line* measurements, with all draw-backs of long response times, a high degree of manual preparation or automated instrumentation. Moreover, *off line* analysis include biases due to manual preparation. For example, the gold standard for viability assessment is counting colony forming units or staining a sample with a viability dye (Davey, 2011). Usually, an accurate single-cell based analysis becomes difficult under such conditions. Nevertheless, such viability tests is of huge importance for beer and wine production, as well as for dairy starter cultures (e.g. for lactic acid bacteria). The viability directly decides on the product quality, but also on the process efficiency and the ability to cope with different stress factors, which are intrinsic to the process.

Changes in cell physiology can interrelate with the cell morphology. The morphology of cells is altered by means of environmental stress (Albertin, et al., 2011; Timoumi, et al., 2017), as e.g. in large-scale production due to gradient formation, or in general under nutrient starvation and high shear stress. Since the cell status might be related to the cell morphology, process analytical tools for monitoring it on a single-cell basis need to be explored.

1.2. **Thesis outline**

This thesis consists of a *Literature Research* section, which is divided in three chapters:

Chapter 1 (*Environmental conditions in industrial-scale bioprocesses*) provides a general overview on the environmental conditions, with which the cells have to cope in industrial-scale bioprocesses. In the first part the most widely used cultivation modes and technical limitations due to scale-up are described. The second part provides a short review of scale-down approaches used until now to reproduce those conditions in lab-scale. Finally, the industrial relevance of *C. cohnii* and *S. cerevisiae* is discussed.

Chapter 2 (*Morphology and physiology, a tight relationship*) points out the phenotypic variability in microbial cultures and its relation to morphological cell dynamics. The population heterogeneity, which result from the single-cell specific response to the cultivation conditions, but also from cell cycle events will be discussed. A section pointing out the relevance of single-cell information is included.

Chapter 3 (*Analysis of the single-cell morphological heterogeneity*) provides a short overview on experimental single-cell morphological analysis, making a differentiation between imaging and non-imaging techniques, and evaluates it's *in situ* applicability.

Additionally, three publications resulting from the work executed during this thesis are enclosed:

Publication 1 (*Single-cell-based monitoring of fatty acid accumulation in Crypthecodinium cohnii with three-dimensional holographic and in situ microscopy*).

The single-cell size distribution was tracked for bioreactor cultivations, as well as for testing various medium compositions in terms of growth and lipid accumulation. Morphological heterogeneity was monitored with a photo-optical sensor and holographic microscopy. The accumulation of the lipid product could be quantitatively detected based on the cell size distribution. It was concluded that the diameter, circularity and phase-homogeneity of the microalgae *Cryptecodinium cohnii* changed depending on the process stage or media composition.

Publication 2 (*Sterol synthesis and cell size distribution under oscillatory growth conditions in Saccharomyces cerevisiae scale-down cultivations*)

In order to mimic large-scale oscillating conditions in lab-scale, two scale-down systems were used. The cell response to those conditions on the metabolite accumulation of the main carbon and sterol biosynthesis in the yeast *Saccharomyces cerevisiae* was investigated. Alterations in the metabolic activity, especially concerning synthesis rates and intracellular regulation mechanisms within the sterol metabolism, were measured. The size distribution from the holographic microscopy measurements revealed that the cell size distribution changed concomitantly.

Publication 3 (Real-time monitoring of the budding index in *Saccharomyces cerevisiae* batch cultivations with *in situ* microscopy)

Maturation of the yeast *Saccharomyces cerevisiae* became trackable *in situ* on a single-cell level. Based on the relation of budding and non-budding cells, a distinction between growth stages and cultivation conditions was feasible. Moreover, the single-cell distribution of several morphological parameters such as the cell size and aspect ratio provided information on the population heterogeneity and the cell activity.

Finally, a *Summarizing discussion* is highlighting the importance and applicability of the achievements accomplished during this thesis. Future challenges and perspectives are highlighted in the *Outlook* section.

1.3. **Publications included in the thesis**

Post-print version used in thesis:

1) Chapter 4.1 (p. 48-65)
   Marbà-Ardébol, A.-M.; Emmerich, J.; Neubauer, P. and Junne, S. (2017). Single-cell-based monitoring of fatty acid accumulation in *Crypthecodinium cohnii* with three-dimensional holographic and *in situ* microscopy. *Process Biochemistry* 52, 223-232.
   https://doi.org/10.1016/j.procbio.2016.11.003

2) Chapter 4.2 (p. 66-82)
   Marbà-Ardébol, A. M.; Bockisch, A.; Neubauer, P. and Junne, S. (2017). Sterol synthesis and cell size distribution under oscillatory growth conditions in *Saccharomyces cerevisiae* scale-down cultivations. *Yeast* 35, 213-223.
   https://doi.org/10.1002/yea.3281

3) Chapter 4.3 (p. 83-99)
   Marbà-Ardébol, A.-M.; Emmerich, J.; Neubauer, P. and Junne, S. (2018). Real-time monitoring of the budding index in *Saccharomyces cerevisiae* batch cultivations with *in situ* microscopy. *Microbial Cell Factories*, 17, 73.
   https://doi.org/10.1186/s12934-018-0922-y

In all publications listed here, I was responsible for the conception and realization of the experimental work, the interpretation of the results and the main part of the writing.

1.4. **Other publications**

The 4 years PhD project resulted in other publications, which have not been included in this thesis. Some of them are in strict relation with the topic of this work and some others are the result of other collaborations:

1) Marbà-Ardébol, A. M.; Turon, X.; Neubauer, P. and Junne, S. (2016). Application of flow cytometry analysis to elucidate the impact of scale-down conditions in *Escherichia coli* cultivations P. Gil Salvador 2013 Award in Bioengineering category.(November 22, 2013 in the Annual General Assembly of the AIQS). *Afinidad.* **73** (573), 7-15.

2) Junne, S.; Marbà-Ardébol, A. M. and Neubauer, P. (2016). Neue Applikationsfelder für Single-use-Bioreaktoren. *BIOspektrum.* **22** (1), 96-99.
DOI: 10.1007/s12268-016-0660-9.

3) Lorenz, E., Runge, D., Marbà-Ardébol, A. M., Schmacht, M., Stahl, U. and Senz, M. (2017). Systematic development of a two-stage fed-batch process for lipid accumulation in *Rhodotorula glutinis*. *Journal of biotechnology* **246,** 4-15.
DOI: 10.1016/j.jbiotec.2017.02.010.

4) Marbà-Ardébol, A. M., Emmerich, J., Neubauer, P. and Junne, S. (2017). *In situ* microscopy for real-time determination of single-cell size distribution and activity in microbial cultures. *13. Dresdner Sensor*-Symposium 201 Vol. P2. *Prozessmesstechnik* 222 - 225 (Hotel Elbflorenz, Dresden).
DOI: 10.5162/13dss2017/P2.10.

5) Marba-Ardebol, A. M., Emmerich, J., Muthig, M., Neubauer, P and Junne, S. (2018). *In situ* microscopy for real-time determination of single-cell morphology in bioprocesses. *Journal of Visualized Experiments*, submitted.

1.5. **List of abbreviations**

ANN	artificial neural network
C. cohnii	*Cryptecodinium cohnii*
DCW	dry cell weight
d_{32}	Sauter mean diameter
d_F	Feret diameter
DHA	docosahexaenoic acid
DHM	digital holographic microscopy
DO	dissolved oxygen
E. coli	*Escherichia coli*
FCM	flow cytometry
ISM	*in situ* microscopy
ratio C/N	ratio carbon/nitrogen
PFR	plug flow reactor
S. cerevisiae	*Saccharomyces cerevisiae*
STR	stirred tank reactor
two-CR	two-compartment reactor
three-CR	three-compartment reactor

2. Literature research

2.1. Environmental conditions in industrial-scale bioprocesses

Nowadays, the competition in bioprocesses is growing due to the raise of biosimilars and the expiration of patents, as well as due to an increment in the demand of industrial bioproducts (enzymes and small molecules), of bioenergy, and of chemoenzymatic processes, which have to be competitive against existing chemical processes. Meanwhile productivity and quality-by-design aspects need to be improved and controlled, development times need to be kept short and costs need to be reduced (Konstantinov and Cooney, 2015).

Cultivation conditions in the lab-scale are often far away from large-scale operation. Consequently, lower yields are often detected for both, biomass and growth-associated products, when scaling-up. Therefore, **large-scale constraints should be already considered in the early process development steps** (Noorman and Heijnen, 2017). This means to recreate in the lab-scale the cultivation conditions cells will encounter during production, by considering e.g. the feed stock and the chosen operation mode that will be applied in the production scale (**Figure 1**), as well as the intrinsic technical limitations of the large-scale, while analyzing how the cell phenotype is accordingly influenced.

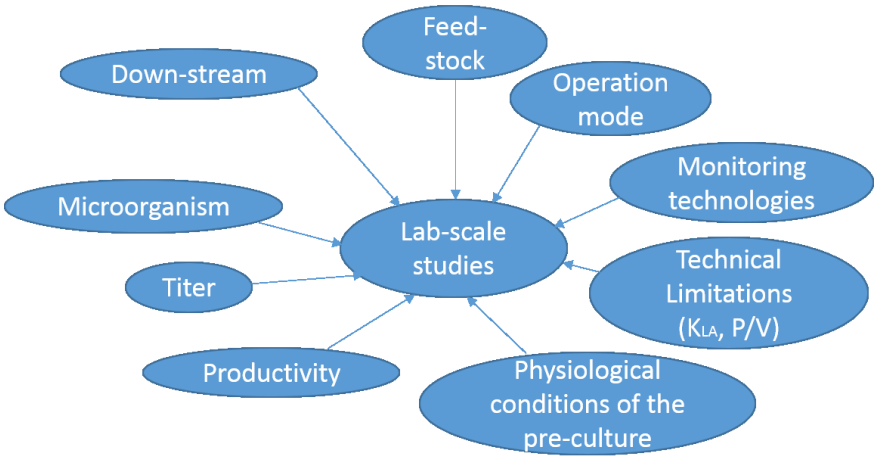

Figure 1. Points from the large-scale conditions to be considered in lab-scale studies.

In order to be competitive, **processes should be robust against variations**. A critical issue, which has to be considered, is the inherent variability of raw materials (Losen et al. 2004; Unthan et al. 2014, Kasprow, Lange et al. 1998), since mostly complex media is applied (cane or beet molasses, starch hydrolysates of maize, cassava, wheat and raw sugars). Its composition is usually not well defined and there is a large batch-to-batch variation depending on quality and availability (regional, seasonal, price or regulations), which become even more crucial for bulk production with the envisaged concept of a bio-based economy. This variability can affect both, the upstream and the downstream operations.

Besides, **processes need to be flexible** in terms of productivity, since the demand forecast is changing rapidly or is even falsely predicted. Consequently, a **better understanding and control of the process is needed**. Therefore, in the following chapters first, the intrinsic conditions and limitations of widely applied operation modes are presented (2.1.1). This decision will determine the boundary conditions of the process. Secondly, the limitations of the transport phenomena and their consequences are discussed (***Error! Reference source not found.***). Then, scale-up and scale-down accomplishments, hallenges and limitations are described (2.1.3). Finally, the industrial relevance of *C. cohnii* and *S. cerevisiae* is presented, as they were exemplarily investigated during the practical part of the present research work (2.1.4).

2.1.1.Cultivation modes

With the exception of continuous processes like wastewater treatment or bioenergy production, **the majority of bioprocesses nowadays are operated as a batch or fed-batch** (Neubauer and Junne, 2016). Although batch mode is considered flexible when low volumes of different products need to be produced, it is also characterized by a lack of control in the cell growth. During a batch process, eventually followed by a fed-batch process, cells are passing different growth phases where problems associated with catabolic regulation, oxygen limitation and heat generation may appear. These changes are more drastic during batch growth and can lead to various physiological states. However, batch-mode is applied for the production of beverages, probiotics and antibiotics.

Many commercial bioprocesses are operated in fed-batch mode under substrate limitation. As high volumetric yields of a product can only be reached by high cell densities, the substrate feed must be highly concentrated. In a substrate limited fed-batch the cell growth rate is a function of the feed rate and a quasi-steady state is achieved during a certain period of time. By controlling the growth rate or rather the feed rate, the reproducibility of the process can be improved (Jenzsch, et al., 2006). Moreover, a controlled feed can also avoid oxygen limitation and by-product accumulation and guarantees aerobic growth even at high cell densities. Another advantage of this operation mode against batch mode is the possibility to change the cultivation conditions to trigger the cells to another phase, for example by changing the feed composition, by temperature shift or addition of an inducer in recombinant bioprocesses. In this way, the process performance can be optimized by maximizing the cell concentration before the product of interest is produced decoupled from growth.

Continuous processes can increase the yield and reduce the volume (Croughan, et al., 2015). For the production of primary metabolites, which are associated to the growth of the organism (organic acids, amino acids), continuous bioprocessing usually is superior. This is also the case for unstable products (e.g. certain enzymes and blood coagulation factors), since the residence time inside the reactor needs to be short (Ozturk, 2014). Due to the steady state, the process can be controlled comparably easily by

the speed of the feed pump, i.e. the residence time. Unproductive turnaround times can be reduced (e.g. cleaning and sterilization), hence the productivity increased. Therefore, continuous processing or at least repeated batch and fed-batch procedures during upstream is an interesting opportunity for future bioprocesses.

Moreover, if the product of interest can be excreted into the supernatant, biomass retention can increase the productivity due to the possibility of cultivation during long period of times at high cell densities (Sieck, et al., 2017). This continuous mode of operation, called perfusion, consist of continuous harvesting of supernatant and concomitant supply of fresh medium, while cells are retained in the bioreactor.

Nevertheless, there are some drawbacks, as the risk of infection (Desai, 2015) or spontaneous mutation of the microorganisms (Barrick and Lenski, 2013), which make continuous modes less attractive to an application with low tolerance of risk and high regulation procedures (Reay, et al., 2013). Moreover, down-stream costs may increase when the titer is diluted due to the constant harvesting. Regarding process development, it is easier to transfer a batch process into the large-scale than a fed-batch or a continuous process, which requires improved monitoring and control.

For all cases, **monitoring is necessary to document repeatability as quality control and ensure a proper operation regime,** according the required regulatory boundaries like e.g. set by the U.S. Food and Drug Administration (FDA) (Rathore, et al., 2015).

2.1.2.Scale-up related challenges

The first drawback that faces scale-up is the **limitation in the power of mixing and consequently the limitations in mass transport**. Due to their non-linearity performance, transport phenomena are difficult to scale up in a bioprocess. Mixing times in the lab-scale are lower than 5 seconds, but increase at least by an order of magnitude in industrial-scale bioreactors (Hewitt and Nebe-Von-Caron, 2001). Mixing times in the range of several minutes were detected in bioreactors running at a scale of 120 and 150 m^3 (Junker, 2004; Namdev, et al., 1992). Therefore, several related growth parameters like substrate, O_2, CO_2, or side metabolites, but also physical parameters like temperature or pH are not evenly distributed.

Although the sensor technology is constantly improving, published literature of gradients measurements in the large-scale is rare. Only recently, the investigation of the spatial gradients in the liquid phase of a biogas plant has been published (Kielhorn, et al., 2015). A reason could be that bioreactors in the production scale have hardly changed with the time, so the feasibility of applying new technologies may be difficult. Regulations and costs restrictions may have become more relevant with the time as well. Therefore, gradient formation and other scale-related stresses are often not

considered, as the sensitivity of the physiological state of the organisms to these stresses remain to be investigated. Nevertheless, recent reviews are pointing out the importance to perform a proper analysis of the physiological state under large-scale environmental conditions (Neubauer and Junne, 2016).

The most important spatial and temporal heterogeneities and the physiological cell response to them will be discussed in detail below.

2.1.2.1. Substrate gradients

Substrate gradients appear in high cell density fed-batch cultivations, since the power input is restricted. If cells cope with a substrate concentration above a critical value, an overflow metabolism can occur (30 mg L^{-1} of glucose is reported for *S. cerevisiae* and *E. coli*), which implies by-product formation due to the Crabtree effect (yeast) or due to the redirection of acetyl CoA from the Krebs cycle (bacteria) (Hewitt and Nienow, 2007). In contrast, when cells suffer from glucose starvation, they have to shift to an alternative carbon source (ethanol, lactate or acetate among others). A shift from one carbon source to another results into reduced growth.

Glucose gradients were measured by sampling at three different stirred tank bioreactor heights in a fed-batch mode, either with a working volume of 9 m^3 (Bylund, et al., 1998), 22 m^3 (Enfors, et al., 2001), or 30 m^3 (Larsson, et al., 1996). These studies showed that gradient formation directly depend on the mixing characteristics at the feeding position. Even a 400 times higher glucose concentration than the average could be encountered when this position was not well-mixed, e.g. when feed addition was at the top. Moreover, cells are exposed to two types of substrate gradients in the large-scale bioreactor. They are exposed to rapidly fluctuating high substrate concentrations when they circulate in the feeding zone, whereas cells circulating between all zones in the liquid phase cope with a decrease of substrate concentration with the distance to the feed point. It is important to note that although multiple feeding points at well-mixed zones were considered, usually any addition in the bioreactor is dosed from one single spot (Larsson, et al., 1996), due to concerns about contamination, pipe blockage or mechanical stability. Despite of the fact that the optimal position of any feed addition is near the impeller, where the maximal specific energy dissipation rate is encountered, surface addition is often applied in large-scale. Consequently, substrate is almost depleted in the middle and bottom parts of the reactor (Neubauer and Junne, 2016). The assumed substrate concentration and dissolved oxygen in large-scale fermenters with feed addition from the top and at the bottom are depicted in **Figure 2**.

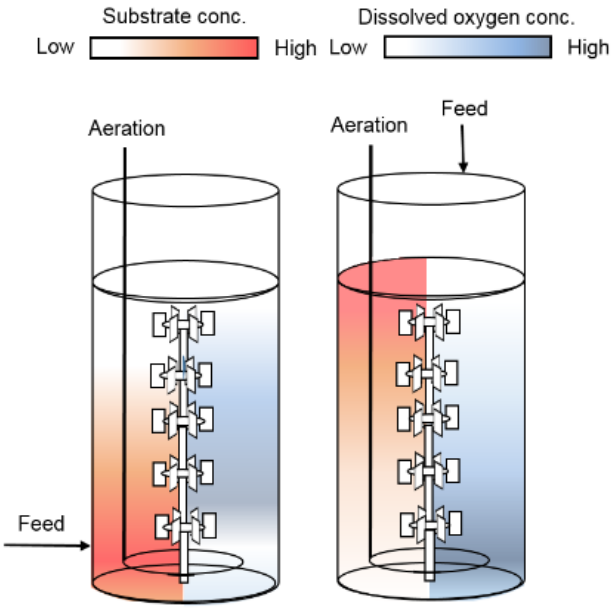

Figure 2. Suggested distribution of substrate and dissolved oxygen (DO) concentration in large-scale bioreactors during a nutrient-limited fed-batch process

2.1.2.2. Oxygen gradients

Close to the feeding zone, the high substrate consumption rate leads to a volumetric oxygen demand of the culture that exceeds the oxygen transfer rate to the liquid phase. This is often the limiting-rate in aerobic processes due to the low solubility of oxygen in the medium (Garcia-Ochoa and Gomez, 2009). Gas solubility in liquids is always low and a function of temperature, pressure, concentration and type of salts dissolved in it. Under the absence of oxygen, some organisms can perform anaerobic respiration when an alternative electron acceptor is present, as for example during the use of nitrate by some bacteria (*E. coli* or *C. glutamicum*). Otherwise, many organisms can grow without using the electron transport chain, e.g. yeast. However, this anaerobic growth is associated with a low energy yield compared with that observed at completely oxidative processes (Rodrigues, et al., 2006).

In contrast, e.g. in the lag-phase, high oxygen concentration can lead to oxidative stress. The accumulation of intracellular reactive oxygen species can damage lipids, proteins and nucleic acids. Effects on lipids include a decrease in membrane fluidity, specific ion permeability or activity of membrane receptors. Damages on proteins compromise their structure, and therefore their functionality (Guan, et al., 2017).

Dissolved oxygen (DO) gradients were measured with a movable sensor in an industrial *Streptomyces* cultivation with a working volume of 112 m^3 (Manfredini, et al., 1983). Although in this study a high viscosity was encountered due to the filamentous morphology of *Streptomyces* (250 -500 mPas), gradients were not only measured in viscous culture broth. An uneven distribution of oxygen was also

measured by Oosterhuis *et al.* in a cultivation volume of 19 m^3, where the viscosity was only 1.5 mPas (Oosterhuis, 1984).

2.1.2.3. Other gradients

So far, the majority of studies focused on effects of dissolved oxygen and substrate concentration. However, **dissolved carbon dioxide (dCO_2) and pH gradients may also be critical scale-up factors**. The dCO_2 concentration can be elevated close to the feed point due to the high consumption rate of carbohydrates in aerobic cultivations. However, not only microorganisms can change the composition of the media and hence the gas solubility, the hydrostatic pressure in large bioreactors caused through the height of the reactor becomes also critical for gas solubility. Thus, elevated regions of dCO_2 can be identified in the lower parts of them. Moreover, high concentrations of dCO_2 may cause acidification of the media.

Baez *et al* studied the effect of dCO_2 constant exposure and oscillating dCO_2 conditions in a two-CR (STR-STR), under different mean circulation times. The time of exposure to high dCO_2 concentrations came out to be critical, since the lowest circulation time (50 s), as present in large-scale bioreactors, had little effect on growth and recombinant protein production of *E. coli* cultures (Baez, et al., 2011). However, a permanent exposure to high dCO_2 trigger the acid stress response of the cells.

Additional gradients result from the dosification of the acid/base addition for pH control. As pointed out above, any feed is bound to the flow regime in the region of addition. Moreover, pH control is based on one point measurements, and it is pulse-wise dosed. A lower number of studies dealing with pH fluctuations have been published in comparison to substrate and oxygen gradients. However, they have been showing performance losses, thus it may be an underestimated parameter. Oscillating exposure of cells to high pH zones led to a negative effect on the viability and cell growth on *E. coli* fed-batch cultivations (Onyeaka, et al., 2003). *C. glutamicum* was more sensitive to pH fluctuations than to oscillating oxygen availability (Limberg, et al., 2017).

2.1.2.4. Heat transfer

The height to diameter of microbial bioreactors is usually in a range of 3-5. Large-scale volumes are in between 100–200 m^3 (Wittmann, et al., 2016), but they can increase up to 500 m^3 like some beer fermenters (Nienow, et al., 2011) or lysine production (Eggeling and Bott, 2015). **Heat exchange surface may sometimes become the limiting factor rather than the oxygen transfer in high-cell density processes** (Hewitt and Nienow, 2007)**.** When scaling-up heat release scales with the volume of the reactor, whereas the relation between surface area to volume is dramatically reduced, and thus the cooling capacity. The installation of cooling coils or cooling baffles can improve the heat exchange. In contrast, the limited heating rate can be beneficial for the cells, when increasing the temperature in

order to shift to a production phase. Low heating rates reduce negative effects associated with the heat shock stress response as showed in Caspeta *el al*. The production of a recombinant protein using a thermo-inducible expression system showed a correlation between by-products accumulation and heating rate. The highest productivity was achieved with the lowest heating rate, which means to mimic the heating conditions encountered in the large-scale by induction (Caspeta, et al., 2009).

2.1.3.Scale-up/scale-down

Although some successful examples in scaling-up can be found, **there is no standard criteria ensuring success**. Some recommendations are listed (Junker, 2004; Takors, 2012) by taking into account physical similarities between scales. Mainly three scales can be differentiated when scaling, namely the lab-scale for elementary studies, the pilot plant for the process optimization, and the production scale. Besides, there is the micro-scale, which can be used for high-throughput investigations.

Mostly used parameters in scaling-up are the geometry of the vessel (height to diameter ratio), the agitator tip speed, the volumetric power input (P/V), the oxygen mass transfer rate (K_La), and the Reynolds number (Neubauer and Junne, 2016). All of them are physical properties that affect mass and heat transfer. These parameters cannot be scaled in the same way due to technical and economic restrictions. Besides, it is important to know the interaction between each of them, and that these relations use to change with the scale.

The energetic expenses increase drastically when increasing the scale. Typical scale-up volumes are in a range from 10 L in lab to 1 m^3 in pilot scale, followed by 10 to 500 m^3 in the production scale. A 10-fold increase in the reactor size reduces the specific power input about two-thirds (Bailey and Ollis, 1977). Consequently, the criteria of constant mixing time can hardly ever be applied for scaling-up, since it is greater of what is economically or technically feasible. It is therefore inevitable that the mixing time increases with the scale. Mixing times are normally experimentally measured (Nielsen, et al., 2003), but they also can be approximated through correlations (Oosterhuis, 1984).

In order to consider large-scale conditions to develop or optimize bioprocesses, scale-down simulators can be used. They mean to mimic the industrial-scale conditions in order to study the consequence of gradient formation in the lab or pilot-scale, empirically or through mathematical models. This subject was discussed in depth in some recent reviews (Delvigne, et al., 2017; Neubauer and Junne, 2016). The strategy of scale-down approaches is based on the comparison between a reference culture in a well-mixed reactor, where homogeneous conditions are assumed, with another one, where cells cope with oscillatory conditions, as it occurs at large-scale. **Meanwhile the reference system usually is a STR, different approaches can be applied for mimicking the oscillations** (Neubauer and Junne, 2016), which can be cyclic or stochastic.

Although it is demonstrated that scale-down systems are reliable for studying large-scale conditions (some examples are presented below), their application is not yet a standard step in bioprocess optimization and development, there exists no standardization. This may be due to the empirical design associated to them and the assumptions made to conduct such scale-down studies. As previously noted, there is a lack of industrial-scale data, which makes it complicated to proof the validity of the various approaches. A huge variability of the conditions in the large-scale along with confidential issues have let to this scenario as well. Different scale-down set-ups, each of them mimicking different gradients distributions, have been applied and compared with one another (**Table 1**).

Table 1. Overview of published studies comparing the effect of different scale-down set-ups.

Cultivation mode **Scale-down comparison**	**Organism**	**Observations**	**Reference**
Fed-batch mode 1) STR with fluctuating aeration 2) Two-STR (one STR with oxygen limitation and one without).	*G. oxydans*	- different gluconic acid production curves between 1) and 2)	(Oosterhuis, et al., 1985)
	S. cerevisiae	- same biomass yield - metabolic imbalance in 1) (accumulation of some metabolites e.g. acetic acid)	Sweere, et al., 1988
Batch followed by fed-batch mode Sugar concentration and dissolved oxygen oscillations. 1) STR 2) STR-PFR	*E. coli*	- almost the same biomass yield - stronger stringent response in 2) - higher cell segregation in 2)	Delvigne, et al., 2009
Fed-batch mode Sugar concentration and dissolved oxygen oscillations. 1) STR-PFR 2) STR-PFR-PFR	*C. glutamicum*	- similar biomass yield - similar lysine yield	Lemoine, et al., 2015
	E. coli	- different biomass yield - lower viability in 2)	Marba-Ardebol, et al., 2016
Batch mode 1) Two-STR 2) STR-PFR	*C. glutamicum*	- similar growth reduction - similar lysine yield	Limberg, et al., 2016

Cyclic oscillations can be achieved by applying pulse feed of some growth related parameters (aeration, substrate) in a one compartment reactor e.g. continually changing oxygen concentration in the inlet gas flow (Sweere, et al., 1988b) or based on ON/OFF DO-feed control (Delvigne, et al., 2009). Pulse feed experiments are used for studying metabolic shifts of physiological parameters under some disturbance that appears in large-scale.

Stochastic extracellular fluctuations can be achieved by the compartmentation of the reactor, where not only spatial, but also temporal gradients are created, as it occurs in large-scale. Usually, one STR is simulating a zone with rather ideal conditions, whereas in another compartment/s cells are undergoing the limitation or excess of one or more growth related parameters.

When using a two-CR that consists of two STRs, the residence time distribution of the cells in both compartments is broad and not defined, and probably a lot of cells are exceeding the time coping with stressful conditions. If cells should cope with spatial and temporal defined gradients one of the STR compartments can be changed to a plug flow reactor (PFR), in which the mixing regime can be characterized through the Bodenstein number (George, et al., 1993). This non-dimensional number is a function of the residence time and the aeration rate, which ensures a plug flow regime. The formation of the desired gradients should be defined with large-scale measurements, or with predicted values, which originate from Computational Fluid Dynamics (CFD) studies (Bylund, et al., 1999). PFRs can be equipped with static mixers to provide efficient mixing of gas and liquid, while the plug flow regime is maintained (Neubauer and Junne, 2010). Besides, the possibility to install sample and sensor ports along the PFR module allows the measurement of gradients and metabolites after defined residence times (Junne, et al., 2011). Up to now, multiple compartments (mostly two) are the most applied set-ups, mainly to mimic DO and substrate gradients of fed-batch cultivations, but also pH fluctuations (Amanullah, et al., 2001).

On the basis that all scale-down systems are a simplification of the real gradient concentration profile, the reduction of the large-scale conditions to only two zones neglect some extreme limitations presented in this scale. Therefore, a third compartment has been added, which extends the variability of areas that can be simulated. Considering e.g. the homogeneous zone (STR compartment with aeration) with the feed zone (PFR-compartment with feeding) as before, the third compartment can be added to mimic a zone with strong starvation far away from it (a second PFR without feeding) (Lemoine, et al., 2015; Marba-Ardebol, et al., 2016), where substrate limitation and oxygen depletion could be encountered. The cells circulate stochastically between the three compartments.

The potential of scale-down to observe the behaviour of the large-scale process has been proven for various microbial cultivations, e.g. when achieving the same biomass yield as in the large-scale (Xu, et al., 1999). However, if cells are shear sensitive like cell culture or algae cells, the peristaltic pumps used in multi-compartment reactor systems can already influence the process performance (Nienow, et al., 2013). Therefore, control runs must be performed to separate the cells response from each effect (Brunner, et al., 2017), e.g. pH fluctuations from shear stress.

The application of stressful conditions, however, can have both, positive and negative effects, a case-dependent study is always necessary. It was demonstrated that large-scale conditions can have a positive effect on the process. The gassing power of yeast in a dough (quality parameter of Baker's yeast) was increased for sweet doughs in both scale-down experiments and production bubble column reactor (215 m^3) in comparison to lab-scale homogeneous conditions (George, et al., 1998), despite the lower yield obtained. This did not only result into the study of productivities, but also of cells quality and/or viability. Flow cytometry (FCM) measurements showed that gradients encountered in the large-scale can provide higher viability than the homogeneous conditions of the lab-scale to some cultures, although the occurred losses in biomass. Scale-down systems and production scale viabilities were in agreement to each other (Enfors, et al., 2001; Hewitt and Nebe-Von-Caron, 2001). Results from Delvigne *et al* point in the same direction. FCM was applied for the study of a transcriptional reporter gene based on the green fluorescent protein (GFP) on a single-cell basis. *E. coli* general stress response under scale-down conditions (excess, limitation and starvation of glucose and exhaustion of oxygen) was monitored using a prpoS::gfp fusion. A significant drop of the GFP content was observed for the heterogeneous conditions (Delvigne, et al., 2009). This reduction was associated with a segregation in the population heterogeneity. *S. cerevisiae* reporter strains have been also applied for investigating the cell robustness against freeze-thaw stress and growth on ethanol in a continuous two-STR scale-down cultivation. Sugar concentration and dissolved oxygen oscillations were encountered. One strain reporter was related to growth, whereas the other was related to ethanol growth. FCM measurements evaluating freeze-thaw stress reveal that the membranes of cells growing with higher dilution rate appear to be more robust towards freeze–thaw stress, in comparison to cells growing at lower dilution rate. In terms of ethanol consumption, cells cultivated in one-compartment reactor showed no growth on ethanol, whereas 64 % higher fluorescence was detected in compartment reactor cultivations. The population heterogeneity increased as well (Heins, et al., 2015). The response of reporter genes in combination with scale-down experiments with PFR compartments, as described for several bacterial processes, remain to be investigated for yeast cultivations.

Computational approaches provided a higher resolution of the large-scale system (Larsson, et al., 1996), when combining kinetic data of the organisms (relevant metabolic reactions) with the description of fluid dynamics (mixing times, mass transfer and flow regime). An Euler-Lagrange

approach was used for the description of an individual cell behavior, as a result of the interaction with spatial and temporal bioreactor heterogeneities. This approach was applied for the simulation of a 900 L process at fed-batch mode when cultivating *S. cerevisiae* (Lapin, et al., 2004) and *E. coli* (Lapin, et al., 2006). Recent studies have enabled an even higher resolution by monitoring the lifetime of millions of cells in parallel (Haringa, et al., 2017). Population balance models can be coupled to CFD models for the investigation of population segregation, as a response to the environmental conditions. Additionally, the transfer of physiological conditions, if possible with single-cell based measurements, shall be conducted to prove the reliability of the scale-down approach for a representative simulation of the large-scale.

Nevertheless, losses of process performance during scale-up are still a reality. George *et al.* observed a decrease of the biomass yield of a yeast process of about 7% when a 10 L fed-batch cultivation was compared with the industrial-scale of 210 m^3 (George, et al., 1998). Bylund *et al.* observed that the biomass yield was decreased by 20% when scaling up an *Escherichia coli* cultivation from 3 L to 9 m^3 (Bylund, et al., 1998). **This shows the relevance of scale-down studies for an economically feasible bioprocess development, if the losses can be considered in an early stage, and eventually reduced through strain and process optimization.**

2.1.4.Industrial relevance

2.1.4.1. Heterotrophic algae *C. cohnii*

Heterotrophic marine organisms, such as *Crypthecodinium and Schizochytrium,* have been used to produce *n*-3 long-chain polyunsaturated fatty acids (*n*-3 LCPUFA) in commercial quantities, namely docosahexaenoic acid (DHA). While *Schizochytrium* produces relatively high amounts of ω-6 docosapentaenoic acid (DPA), other PUFAs beside DHA represent less than 1% in *C. cohnii* (Sijtsma and De Swaaf, 2004). DHA benefits on human health are ranging from an essential role in the growth and functional maintenance of the brain and retina in infants and adults, to a reduction of cardiovascular disorders. For a review, see, for example (Matos, et al., 2017), in which also functional food products from microbial algae are described.

Fatty acids that are constituted of more than 18 carbon atoms should be obtained from the food, since it is hardly possible to synthesize these in the human body. Although sea fish is the major source of long-chain PUFAs in human nutrition, the natural source are microalgae, which are consumed by the fish (Mendes, et al., 2009). Nowadays, and despite of healthy, economic and environmental drawbacks, the source of DHA for human consumption is fish oil. Since small fish is caught from the sea to provide fish oil, it is not sustainable and leads to the problem that the nutrition of larger fish is withdrawn from the sea, e.g. to feed fish in aquacultures. Therefore, the cultivation of heterotrophic algae could be a

sustainable solution. Besides, residual microalgal biomass could be utilized to produce biogas, bio-ethanol or bio-fertilizer.

The expected market potential for DHA is estimated to exceed USD 300 million (Kothari, et al., 2017). Recently, *Veramaris*, a joint venture between DSM (Heerlen, Netherlands) and Evonik Industries AG (Essen, Germany) will produce EPA and DHA from heterotrophic marine algae for animal nutrition, mainly in aquaculture like salmon production (Tocher, 2018). An investment volume of USD 200 million demonstrates the economic relevance of the process (DSM, 2017). However, several challenges have to be overcome for a large-scale process. E.g. the risk of contamination should be minimized, since cells grow in rich media. The supply of sufficient oxygen at moderate shear-forces is also crucial like the monitoring of the intracellular product accumulation, which is performed through sophisticated gas chromatographic analysis.

2.1.4.2. Budding yeast *S. cerevisiae*

Saccharomyces cerevisiae, also known as baker's yeast, is one of the yeast species most commonly used in industrial biotechnology. The eukaryotic microorganism is characterized by its high rate of division and its easy cultivation. As its name is indicating, this yeast has been generally used for the baking process. *S. cerevisiae* is a facultative anaerobic microorganisms, which allow its application for the production of alcoholic beverages such as wine, beer and cider.

S. cerevisiae is also recognized by the US Food and Drug Administration (FDA) as a GRAS organism and nowadays widely used for the production of recombinant proteins, enzymes and vitamins. For an extensive review, see (Demain and Martens, 2017). The availability of its entire genome sequence enables the genetic modification of the model organism. An advantage over prokaryotes as a production strain is the secretion of the products into the medium, which greatly facilitates a later purification. In addition, *S. cerevisiae* has various posttranslational modifications that are essential for the correct folding of enzymes and other proteins due to the eukaryotic expression system. Therefore, *S. cerevisiae* carries out proper folding of many human proteins. Insulin and insulin analogs are the main biopharmaceuticals produced by yeast (Baeshen, et al., 2014), and the global insulin market is expected to grow to more than USD 32 billion by 2018 (Nielsen, 2013).

In addition, the yeast *S. cerevisiae* has a high ergosterol-phospholipid ratio of 3.3 mol mol^{-1} in its cell membrane (Zinser, et al., 1993). Besides ergosterol, other intermediates of the post-squalene pathway have many applications in the cosmetic and pharmaceutical industry or as nutritional supplements (Demain and Martens, 2017). Synthetic biology allowed the successful reconstitution of the biosynthesis pathway for hydrocortisone in *S. cerevisiae* by the expression of 8 exogenous proteins and the deletions of 4 yeast genes. The ergosterol pathway was redirected to produce the cholesterol

substitute campesterol that was transformed into hydrocortisone by the classical mammalian pathway. Hydrocortisone can be extracted from the culture broth as the predominant steroid (Szczebara, et al., 2003).

However, although the engineering of an expression system and scale-up can be successful, the process can fail as well. In 2013, the precursor to artemisinin, which is the most effective drug against malaria, was produced with an engineered *S. cerevisiae* strain. They claim its commercialization at a fair and sustainable price, as it was part of a consortium with ”The Bill and Melinda Gates foundation”. However, this drug met market resistance. The increment of the agricultural artemisinin source production, which was until the biotechnological process appeared the only source of artemisinin, led to an excess supply and the prices sank. In addition the improvements in diagnosing malaria before administer medicine are reducing the demand as well (Nature News, 23 February 2016).

Another large area of application for *S. cerevisiae* is the production of bioethanol. Approximately 100 billion liters of ethanol are produced per year from sugar cane and corn starch. *S. cerevisiae* can reach 18 % of ethanol concentrations in the fermentation broth (Lin, et al., 2013). However, *S. cerevisiae* cope with several stress factors during the production of biofuels, hence engineered strains have been applied for improving productivity. E.g. the possibility to metabolize C5 sugars increases the yield when using lignocellulosic biomass as raw materials. Thermotolerant strains allow process temperatures (ca. 40 °C) that are less cooling demand and better for the hydrolysis of the feedstocks. Alcohol toxicity can limits bioethanol titer and productivity, as well as compromise cell viability. Therefore, tolerance against alcohol has been improved as well (genetically or by changing process conditions e.g. pH of the fermentation) (Demain and Martens, 2017).

2.2. Morphology and physiology, a tight relationship

The only factor that determines the yield of a process is the physiological state of cells (Fernandes, et al., 2011), which is often related to the morphological state, so there is a relationship between form and function. As presented in chapter *2.1.*, **process parameters and physical properties are not straightforward transferable across the different scales. Morphological features may be more applicable as scale-up and process performance evaluation criteria**, since microorganisms are either the final product or the biocatalyst of the process.

Morphology is easier to study and analyze in comparison to physiological, metabolic or genetic features, and it can be measured both in lab-scale scale and in large-scale. From the very beginning, the morphology of the cells has been analyzed, like Emil Hansen did with brewing yeast (Rank, et al., 1988). He separated the cells considering their morphology and showed that different pure cultures provide unique and reproducible industrial fermentations. Another example is *Penicillium chrysogenum*, in which the pellet size distribution decides about the productivity of penicillin. Free filaments increase the viscosity and lead to insufficient oxygen mass transfer (Bellgardt, 1998).

The term of morphology can include several parameters such as colony morphology, microscopic appearance of the cells (shape, structure, form or chain formation), flocculation profiles and formation of agglomerates. However, one of the most used attributes is the cell size. The mean cell size of one species typically differ very little. **There is evidence that cells are able to monitor and control their size** (Bisova and Zachleder, 2014; Taheri-Araghi, et al., 2015; Turner, et al., 2012) in order to keep a certain degree of size homeostasis (Cook and Tyers, 2007). Moreover, in unicellular organisms like algae, yeast or bacteria the ratio of surface to the volume can play an important role for the adaptation to environmental conditions, like nutrient availability (Brauer, et al., 2008). Most of these organisms increase their size only by two or even less during their cell cycle.

The cell size is directly related to the internal biosynthesis. Not only is the size of the organelles often proportional to the cell size (nucleus, mitochondria, vacuole…), but also most of the proteins and mRNAs increase accordingly (**Figure 3**). The organism's metabolism and heat production are closely related to the body mass, as well as with the surface area and rate of heat loss. Therefore, there is a tight relationship between the cell's metabolism and their shape (Chan and Marshall, 2010). In contrast, the amount of DNA is not proportional to the cell size (**Figure 3**).

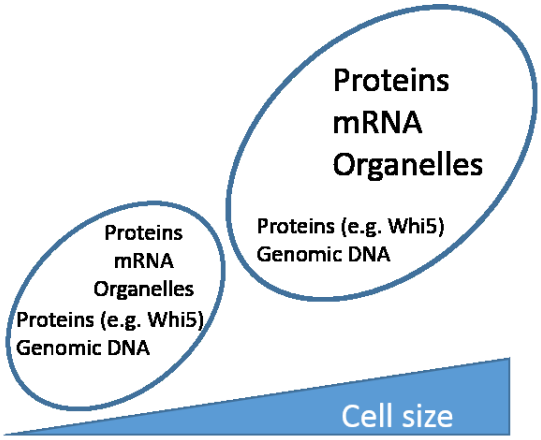

Figure 3. Molecular components that increase in dependence of the cell size. Adapted from (Schmoller and Skotheim, 2015)

Cell morphology can be influenced by cell cycle (2.2.1), cultivation conditions (2.2.2) or cell aging. The linkage between morphology and production performance should be investigated, in order to allow a better way of process monitoring, development and optimization (Gao, et al., 2014). Nevertheless, in bioprocesses, as well as in nature, a dynamic diversification is present (Delvigne and Goffin, 2014). **The overall productivity of the process depends on the phenotypic distribution (2.2.3)** (Lindmeyer, et al., 2015).

2.2.1.Cell cycle

Due to the great importance of size in cellular processes, many cells control it by connecting growth with cell-cycle events and division. Although there have been efforts in order to elucidate the mechanisms of such a control for different types of unicellular organisms, they have remained elusive (Schmoller and Skotheim, 2015). Investigations came out with different models for cell cycle control, mainly “timers” and “sizers”.

A proposed cell cycle control system is that **cells stay at each cycle phase for a specific amount of time (“timers” models)**. However, this model cannot explain some physiologic events, as e.g. when cells grow at a rate proportional to their volume (Turner, et al., 2012).

Cells actively monitor their size and regulate the cell cycle taking into account some critical size checkpoints (“sizer models”). A critical size or a critical size per DNA content is required for advancing through the cell cycle at DNA replication initiation or division. One of the most recognized prokaryotic cell cycle theories is the Cooper-Helmstetter model (Willis and Huang, 2017). This theory can be considered as a “sizer”, since it relates the DNA replication (initiation) with a certain constant ratio of cell mass to DNA replication complexes. **Cells need to “sense” their size, if they are actively controlling it** (Turner, et al., 2012). As pointed out before, most macromolecules accumulate in proportion to cell

size, but some do not. One of the proposed sensing mechanisms is the utilization of cycle inhibitor proteins that do not increase proportionally to the cell size, so they generate size-dependent concentrations (Schmoller and Skotheim, 2015). This control was shown through the analysis of the cell cycle of budding yeast cells (**Figure 4**).

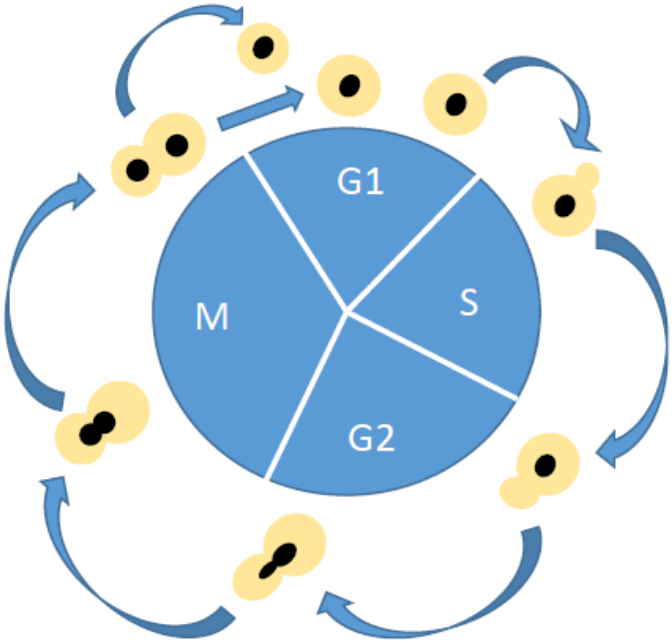

Figure 4. Budding yeast cell cycle: it is usually divided in 4 phases, G1, S, G2 and M. The M phase of the cycle corresponds to mitosis. This phase is followed by the G1 phase, which corresponds to the interval between mitosis and initiation of DNA replication. During G1, the cell is metabolically active and continuously grows but does not replicate its DNA. G_1 is followed by S phase, during which DNA replication takes place. The completion of DNA synthesis is followed by the G2 phase, during which cell growth continues and proteins are synthesized in preparation for mitosis.

The proportion of the cell cycle activator Cln3, which scales with size, and the cell cycle inhibitor Whi5, which does not, results in cell size control. Cln3 is maintained constant during G1, whereas Whi5 is diluted. However, this alone cannot explain that smaller cells at birth grow proportionally more than larger cells in the subsequent division cycle, since they need to achieve a size threshold for exit from the G1 phase (Di Talia, et al., 2007). An additional mechanism was found: larger cells are born with lower Whi5 concentrations, since larger and smaller cells are born with nearly the same number of Whi5 molecules. The expression of this protein is mainly during S/G2/M phases, therefore its synthesis is mainly independent from cell size. However, certain diversity is existing, since this inhibitor-dilution model is stochastic. Irregularities in these processes affect fitness and function (Schmoller and Skotheim, 2015). Moreover, different regulation between mother and daughter cells exists. A certain cell size is required to proceed to budding. However, small mother cells can proceed more rapidly

through the G1 phase in comparison to daughter cells of similar size. Moreover, the time spent in the G1 phase decreases with the number of cell cycles a mother cell has undertaken.

Although cell size is controlled by regulating division in response to growth, this will depend lastly on the environmental conditions. Despite of the fact that remarkable differences can be encountered between cell cycles of bacteria and budding yeast, a positive correlation between cell size and nutrient availability exists for both. On rich media cells grow quickly and divide at a larger size, whereas cells grow slowly and divide at smaller size under poor conditions (Willis and Huang, 2017). However, not all cells of a culture respond equally to the environment. The viability of each cell is affected differently after an environmental stress depending on the cell cycle phase, and on the age of cells (Carlquist, et al., 2012). Under certain stressful conditions, cells can become quiescent. This is seen as an advantage in some cases, in order to preserve the cell integrity. A typical example can be found in the brewing industry, where some cells enter in a quiescent G0 phase under ethanol stress. These cells are not contributing to the ethanol production, but they can be reactivated in a following cultivation (Carbó, et al., 2015).

If different and defined cell shape patterns can be differentiated during the cell cycle, the classification in categories of these patterns and the posterior quantification of its occurrence along the time can provide information about the cell growth activity and cell vitality (Saldi, et al., 2014). E.g. the proportion of cells that are in the maturation state at a time in budding yeast cultivations (budding index, BI), provides information about the growth vitality (Brauer, et al., 2008; Porro, et al., 2009). Besides, the product synthesis is usually a function of the cell cycle phases, which is normally blocked for DNA replication and the cell division (Müller, et al., 2010) and hence the accumulation or secretion rates of microbial products too. This is the case of the polar lipids in *C. cohnii* algae cells, which increase stepwise mainly in the growth phases (G1 and G2) (Kwok and Wong, 2005). On the other side, the non-growing morphological states use to contribute to product synthesis of secondary metabolites (Lange, et al., 2017).

The morphology is not only influenced by the cell cycle, but also the cultivation conditions, or in fact the lifeline of each cell along the reactor make the morphology a dynamic and unique property of each cell.

2.2.2. Influence of environmental conditions on the cell morphology

Although usually stressful conditions are associated with negative effects, they may be controllable and in some cases even favorable for bioprocesses. Only unusual conditions are exceeding the ability of the cells to react. As already mentioned in this work, there is a relation between physiological and morphological cell status. Further is the relation of physiologic states to certain process performances, through the elucidation of their effect on the cell morphology. **Figure 5** is showing environmental stress conditions cells may suffer during cultivation conditions, which may have an effect on their morphology.

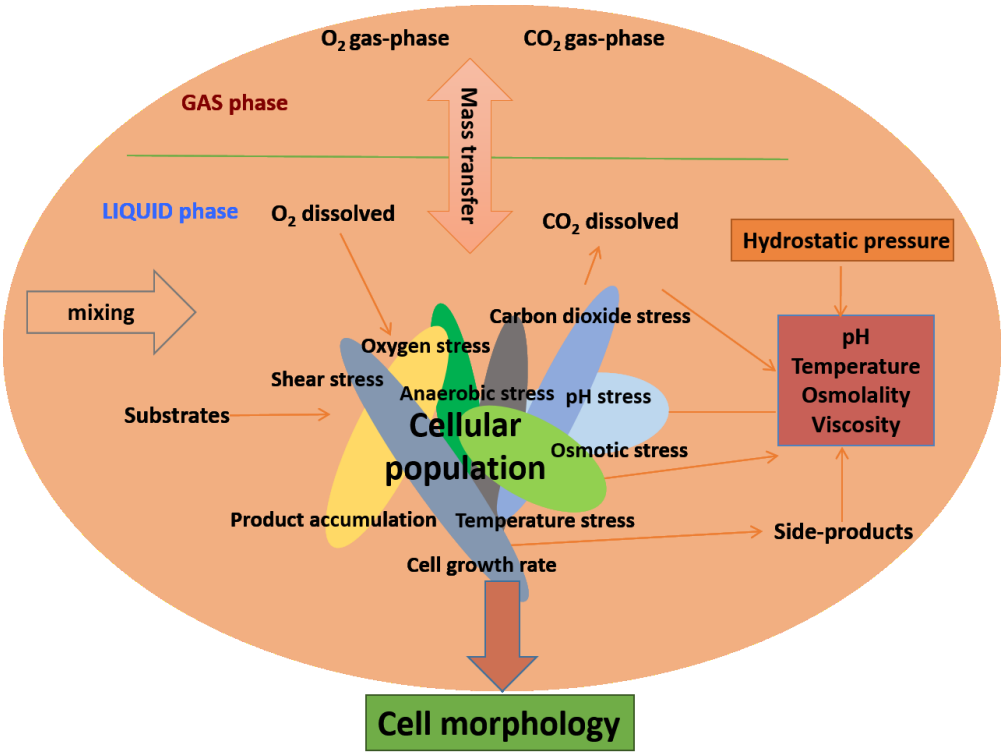

Figure 5. Environmental stress conditions cells may suffer during cultivation conditions can affect their cell morphology. Adapted from (Lemoine, et al., 2017).

Cells size can change dramatically as a function of extracellular conditions. For example, unwanted carbon starvation or adaptation to the stationary phase can be observed in gram-negative bacterial cells, since the reductive cell division increases the surface/volume ratio and therefore cells become smaller (Chung et al., 2006) and rounder (Navarro Llorens, et al., 2010). The cell response to the media composition and toxicity, in terms of morphology and cell cycle, were also studied with algae cells. Cell cycle arrest, formation of multicellular aggregates or changes in the cell size and shape were some of the responses (Khona, et al., 2016; Machado and Soares, 2014; Marbà-Ardébol, et al., 2017).

One study evaluated the same strain under different abiotic backgrounds by considering its morphological profile. Different aeration rates, substrate concentrations and repitching regimes (re-

use of the yeast cells for the inoculation of several consecutive batches) among other parameters were applied (Bühligen, et al., 2014). It was found that the replicative age of the cells (the number of bud scars) was correlated with the size of the cells in the three different processes investigated. Moreover, a significant correlation between the cell size and the gravity (total amount of dissolved solids in water) was detected. In a similar way, an optimization strategy based on the maximum population size in food-processing yeast strains (carrying capacity) was proposed (Albertin, et al., 2011), since a correlation with the maximum CO_2 production was found. This approach could be used for baking, brewing, and wine making.

Cell aging is also associated with morphological changes such as increment of the cell size, cell surface wrinkling, decrease in cell turgor and bud scar number, among others. Those parameters have been detected through bright field, fluorescence or confocal microscopy. The aging of cells can be observed with the cession of the net increment of cell concentration, at the same time that the cells enhance the accumulation of storage compounds (Maskell, et al., 2003); or with a replicative scale, which represents the number of times a cell has divided itself.

Gradients encountered in the large-scale can led to alterations in cell physiology, which is the result of the different micro-environments the cells are exposed to and the different adaptation responses. Some parts of the reactor provide optimal conditions, while others have limitation and/or excess of growth related parameters. Latter can generate undesired cell states, which will reduce the efficiency of the process. While offering a suboptimal performance, those cells are consuming nutrients, which even may lead to the overall failure of the process (Rosano and Ceccarelli, 2014). The analysis of the statistical relevance between morphological and physiological changes under different fermentation conditions, but also time-dependent morphological features can improve the estimation of the physiological responses to different environments and its impact along the time (Ohnuki, et al., 2014).

In bioprocesses cultivation conditions are modulated in order to control the behavior of the cells through exposing them to a determined environment. Examples of widely used **process cultivation conditions that influence the cell morphology** are listed below.

2.2.2.1. Growth disruption for intracellular product accumulation

Intracellular accumulation of side products is one of the most established responses of a wide range of microorganisms (filamentous fungi, microalgae, yeast or bacteria cells), when cell growth is disturbed (e.g. by the limitation of a primary nutrient or temperature shift). This adaptation is in detriment of cell proliferation, but they can still assimilate the carbon source (Vitova, et al., 2015; Zhu, et al., 2016). Under such circumstances, cells change their shape and size. Eukaryotic organisms tend to accumulate lipids, also called single-cell oils (SCOs). Some examples are the oleaginous yeast *Yarrowia lipolytica*

(Xie, et al., 2015) or *Rhodotorula glutinis* (Lorenz, et al., 2017). Oleaginous organisms can accumulate lipids beyond 20% in relation to their dry body mass, primarily as triacylglycerols and fatty acids. Usually, a highly optimized carbon-to-nitrogen (C:N) ratio is applied in order to increase lipid accumulation.

Nowadays, microbial SCOs have gained attention for the sustainable production of biodiesel (Jin, et al., 2015) from lignocellulose conversion, low-value bio-waste and/or wastewater, as well as for the production of other added value products like pigments (e.g. b-carotene or torulene) or polyunsaturated fatty acids (Qin, et al., 2017). Therefore other limitation like phosphorous or sulfur have been recently applied due to difficulty in reducing nitrogen content of certain substrates. In contrast, in prokaryotes, although some species can accumulate neutral lipids, Polyhydroxyalkanoates (PHA) are the most common storage compounds. The bacteria *Ralstonia Eutropha* can accumulate up to 79% of this biopolymer in its dry cell weight (Budde, et al., 2011).

2.2.2.2. Mechanical stress

Mechanical stress can be used to control the morphology of some cells types, like fungi (Serrano-Carreón, et al., 2015), or to increase the photosynthetic activity and growth in microalgae cultivations. Each specie, as a function of the cell concentration, has a different mixing optimum depending on the sensitivity of the cell membrane and other morphological structures like the flagellum (Leupold, et al., 2013). Moreover, some cells are shear-sensitive to mechanical agitation as usually performed in a stirred tank reactor, and hence other reactor concepts are more appropriated in order to avoid losses (Hillig, et al., 2014b). Smaller cells tend to be more robust against agitation (Overbeck et al., 2015), although the presence of filaments and agglomerates can increase the sensitivity against shear forces. In general, the disruption of cells due to mechanical stress leads to higher lysis rates, foam formation and a decrease of the product yield, subpopulations can occur.

2.2.3.Single-cell heterogeneity. Morphological variability in microbial cultures

Cell heterogeneity can be considered regarding different phenotypic subpopulations within a culture, or as regards of the variability between each single-cell in an isogenic culture. **Cell heterogeneity is regulated stochastically** mainly through intracellular biochemical reactions, which depend on some low biochemical reactant concentrations, such as promoters (intrinsic noise). Moreover, **the uneven availability of some biomolecules, due to cell division or environmental factors such as extracellular fluctuations, implies an extrinsic noise, which contributes also to the variability within a culture** (Binder, et al., 2017; Lemoine, et al., 2017; Silva-Rocha and de Lorenzo, 2010).

Mutations usually do not have a large influence on the product synthesis, otherwise the new mutant must have a higher growth rate than the original organism, or longer times for growing than the

timescales of batch and fed-batch cultivations (Ryall, et al., 2012). However, it can be different when working with genetically modified organisms, since there is the possibility that the mutation disbands or that the plasmids get lost (loose of the engineered capacity), allowing the wild type to appear again. The wild type has the advantage to be less energy demanding, and therefore can threat the productive organism (Müller, et al., 2010).

Cell cycle is based on unbalanced events like an uneven cell division, variation in gene copy numbers or epigenetic modifications, which contribute to a variation in the metabolite and protein concentration, hence generating low and high performing variants. For example, different resistance again antibiotics between genetically identical bacteria has been detected (Geiler-Samerotte, et al., 2013). Regarding cell size, cells undergo always an asymmetric division. This is clearly accepted when the division occurs e.g. by a bud mechanism. However, it is also occurring through a binary fission, where a variation is encountered, and therefore the capacities of the cell may be affected.

Cell aging has also to be considered, since the **descendants may differ from their ancestors**. Consequently, the capacities of the cells can be altered in the aged population distribution (Delvigne and Goffin, 2014). The generation time increases with the age, since the reproduction abilities decrease. Various senescence factors are not present any more, while growth rates and metabolic efficiency are going down as well. Age factors can be transferred to the daughter cell depending on the age of the mother, either by generating an aged daughter or the mother can keep them. An asymmetric distribution of the damage ensures a certain population of the cells to be “damage-free”, which results in a higher growth rate and therefore contribute to the viability and vitality of the culture. This is the case of the budding yeast cell *S. cerevisiae*, where the aging factors, such as carbonylated proteins caused due to oxidative stress, remain in the ageing mother cell (Shcheprova, et al., 2008). This fragmentation between daughter cells and different ages of mother cells is a necessity for re-using yeast cells for several batches (repitching) in brewery. Old cells have a higher flocculation potential, ferment more efficiently and at a higher rate compared to younger mother cells or daughter cells. However, they have low viability and may flocculate too early and have a reduced generation time, but if only daughter cells are present, the lag-phase can be prolonged too much and this can affect the flavor. On the other side, older cells can recover faster from a stress than daughter cells. Therefore, it is important to have a certain amount of old cells in the yeast slurries, since the last part of the fermentation with nutrient depletion and high ethanol contents is very stressful for the cells. The optimum cell age distribution could be classified through cell size measurements in yeast slurries for the repitching (Powell, et al., 2003).

Due to the productivity losses observed when scaling-up, population heterogeneity in bioprocesses has to be avoided (Martins and Locke, 2015). Studies based on the different productivity of

subpopulations showed that the variation between them can be significant, since any improvement on the overall productivity may be limited by low performance subpopulations (Xiao, et al., 2016). However, in contrast to what was expected, **the reduction of the population heterogeneity does not has to imply an improvement in productivity**. Continuous and synchronized cultures succeeded in the reduction of the cell variability, but failed in improving the productivity. Moreover, the synchronization cannot be maintained permanently. Concerning this, the cells can switch from a producing state to a non-producing state and vice-versa (Delvigne and Goffin, 2014).

In connection to the environmental conditions of large-scale bioprocess, other mechanisms have been proposed, in which cell **heterogeneity enables the persistence of a culture under fluctuating environments**. Delvigne *et al*. studies already pointed out that the stringent response of bacteria cells against oscillating conditions is based on a cell population segregation (Delvigne, et al., 2009). Other authors recently showed the relation between different levels of substrate limitation and substrate shifts, with phenotypic heterogeneity in metabolism. This heterogeneity allows cells to cope with substrate fluctuations (Schreiber, et al., 2016). Ackermann *et al* observed that slowly growing cells have a higher chance of surviving sudden exposure to antibiotics (Ackermann, 2015). Despite of these results, **population heterogeneity in industrial-scale is not yet considered very often.**

Consequently, in order to detect and quantify the heterogeneity of a population in industrial bioprocesses, **process analytical tools on a single-cell basis are needed.** These must provide sufficient data in short time, so that a representative and statistically valid sample is obtained.

2.3. **Analysis of the single-cell morphological heterogeneity**

The process analytical technology (PAT) initiative (Food and Administration, 2004) has driven the implementation of reliable tools suited for analyzing and controlling the critical process parameters (CPPs) and the performance quality attributes (CQAs). They can give feedback on the process state and reduce the risk of failure (Gomes, et al., 2015). Therefore, they should be considered for the whole process and development. Consequently, the final product variability can be managed in order to meet the specifications demands, while reducing costs associated with wasted materials and time.

Usually, physical (stirred speed, weight of the vessels…) and chemical properties (analysis of the liquid and gas phase of the bioreactor) are in the spotlight (Sonnleitner, 2012), whereas the solid phase (cells) is normally not monitored, but sampling is used (Beutel and Henkel, 2011).

Common analytical tools beyond a few for traditionally measured parameters are still *off line* and/or *at line* techniques. However, the behavior of cells are extremely dynamic and sensible to environmental changes, e.g. during sampling. Therefore, *off line* measurements can be inaccurate. *In situ* measurements, which are performed directly in the culture broth, provide more reliable results, because a large number of cells are analyzed simultaneously. Alternatively, *on line* measurements can be conducted through a bypass, in which a representative sample of the culture is withdrawn from the reactor and analyzed aside, but close to the reactor. However, when a bypass is applied, the sample may be modified through staining or lose its sterility; accordingly, the sample should be discarded. Besides, even if this is not happening, attention should be paid to cell stress such as oxygen depletion, temperature or shear forces along the bypass, as well as to the heterogeneity of the bulk culture in comparison to the measured sample, which may query the results of the measurement (Vojinović, et al., 2006).

In situ sensors must not have interferences due to the media (complex and water-based), gas bubbles or to stirring speed changes. Sterilization processes must not compromise the performance of the sensor e.g. by not altering previous saved calibrations. Moreover, they should be long-term stable and cover the whole variability of the process (for example dilutions procedures are not any longer possible).

From the different experimental methods capable to assess the single-cell heterogeneity, until now, the physical characterization through microscopy is the only one that can be applied *in situ* in the reactor cultivation (Camisard, et al., 2002; Wiedemann, et al., 2011a); whereas for studying the gene expression, protein analysis or metabolite analysis sampling (*off line*) or a bypass system is needed (González-Cabaleiro, et al., 2017; Zhang, et al., 2015). A differentiation regarding the measurement location of the sensors is done in **Table 2**.

Table 2. Sensor measurement regarding its possibility to be coupled to the bioprocess and its sample preparation.

	Sampling	**Sample preparation**
in situ	None. Measurement directly in the culture broth in the bioreactor.	None
in line/at line/bypass	Automatic sampling. Recirculation loop or disposal of the sample after measurement.	Quick. Dilutions and/or staining possible.
off line	Manual sampling. Posterior analysis.	Laborious and time consuming.

Data generation and transfer can be continuously or discontinuously processed, but more important is that the measurement time is shorter than the process dynamics (Sonnleitner, 2012). Only then, real-time measurements are capable for process control. When the upstream process is monitored in real-time, consequently the down-stream process can be adapted (Warikoo, et al., 2012). *In situ* sensors use to have shorter delay times, since sampling and subsequent preparation is avoided.

Single-cell based monitoring is not frequently applied yet (Fernandes, et al., 2011) due to the lack of suitable tools. Consequently, the information behind the origin of population inhomogeneities and the appearance of subpopulations is not considered.

As pointed out in the previous chapter (2.2), the morphological assessment of cells can be advantageous compared with engineering parameters due to the close relation with the cell physiology. Further, statistical information about population heterogeneity is detected, when morphology is measured on a single-cell level. Several other parameters might be correlated with morphological features at a time (**Table 3**).

Table 3. Morphological parameters that can be assessed through microscopic analysis.

Parameter
Cell size
Cell shape (max. length and width, circularity, perimeter)
Mobility
Aggregates
Color
Contaminations
Occurrence, amount of other particles
Cell organelles, lipid droplets

Morphological parameters can be obtained through a vast array of techniques (**Table 4**). Some of them are briefly explained below. It is important to pay attention to the techniques that allow a quantification rather than a quality assessment, like imaging techniques through digital image analysis.

In order to avoid qualitative interpretations, the morphology of the cells should be described through quantifiable parameters e.g. the perimeter, the circularity or the ratio in between the max. Feret diameter and the min. Feret diameter. The differentiation between budding and not budding yeast cells could be also obtained through the derivative of the curvature along the periphery (Nguyen, et al., 2017).

Table 4. Classification of single-cell analysis tools based on its *in situ* applicability.

Non-imaging techniques	**Analytical Method**	**Measuring principle**
Off line or at line	Coulter counter	Electrical current exclusion, change in resistance due to volume displacement.
	Microchannel resonators	Buoyant mass. It is dependent on the amount of biomass in the cell.
	Flow cytometry	Light scattering and/or fluorescence.
In situ	Laserlight backreflection	Chord length distribution
Imaging techniques		
Off line or at line	Fluorescent microscopy	Fluorescence
	Imaging flow cytometry	Light scattering, imaging and/or fluorescence
	Phase contrast microscopy	Separate the illuminating background light from the specimen scattered light.
	Digital Holographic microscopy	Hologram (phase and intensity)
In situ	Photo-optical microscopy	Imaging

2.3.1.Non-imaging techniques

2.3.1.1. *Off line* or *at line* techniques

Coulter counter

The principle of measurement of the coulter counter is the electrical current exclusion. When a single cell passes through a defined size aperture, a voltage pulse occurs, which is proportional to the cell volume, since there is a volume displacement of the conductive liquid where the cell is suspended in. Therefore, the cell diameter is calculated from the cell volume and not the other way around.

Moreover, this technology supports high speed analysis (thousand cells per second) by flowing the cells through a microfluidic channel (Xu, et al., 2016), working as an impedance FCM (Bryan, et al., 2012), which can be applied *in line* with a recirculation loop. However, as it occurs usually at FCM

measurements, the dilution of the cell concentration and the flow rate should assure that only one cell at a time passes through the signal light beam, otherwise artifacts are created. The cells need to be suspended in a specific ionic environment to be analyzed, where environmental changes may affect the physical properties of cells.

The coulter counter provides a cell size distribution and a cell count. Due to its principle of measurement, it can be applied to a large range of cell sizes (including bacteria, yeast and cell culture), but it does not allow to discriminate between cells except by size, hence budding cells or aggregates are also depicted as single particles (Tibayrenc, et al., 2010).

Microchannel resonators

The measurement principle of this technique is based on the Buoyant Mass of the cell. The system consists of a cantilever sensor suspended in a vacuum cavity that resonates at a frequency proportional to its total mass. A microfluidic channel is embedded in this cantilever. When a cell transits the microchannel, a certain amount of fluid is displaced and the resonance changes in relation to the difference in between the densities of the cell and the fluid, as well as to the volume of the cell (Lewis, et al., 2014). From this measurement the mass and the size (equivalent sphere) of the cells can be calculated, as well as the cell count.

The main source of error of the measurement is the variation of the resonance depending on the position of the cell in the cantilever tip. However, the heterogeneity of a cell culture is higher than this source of variability.

The measurement of the cell mass can be performed on the femtogram scale, allowing the determination of the growth rate even within different cell cycle phases for bacteria, yeast or mammalian cells (Godin, et al., 2010). Nevertheless, it is not providing real time measurements, since less than 1,500 cells per hour are measured (Bryan, et al., 2010).

Flow cytometry

Flow cytometry is a combination of fluidics, optics and electronics systems. The single-cell measurement is possible because the sample is injected into the laminar flow of the sheath fluid with a slightly higher pressure. Consequently, the hydrodynamic pressure constrain the sample and thereby only one cell passes the laser light at a time. As pointed out before for the Coulter counter, a compromise between concentration of the sample and the speed of analysis has to be found, (Shapiro, 2003). Light scattering and/or fluorescence are captured, filtered spectrally, and converted into electrical signals through photodetectors.

The cells are characterized based on their light scatter properties, the relative size distribution is associated to the forward scatter measurements, while the side-scatters are used to give information about the granularity/complexity of the cell. If exogenous dyes are used, viability, vitality, respiration capacity or intracellular product accumulation can be determined, as well as when the cells express reporter genes based on the synthesis of a fluorescent protein associated to certain cell responses. The whole spectra of microorganism cells sizes can be covered with this technique: cell lines, algae (Hillig, et al., 2013), yeast (Back, et al., 2016) or bacteria (Marba-Ardebol, et al., 2016).

The main advantage of this method is the amount of events that are measured per sample point (10^6), and the multiple parameters that can be obtained at a time, although one must always take into account that values are relative and not absolute. Even though calibration beads of different sizes are available (Mittag and Tárnok, 2009), they have not yet been successfully applied for quantifying microorganism, but for bigger cells like cell culture.

Over the last few years, a lot of studies about FCM have been published. However, more standardization and optimization is necessary, if results should be comparable. To do so, stain concentration, incubation time and temperature, fixation procedures and controls need to be taken into account. These parameters will depend on the organism and cultivation conditions (media matrix), but also on the instrument. The mechanism behind each dye should be in focus in order to obtain systematic conclusions (Buysschaert, et al., 2016).

FCM analysis can be performed *off line* after the fixation of cells; *at line* by washing, diluting and staining the cells; or *in line*, when sampling, staining, measurement and data analysis steps are automatized (Besmer, et al., 2014; Brognaux, et al., 2013a; Hammes, et al., 2012). Despite of this automation, some minutes are necessary from the time a sample is taken, until the results are provided.

This technology has been applied to assess cell growth, intracellular product accumulation, metabolic activity, scale-down effects, optimize pre-culture conditions (Bouix and Ghorbal, 2015) or detect contaminations.

2.3.1.2. *In situ* techniques

Laserlight backreflection

This technique measures the laser light, which is reflected backwards when hitting a particle. A distance to the probe is defined, where a circular path is scanned. When the light interferes a particle, only the light, which is reflected directly backwards is measured. The intensity of the reflected light, measured by the duration of this event, is a measure of the cord length. The single-cell size distribution is not directly measured, but the size and shape of the particles are related to the chord length distribution.

This technology allows high throughput measurements, since the pulsed laser beam can detect thousands of particles within a second and it can be directly coupled to the reactor and sterilized.

The laser wavelength and energy must be adjusted depending on the microorganism size and shape. Cell concentrations measurements can be accomplished, since only particles in the focal plane are counted, while defocused particles are suppressed. Flocculation studies (Ge, et al., 2005; Xue, et al., 2010) and scale-down studies have been investigated by correlating *off line* and *at line* results such as cell viability or agglomeration (Brognaux, et al., 2013b; Lemoine, et al., 2015).

2.3.2.Imaging techniques

Imaging techniques can be generalized by splitting the work-flow into three steps: image acquisition, particle-identification and data-analysis. The acquired image requires usually a data preparation step before feature extraction, which includes preprocessing or filtering to reduce the noise, followed by a determination and segmentation of the particles of interest (Kan, 2017). After that, machine learning algorithms in combination with the image annotation of specialists can be applied. In this way, the analysis can be standardized at the same time that the user can act on the results to improve them (Sommer and Gerlich, 2013).

2.3.2.1. *Off line* or *at line* techniques

Fluorescent microscopy

Fluorescence sensors have been applied to several platforms to monitor proteins, RNA or DNA, but also cellular properties such as the membrane potential, cell cycle or redox state. However, the major limitation of fluorophores is its specificity and the cell membrane permeability (Specht, et al., 2017). These challenges can be avoided when using fluorescent proteins, which can be expressed e.g. at different cycle phases (Leitao, 2017) or due to some stress responses (Di Talia, et al., 2009). This technology has been applied for high throughput and screening investigations (Torres, et al., 2016). Although the spectral overlap is limiting the recognition of several parameters at once, the combination of imaging and fluorescent dyes offers the possibility to obtain hundreds of parameters in parallel (Okada, et al., 2014).

Fluorescence microscopy is useful to study cellular dynamics, if the fluorescence signal is related to reporters or proteins. The time-lapse fluorescence microscopy allows to gain a video sequence, which shows the cellular dynamics and motions in real-time (Di Talia, et al., 2007; Hansen, et al., 2015).

Imaging cytometry

Imaging flow cytometry (IFC) is going one step beyond conventional FCM. Gating decisions can be performed under consideration of informative and quantitative sample characteristics provided by cell

images, such as the cell size, shape, distribution or location of labeled biomolecules within cells (Han, et al., 2016), which results in a multi-parametric analysis of high-volume cell populations.

The major limitation of IFC is the time required for acquiring, storing and processing a massive number of cell images with a real-time data analysis. Nevertheless, when supervised machine learning models are applied, features can be extracted from the bright field and the typically ignored dark field. Studies have evaluated mammalian cells both fixed and live, as well as fixed yeast cells without staining (Blasi, et al., 2016).

Digital holographic microscopy

A laser or LED, which provides coherent (monochromatic) light, is split inside an interferometer into a reference and an object beam. The object changes the light, whereas the reference beam remains unaffected. Both beams interfere and the charge-coupled device (CCD) records the optical phase and amplitude (intensity) digitally as a hologram (**Figure 6**).

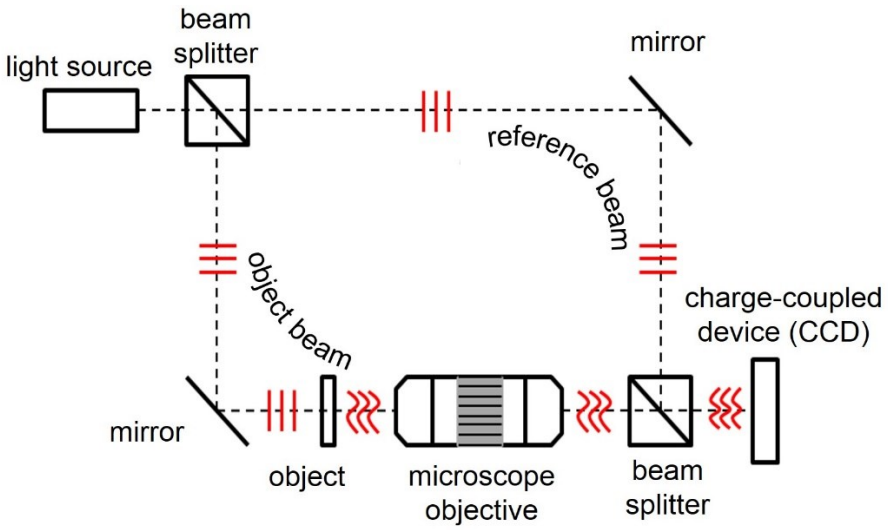

Figure 6. Principle of a digital holographic microscope in Mach Zehnder interferometer configuration (adopted from Robert Spann Master Thesis).

The phase depends on the refractive index ratio of the object to the surrounding material and the thickness of the sample. The intensity depends on the absorption and light scattering. The cellular size, volume and phase homogeneity among other parameters can be determined through this information.

This method has been applied for assessing the harvesting process of adherent cells in real-time (Viazzi, et al., 2015); but also in cells suspensions, where diluted samples were measured *ex situ* (Marbà-Ardébol, et al., 2017). Moreover, the possibility to connect the technology as a bypass through a flow cell is already feasible (Mathuis and Jooris, 2013). The necessity of sampling or of a bypass system can be turned to an advantage. It offers the possibility to dilute for an accurate measurement for high cell densities, when an *in situ* measurement may be limited.

In contrast to traditional optical microscopy, the third dimension can be obtained by the evaluation of the phase and the amplitude signals. If the refraction index of the cell is unknown, as it occurs with cells containing organelles with varying refractive index, only relative volumes can be measured, since the thickness and refractive index cannot be decoupled (Shaked, et al., 2011). However, Rappaz *et al* correlate the phase of the fission yeast *Schizosaccharomyces pombe* to its dry mass and cell area. Therefore, the state of fission can be calculated through DHM measurements (Rappaz, et al., 2009).

Sometimes the time scale can be recorded as well, and hence trajectories of cells become trackable as long as they remain in the field of view. The mobility of the cells can be associated to different growth status (Lewis, et al., 2006).

Cell culture, algae and yeast cells have been investigated. However, in order to assess smaller cells like bacteria, labeling or a software adaptation is normally necessary to enhance the resolution of the cells, since they are weak-scattering particles (Nadeau, et al., 2016).

2.3.2.2. *In situ* (photo-optical sensors)

Photo-optical *in situ* measurements are conducted by coupling a photo-optical probe to an automated image analysis. Several challenges appear when measuring directly in the culture broth, since several phases are present: liquid (media), solid (cells) and air bubbles in aerated systems, or even fat, as it is sometimes used as a carbon source. Other disturbances can be undissolved particles from the media, antifoam or foam formation. Moreover, high cell densities can lead to overlapping events. Therefore, mechanical sampling or a bypass system were used at the beginning for avoiding disturbances, at the same time that cells become sharper when they are not in movement. However, these mechanisms may influence the cell performance, while the system maintenance is increased (Havlik, et al., 2013b).

Efforts to develop *in situ* microscopes (Bluma, et al., 2010; Suhr and Herkommer, 2015) resulted in prototypes without mechanical sampling, where the sampling volume is defined by the focus of the microscope, which favors sterility and reduces maintenance. (Vojinović, et al., 2006). Firstly, they were applied for the visualization of animal cells and their viability determination (Wiedemann, et al., 2011a). Afterwards, even yeast cell concentration and osmotic stress responses could be detected *in-situ* (Camisard, et al., 2002). Only recently, the biomass concentration of high cell densities of yeast (biomass concentration of *Pichia pastoris* up to a concentration of nearly 80 g L^{-1} with an standard deviation below 12%) (Marquard, et al., 2016), and bacteria (biomass concentration of *Escherichia coli* up to a concentration of 70 g L^{-1} with an standard deviation of 8%) (Marquard, et al., 2017) could be measured. However, no single-cell analysis was feasible yet at those cell concentrations. The determination of the dried biomass concentration was not predicted through cell count, it was achieved based on a gray scale intensity measurement of the images.

3. **Research hypotheses, scope of work and research goals**

The work presented in this thesis relies on the following key hypotheses:

The application of three-dimensional digital holographic microscopy and photo-optical *in situ* microscopy can provide statistical relevant information of morphological features from captures of the heterotrophic algae *C. cohnii* and the budding yeast *S. cerevisiae* on a single-cell basis. A representative sample of the population can be measured with a relevant observation frequency, compared with the dynamics of the organism (e.g. cell cycle, growth rate and production rate).

> Recent advances in automated imaging technologies allow measurements of single-cell morphological parameters providing further information beyond the size about cellular structures and shape. A representative sample of the population should be measurable during the whole cultivation. Only then the characterization of the interdependencies between physiological responses and morphology becomes possible.

Metabolic information during the cultivation of the heterotrophic microalgae *C. cohnii* can be assessed through the quantification of single-cell morphological features. Conditions can be distinguished into those, in which growth (at a low C/N ratio), and those in which DHA production (at a high C/N ratio) is favored. The intracellular lipid accumulation in the heterotrophic microalgae *C. cohnii* can be predicted.

> There is a tight relationship between a cell's metabolism and its shape: many cells control their shape/size by connecting growth with cell-cycle events and division. The cell size is directly related to the internal biosynthesis. Hence a quantification of the cell morphology can help in the prediction of the whole cell population response as their physiological status can be indirectly determined.

Environmental conditions in industrial-scale bioprocesses can significantly influence cellular heterogeneity. Namely oxygen oscillating conditions, as they occur in aerated large-scale nutrient-limited fed-batch cultivations, significantly influences the morphological heterogeneity among a population of the yeast *S. cerevisiae*.

> Since oxygen is a cofactor in several reaction steps within sterol metabolism, changes in oxygen availability can have an influence on the sterol regulation. Deficiencies in sterol formation can occur, which lead to a decreased growth rate. They might influence the morphological population heterogeneity as well, since cell stress responses to the same adversity can be different (stochastically regulated). This heterogeneity can have an influence on the process performance and yield, e.g. on the budding, the growth rate, and side metabolite accumulation.

Morphological changes can be used to follow the growth status for the budding yeast *S. cerevisiae* during a batch cultivation. The growth rate can be predicted.

> The morphology of the cells is altered by their own growth in response to cultivation conditions. A distinction between the typical growth stages of a batch cultivation can be made based on the cell size and shape distribution.

Generally, this study is focused on the assessment of industrially relevant bioprocess, by addressing the single-cell based morphological monitoring, ideally *in situ* and in real time. This information is compared with *off line* information, which is usually the golden standard.

Mainly two tools, a photo-optical *in situ* microscopy (ISM) probe and three-dimensional digital holographic microscopy (DHM) were used for the *on line* and *at line* observation of the state of cells during cultivation. The ISM (Sopat GmbH, Berlin, Germany) was formerly used for particle size measurements of droplets, gas bubbles and solid chemical particles. The present study used this ISM for the first time for cell recognition. The DHM (Ovizio Imaging Systems NV/SA, Brussels, Belgium) was used to gain data of morphological features beyond the cell size, e.g. circularity and cell surface. The imaging, particle-identification and/or data-analysis of both techniques had to be adjusted in dependence to the organism of interest.

The main research goal was to proof that by applying single-cell process analytical tools *at line* or directly *in situ*, reliable and statistical morphological data, which can be related to cell physiology and process conditions, can be obtained. The process performance can be evaluated within a time that is relevant in comparison to cellular dynamics. This was exemplarily investigated in microalgae and yeast cultivations (see graphical abstract **Figure 7**).

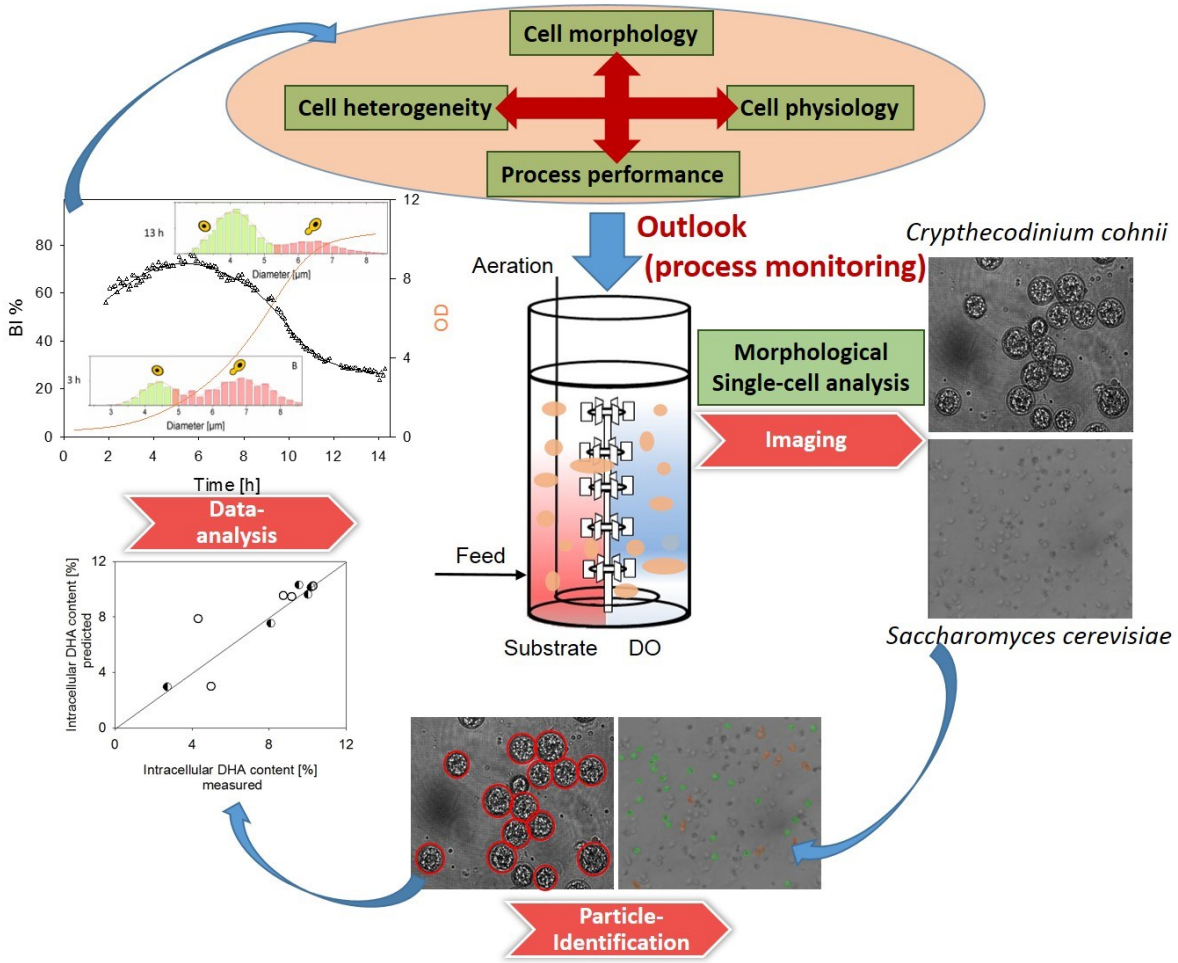

Figure 7. Graphical abstract to summarize the main experimental approach as described in this thesis.

4. Experiments

4.1. Single-cell-based monitoring of fatty acid accumulation *in Crypthecodinium cohnii* with three-dimensional holographic and *in situ* microscopy

Anna-Maria Marbà-Ardébol, Jörn Emmerich, Peter Neubauer, Stefan Junne

Abstract

To date, *on line* monitoring in bioprocesses is restricted to conventional parameters. Presently, advances in microscopy allow the monitoring of single-cell size distributions in a bypass or *in situ*. These data provide information regarding population heterogeneity, substrate conversion, or product synthesis as these parameters are related to the size of the cells. In this study, changes in the single-cell size distribution of the heterotrophic microalgae *Crypthecodinium cohnii* were tracked with holographic microscopy and a photo-optical microscopy probe, which is applicable *in situ*. This algae produces the polyunsaturated fatty acid docosahexaenoic acid (DHA). On the basis of the cell size and broadness of the size distribution, the applied methods enabled to distinguish between cells in the growth and production phase. Under conditions of low growth and high fatty acid accumulation, the cell size kept concomitantly changing. The correlation between cell size measurements and the intracellular DHA content was confirmed by regression analysis. The phase heterogeneity, which was measured by holographic microscopy, changed simultaneously with the DHA synthesis. The amount of information obtained by both digital holographic and *in situ* microscopy is similar to that obtained by flow cytometry but with reduced effort for a real-time analysis.

Keywords: *in situ* microscopy, holographic microscopy, lipid accumulation, heterotrophic algae, polyunsaturated fatty acids

1. Introduction

The present study evaluates the suitability of two techniques, namely three-dimensional digital holographic microscopy (DHM) (Viazzi, et al., 2015) and photo-optical *in situ* microscopy (ISM) (Maass, et al., 2012), for monitoring lipid accumulation in heterotrophic algae without using traditional staining methods or chromatographic analysis. ISM can be used in situ for real-time monitoring. In contrast to many previous reports of on line microscopy in bioprocesses, the microscopes used in this study are commercially available and thus relevant for broader application beyond research.

The cell size of the heterotrophic microalgae *Crypthecodinium cohnii* increases concomitantly with the intracellular content of the polyunsaturated fatty acid docosahexaenoic acid (DHA) (Hillig, et al., 2014b). The traditional method of measuring fatty acid content in a cell by gas chromatography is time consuming, and it only represents an average value of the entire sample. In contrast, single-cell-based analyses such as flow cytometry (FCM) provide more information but also require a large amount of sample preparation time if staining is necessary. Automated FCM can reduce this time of operation, but the method is still required to be conducted *at line* to enable automated sampling, dilution and staining (Delvigne and Goffin, 2014). Moreover, the time of operation could also affect the physiology or viability of sensitive cell types. This can be circumvented with the expression of fluorescent compounds inside the cell; however, genetic modification will be required. Another technique that can be applied to rapidly detect changes in the cell size is microscopy coupled with automated, software-based cell detection. Photo-optical measurements *in situ* or in a bypass have been described in several reports (Belini, et al., 2013; Bluma, et al., 2010). Some approaches included the use of a stop-flow device to capture the sample before a picture is taken, thus minimizing the flow of the cell suspension. However, the involvement of micromechanical parts directly confronted with media components and cell suspension may cause problems. Other approaches allow to capture the cell suspension directly, e.g. by applying immersion lenses; thus, further optical adjustment during the measurement is not necessary (Suhr and Herkommer, 2015). Microscopy tools are applied for determinations beyond biomass concentration (Bonk, et al., 2011; Camisard, et al., 2002; Guez, et al., 2004; Wiedemann, et al., 2011b). The morphological features of a cell can allow to draw a conclusion about its physiological state (Baicu, et al., 2015). The application of *in situ* microscopy in a phototrophic culture of the microalgae *Chlamydomonas reinhardtii* was described earlier (Havlik, et al., 2013a). The same algorithms that are applied for *off line* measurements are usually applicable for *in situ* measurements, although some adaptations may be required. However, the accurate detection of morphological features of undiluted samples at cell densities typically achieved in bioreactor cultivations remains a challenging task. The advantages of a high measurement frequency and the possibility of obtaining a tool for process control when applied *in situ* have to be compared with the disadvantages of a higher background signal and a concomitant loss of accuracy.

Therefore, this study evaluates the monitoring of lipid accumulation in heterotrophic algae in real-time by DHM and ISM without the use of traditional staining methods. DHM uses the absorption of red light from an LED at the edges of particles in comparison to a reference beam that passes through the sample towards a photo-detector to determine the cellular size, volume and phase homogeneity among other parameters. This method is applied for diluted samples *ex situ*. Recent developments enable the user to connect the holographic microscope to a flow cell in such a way that a bypass measurement becomes feasible. ISM as applied in this study consists of a single-rod sensor probe that allows the capture of images within a known focus area in a measurement gap using a high-resolution CCD sensor. Cells continuously pass through this gap because of the movement of the liquid phase and are illuminated with a white flash light.

In our study, various phases of the DHA production process are monitored during lab-scale reactor cultivations with the single-use bioreactor CELL-tainer©. In addition, the effect of different media on growth and lipid accumulation is described. If applied successfully, novel process analytical tools are available for parallel and automated process development and for process control in the case of *in situ* applicability. DHM and ISM could provide suitable information on intracellular DHA accumulation in lipid droplets based on single-cell size distribution in real-time.

2. Materials and methods

2.1. Media preparation and pre-cultivation

C. cohnii culture CCMP 316 was obtained from the Provasoli-Guillard National Center for Marine Algae and Microbiota, ME. Pre-cultures were prepared using a previously published method (De Swaaf, et al., 2003).

2.2. Bioreactor cultivations

Cells were cultivated in the single-use rocking-motion bioreactor CELL-tainer® CT 20 (Cell tainer Biotech, the Netherlands) for 7.5 days. The media composition and cultivation procedure have been described previously (Hillig, 2014). To operate the CELL-tainer at 1 L working volume, expansion channels (Cell tainer Biotech) were used throughout the cultivation to fully cover the electrodes with a sufficient amount of liquid during rocking. In total, 100 mL of pre-culture was used for inoculation. The bioreactor process was started in a batch mode followed by a non-limited fed-batch mode in which the glucose concentration (main carbon source) was maintained between 10 and 25 g L^{-1}. The temperature was maintained at 25 °C. The pH was automatically maintained at 6.0 with 1 M HCl and 1 M NaOH. The dissolved oxygen (DO) levels were maintained by regulating the rotational speed to avoid values below 20% of dis-solved oxygen saturation. In the production phase, sodium acetate was added, and the feed operation was changed to a pH-auxostat mode controlled by acetic acid as described

elsewhere (De Swaaf, et al., 2003). The addition of sodium acetate induced the expression of the enzymes required for the assimilation of acetic acid, which are not active in cells grown with glucose. Previous studies have proven that acetic acid is a suitable additive to enhance DHA synthesis in *C. cohnii* (Hillig, 2014). The liquid volume increased by approximately 1.8 L during the entire fed-batch phase.

2.3. Shake flask cultivation

Shake flask cultivations were conducted in TubeSpin® Bioreactor 600 flasks (TPP Techno Plastic Products, Switzerland) following the procedure and media composition described elsewhere (Hillig, et al., 2014a). Briefly, a working volume of 100 mL was used, and the agitation was set to 230 rpm at an amplitude of 25 mm. The temperature was maintained at 25°C. The cultivation was stopped after 72 h in the batch cultivation mode.

2.4. Screening experiments

To screen for the reduction of the chloride content of the marine media, chloride ions were (partly) substituted by other salts corresponding to a molar equivalent (see table 1). Each experiment was performed in duplicates. Shake flask cultivations were conducted as described above.

Table 1. Substitution of NaCl in shale flask experiments.

NaCl Substitute	Mol-eq. [mol L^{-1}]	Concentration [g L^{-1}]
None (control)	0.34	20.00
$NaNO_3$	0.17	14.45
NaH_2PO_4	0.17	20.40
$K_2S_2O_8$	0.17	45.00

2.5. Microscopy

For monitoring the single-cell size distribution (Fig. S1), the three-dimensional digital holographic microscope oLine-OT40GA (Ovizio, Belgium) and photo-optical probe SOPAT MM 1 (SOPAT,Germany) were used. Cell size distributions were measured either directly in the culture broth (SOPAT) or on a microscope slide (Ovizio). Because the photo-optical sensor was not mounted directly onto the shake flasks or the bag of the single-use bioreactor owing to limited space and the lack of sensor ports, sampleswere obtained and directly filled in 50-mL plastic tubes. The *in situ* microscope was dipped into the cell suspension. By moving the plastic tube up and down, circulation of the fluid through the measurement gap was achieved. In case of DHM, the cell suspension was diluted to an optical density of OD_{492} = 12 and captured on a microscope slide. Table 2 provides an overview of the main characteristics of the microscopes. Several settings such as size boundaries and the applied algorithms

were adjusted for automated algal cell detection with DHM and ISM. Parameters for the detection of algal cells are summarized in table 3.

Table 2. Overview of the main characteristics of the applied microscopes

Parameter	SOPAT MM 1	oLine-OT40GA
Field Depth	2.32 µm	1.5 µm
Camera	2750 x 2200 CCD with 19fps	2456 x 2058 CCD with 15 fps
Interface	GigE Vision	-
Magnification	10 x with an adaptive TV-lense with a magnification factor of 1.6	x 63
Numeric aperture	0.1	0.7
Illumination	Transmission, Xenon flash lamp, 2.6 J, pulse duration 8µs	Transmission, Monochromatic LED at 630 nm
Measuring Gap	200µm	not applicable
Probe length	270mm	not applicable
Probe diameter	24.5mm	not applicable
Software Version	SOPAT v1R.002.0053	OsOne-4.3

Table 3. Parameters for the detection of algae cells in the OsOne software version 4.3 (Ovizio) and SOPAT detection software (SOPAT), recipe file: insitu1lim1k.pss.

Parameter	SOPAT	OsOne
Background	-	2.15
Median cell size (d_{50}) [µm]	18	32
Background detection algorithm	-	Phase variance
Cell detection algorithm	v1R Algo	Local maximum
Apply refocus	yes	yes
Detect invalid areas	yes	yes
Cell minimum size [µm]	8.4	9
Cell maximum size [µm]	23.5	-
Remove image defects	adjusted	9
Split neighbor cells	adjusted	6
Invalid area- sensitivity	-	4

The Sauter mean diameter (d_{32}), which was measured for both techniques, is computed directly from the surface of the cell in the two-dimensional image. It is assumed that the cell is a perfect sphere, and its diameter is equivalent to the diameter of a circle that has the same area as the cell in the two-

dimensional image. The circularity detected by DHM represents the ratio of the cellular area to the square perimeter. The ratio describes the circularity of a cell (1 = exactly circular shape; 0 = no circular shape). The phase homogeneity represents a measure of the spatial closeness of the image of a particle's surface. Values range between 0 and 1, and the maximum value is achieved when the co-occurrence matrix is diagonal. The optical volume is a function of the (unknown) refractive index of the sample and the physical volume.

Cell detection was performed by a software and inspected visually for accurate detection. Whenever cells overlaid each other, they were restricted from being detected. On average, 10 captures were obtained by DHM and 100 by ISM. The slide (cell suspension) was moved between the captures of the holographic microscope (photo-optical probe) to assure the replacement of cells in the image field after each capture.

2.6. *Off line* analysis

2.6.1.Cell growth

Cell growth was quantified throughout the cultivation by measuring optical density, dry cell weight (DCW) and cell count. Optical density was measured in plastic cuvettes at a wavelength of 492 nm with a spectrophotometer (Ultraspec 3000, GE Healthcare, CT). For DCW analysis, 2 mL of culture were centrifuged for 10 min in pre-weighed 2-mL Eppendorf tubes at 21,500 x g, washed with 2 mL of 20 g L^{-1} NaCl solution and centrifuged again under the same conditions. The Eppendorf tubes were then stored in a drying oven (75 °C) for at least 48 h and weighed for DCW determination. Cell counting was performed with a Thoma chamber using a conventional transmission light microscope at a magnification factor of 400.

2.6.2.Cell staining and flow cytometry

FCM measurements were performed with the MACSQuant® Analyzer (Miltenyi Biotec, Germany). The excitation wavelength was set to 488 nm. The obtained data were evaluated using the software FlowJo V10 (TreeStar, OR). Two fluorescent dyes were used separately (no double staining): bis-(1,3-dibutylbarbituricacid) trimethine-oxonol [BOX or DiBAC4 (3)] and Nile red (both from Sigma, Germany). Filters were applied as follows: a bandpass-filter 488/10 for forward scatter (FSC)/side scatter (SSC), 525/50 for BOX and a long-pass filter 655–730 for Nile red-stained cells as described elsewhere (Hillig, et al., 2014b). Briefly, cultivation samples were diluted with phosphate buffer (21.9 gL^{-1} NaCl, 0.35 gL^{-1}KCl, 1.24 gL^{-1} KH_2PO_4, 0.176 gL^{-1} $Na_2HPO_4.2H_2O$) and measured immediately. Cells were stained with a working concentration of BOX 5 µg mL^{-1} for 10 min in the dark. Nile red staining was performed according to a previously published protocol (de la Jara, et al., 2003).

2.6.3.Quantification of carbohydrates and fatty acids

DHA measurement was conducted and analysed with a gas phase chromatograph equipped with a flame ionization detector (GC-FID) as published previously (Hillig, et al., 2014a). Samples were analysed using a capillary column, Varian WCOT fused silica, 25m x 0.25 mm ID, film thickness = 0.12 µm, CP-Sil 5 CB (Varian, Germany). Briefly, conditions were as follows: temperature was maintained at 150 °C for 2 min and then increased at a rate of 15 °C min^{-1} to 250 °C. After 37 min, the column was heated to a final temperature of 280 °C at a rate of 5 °C min^{-1} and was maintained for 7 min. The injector and detector temperatures were set to 290 °C and 300 °C, respectively. The injection volume was 0.3 µL, and the sample was injected in the splitless mode. Nonadecanoic acid was used as the internal standard.

2.7. Calculations

The volumetric substrate uptake rate (R_s) was calculated using the difference in the supernatant substrate concentration within a time interval. Glucose concentration was measured by an enzymatic assay (r-biopharm, Germany) according to the manufacturer's instructions. The dilution induced with the feed rate was considered (eq. (1)).

$$R_s = \frac{\Delta c_S}{\Delta t} + \frac{F}{V_l}\left(c_{S_0} - c_{S_m}\right) \qquad (1)$$

The volumetric DHA production rate was calculated as the concentration difference within a time interval (eq. (2)).

$$R_p = \frac{\Delta c_P}{\Delta t} + \frac{F}{V_l} \qquad (2)$$

3. Results and Discussion

3.1. Two-stage fed-batch cultivation

Fig. 1 shows the cultivation parameters of the 1-L two-stage fed-batch cultivations of the heterotrophic marine microalgae *C. cohnii* in the rocking-motion single-use bioreactor CELL-tainer. Conditions for optimal growth were maintained for 3.3 days before starting the production phase when the C/N ratio decreased below approximately 20 (Feng and Johns, 1991). A clear differentiation can be seen between these two phases in which the cell concentration first increased and thereafter remained almost constant in the production phase (Hillig, et al., 2014b). DHA production ceased after 6.3 days when the intracellular concentration was 10% (w/w), which are rather typical values in a wildtype strain (Ratledge and Wynn, 2002).

Investigations have been previously performed to enhance the lipid production by adjusting the cultivation conditions such as the ratio of nitrate, tryptone and yeast extract or simply the C/N ratio

(Feng and Johns, 1991; Wen, et al., 2002). However, optimization always relied on *off line* analyses that are obtained after the experiment is completed (e.g. the determination of lipid compounds in the cell); there is a need for sampling, sample pre-treatment and quantification of concentrations in real-time. The possibility of rapidly monitoring *at line* or even *in situ* provides the opportunity to measure values in real-time during the experiment.

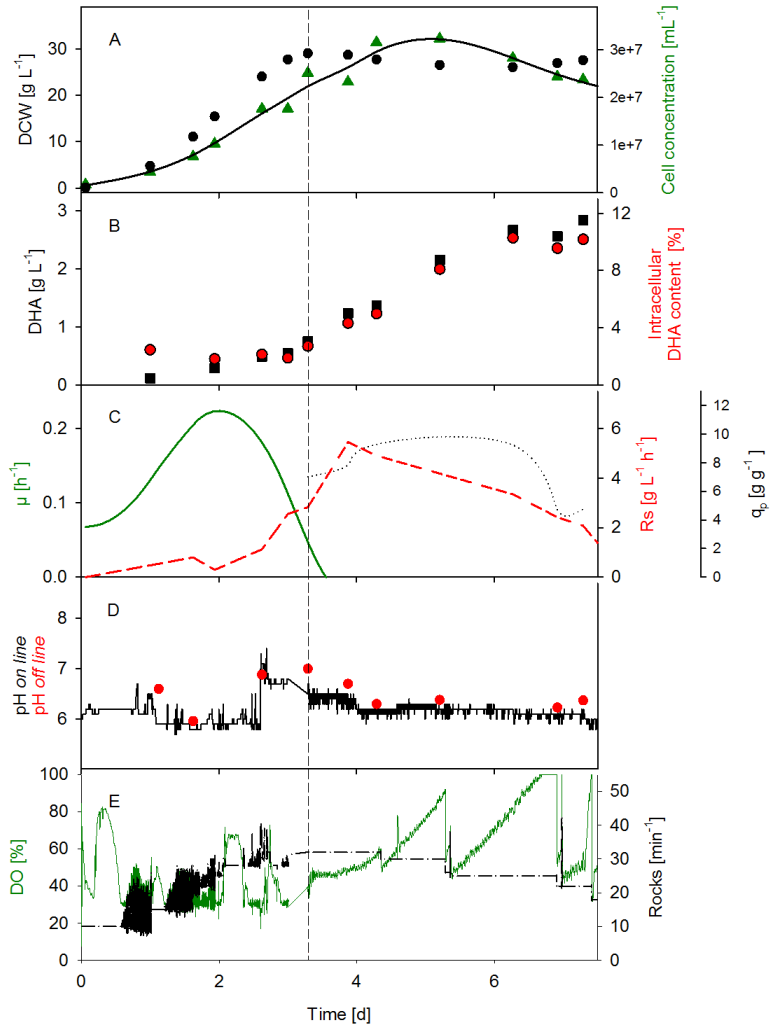

Figure 1. Non-limited heterotrophic 1 L fed-batch cultivations of *C. cohnii* in the single-use bioreactor CELL-tainer. A: Cell concentration (▲) and curve fit (straight line), cell dry weight (●); B: volumetric (■) and intracellular DHA content (●); C: specific growth rate μ (straight line), volumetric substrate uptake R_S (dashed line) and specific product formation q_P (dotted line); D: pH-value as measured *on line* (straight line) and *off line* (●); E: dissolved oxygen saturation (straight line) and rocking rate (dashed line).

In this study, the quantification of intracellular DHA content is of great interest as it is the main product of the process. This should be feasible by the determination of the cell size. Studies using the marine algae *Schizochytrium limacinum* SR21 investigated the effect of accumulating DHA in the cell body weight, which increased almost thrice during the course of cultivation (Chi, et al., 2009). In this case, the cell volume increases by a factor of about three as well. Lipid droplet accumulation in the oleaginous yeast *Waltomyces lipofer* was observed qualitatively *off line* by measuring cell diameter by a flow particle image analysis (FPIA) and FCM using Nile red staining (Raschke and Knorr, 2009). The diameter and fluorescence increased simultaneously, and lipid droplet accumulation was observed with the images provided by FPIA.

Thus, different measurement techniques were applied to observe whether any correlation exists between morphological features and DHA accumulation in *C. cohnii*. Fig. 2 shows the DHA content during the course of the fed-batch bioreactor cultivations as directly determined by GC-FID, FSC and SSC light signals and signals obtained from Nile red- and BOX-stained cells in FCM. Nile red is a selective fluorescent stain for intracellular lipids; their concentrations correlate well with the staining intensity (Fig. 2C). The effectiveness of this methodology for the measurement of neutral lipids was previously demonstrated in the algae Chlorella vulgaris where the correlation coefficient of determination between gravimetric and spectrofluorimetric measurements was R^2=0.99 (Huang, et al., 2009). Nevertheless, this methodology implies times for sampling, staining and analysis. If staining methods should be avoided, FSC and SSC light signals might be suitable. The signals should correlate with the DHA content if the cell size is affected by it. It could be demonstrated that FSC light signals indeed correspond to the cell size, as observed in a microalgae screening where a cell sorting was performed using the two-dimensional distribution of algal cells at red fluorescence (chlorophyll-based auto-fluorescence) against FSC (corresponding to the cell size) (Thi, et al., 2011). In the present study, however, no obvious correlation between the FSC light signal (Fig. 2B) and the intracellular DHA content (Fig. 2A) was observed. This result might be due to a concomitant influence of the lipid droplet content and other cellular compounds on the FSC light signal. The SSC was affected when the DHA content increased; thus, the granularity of the cells changed. In contrast, the intensity of Nile red staining correlated well with the DHA content (Fig. 2C) as previously shown using *C. cohnii* cultures when FCM results were compared with GC-FID measurements (Cooksey, et al., 1987; de la Jara, et al., 2003). BOX staining yielded similar tendencies as Nile red staining because BOX is a lipophilic dye that binds to positively charged proteins or unspecifically to hydrophobic regions such as lipid matrices. In both cases, a relationship is observed during the production phase. In general, parallel-operated bioreactors can be coupled with FCM; thus, this method can be used for a large number of samples (Zimmermann, et al., 2016). An analysis time of several minutes is adequate for most applications in bioprocess optimization and even in screening experiments. Staining as applied in this study required approximately 2 min if cell washing is not performed or automated, e.g. by using plates equipped with filters within a liquid handling station. The costs of FCM are approximately twice as high as those for the microscopic methods if only the cost to buy a functional device was considered. If costs of staining and the limited laser life time are considered, operational costs of FCM are certainly much higher than those for microscopy. Moreover, staining might be affected by a change in environmental conditions such as pH, ion content and side product formation, which can vary because of different growth conditions in parallel experiments. Optical methods for cell size detection might be advantageous if there was no interference of media and cells during auto-detection. Fig. 2A shows the evolution of the average single-cell size as quantified by DHM and ISM. As detected by both methods, the cell size

decreased from approximately 21.5 to 17 µm at the beginning of the fed-batch phase. The reduction in cell size with its growth is most likely linked to maturation. In the following production phase, the cell size increases again to approximately 19 µm. As detected by DHM, the average cell size declines again after 6 days of cultivation in the very late production phase.

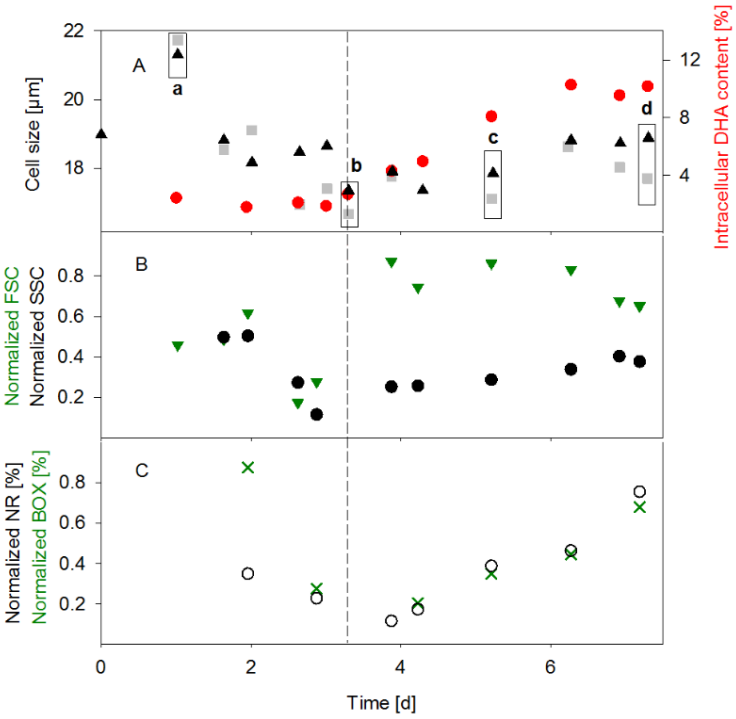

Figure 2. Development of different measurement signals in heterotrophic 1 L fed-batch cultivations with *C. cohnii* in relation to the intracellular DHA content. A: Size detection (as d_{32}) obtained with the DHM (■) and ISM (▲), and intracellular DHA content (●); B: normalized FSC signal (▼) and normalized SSC signal (●) as obtained with FCM; C: normalized Nile-red (○) and BOX signal (X).

The cell size distribution for selected time points is shown in Fig. 3A: after the fed-batch is started (a, straight line), after the growth phase is terminated (b, dotted line), in the middle of the production phase (c, dashed line) and at the end of the production phase (d, dashed and dotted line). The cumulative particle quantity distribution (Q_0) indicates a wider distribution of the particle size (indicated by a smaller slope of Q_0, that is the frequency distribution q_0) at time-point a (maximum frequency distribution q_0 = 0.10). Cells are in an adaptation state, as they were exposed to a greater substrate availability. This situation changed at the end of the growth phase. The d_{32} of cells decreased, and the distribution became much more narrow (time-point b, maximum frequency distribution q_0 = 0.15) as a longer period of similar maturation rates was achieved. This usually leads to a narrow distribution within a cell population. During the production phase, the single-cell size increased due to DHA accumulation (Fig. 3A, time-points c and d, maximum frequency distributions q_0 = 0.13 and 0.12, respectively). If the cell size distribution as measured by ISM is compared with the results of FCM (Fig. 4), the broader distribution at the beginning of the fed-batch cultivation becomes obvious: with the SSC light signal, two populations are visible, of which the larger fraction consists of larger cells. This is also observed with the ISM signal, where a threshold diameter of 19 µm can be assumed to discriminate the two populations. The shift in size in the population between the late growth and late production phase (time-points b and d) can be seen clearly with the ISM and SSC light signals (Fig. 4B

and C). The populations as depicted in the dot plots seem to be quite homogeneous. In summary, the information provided by ISM is in conformity with that by the FCM studies.

Similar trends of Q_0 were obtained by DHM (Fig. 3 B). However, the average d_{32} differs between both methods: for time-point a by 0.4 µm, for time-point b by 0.6 µm, for time-point c by 0.7 µm and for time-point d by 1.2 µm. The difference between the absolute values of the average d_{32} as obtained by both microscopy techniques may be partly due to the different detection algorithms used and number of cells analysed (sample sizes). This will be further discussed in the statistical evaluation section. As measured by both techniques, the degree of population homogeneity was only slightly reduced during the production phase compared with that at the end of the growth phase.

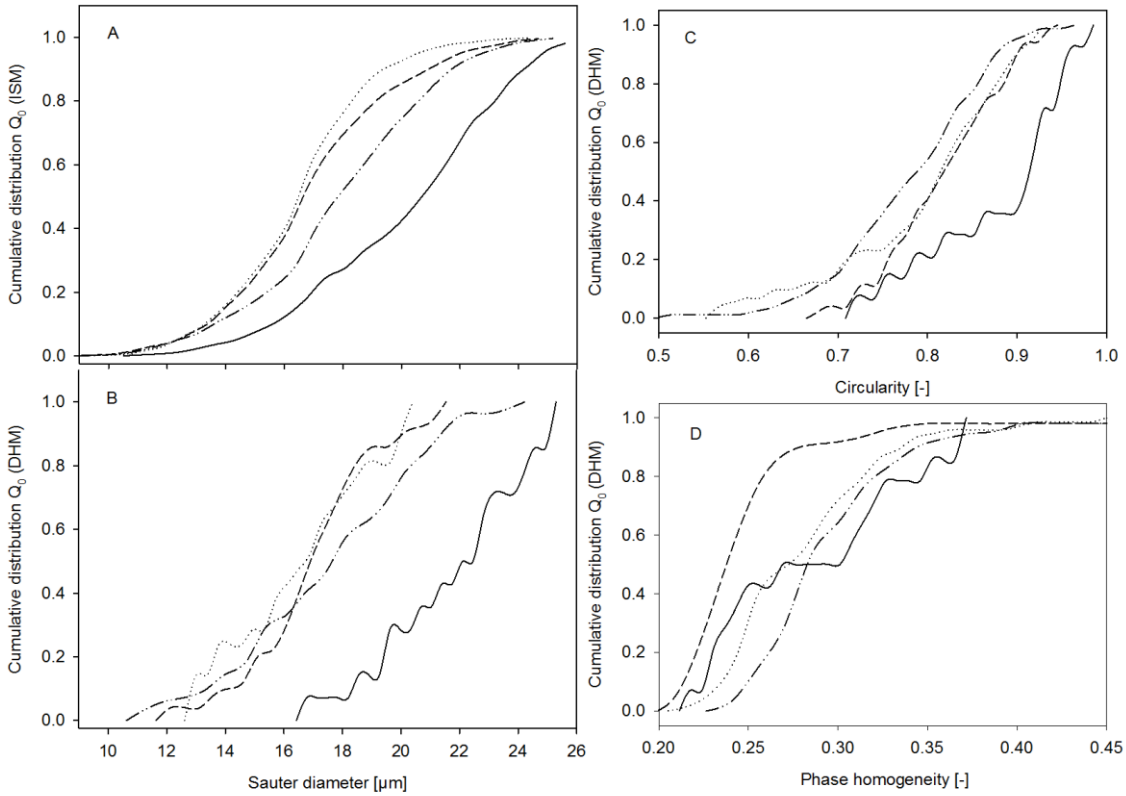

Figure 3. Cumulative single-cell size distribution as measured in heterotrophic 1 L fed-batch cultivations with C. cohnii with the ISM (A) and the DHM (B), cumulative cell circularity (C) and phase homogeneity (D) as measured with the DHM. Values of samples from four time-points of 1 day (straight line), 2.9 days (dotted), 5.2 days (dashed) and 7.3 days (dashed and dotted) are depicted.

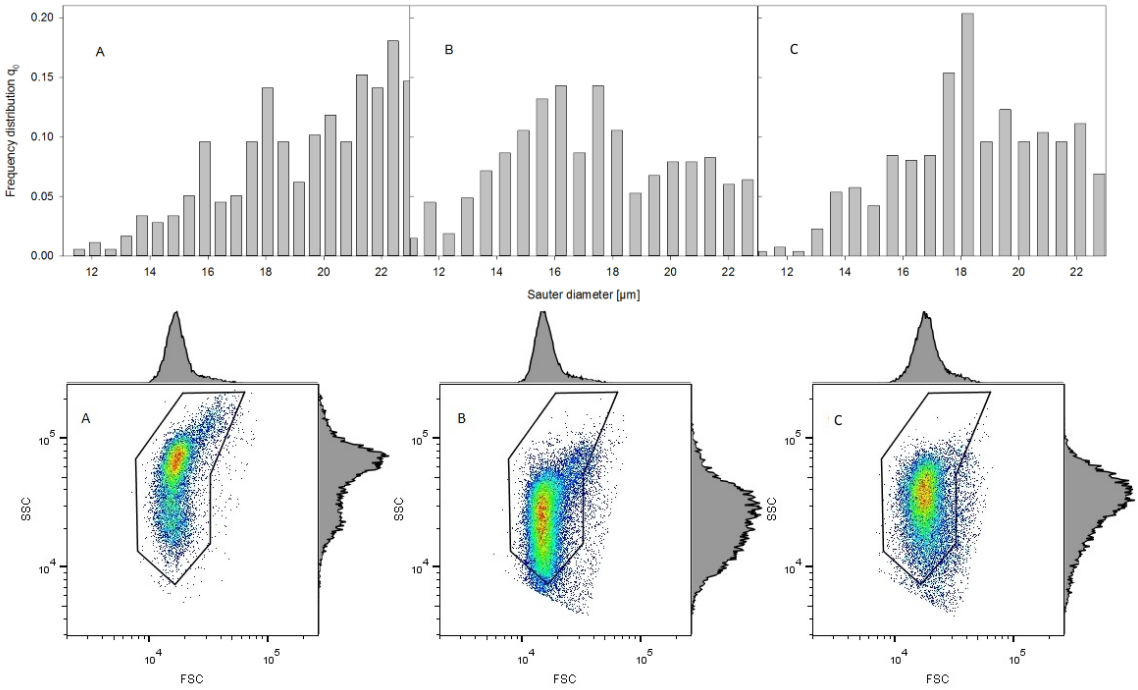

Figure 4. Single-cell frequency distribution as measured in heterotrophic 1 L fed-batch cultivations of *C. cohnii* with the ISM (top row) and forward side scatter (FSC) and side scattered light (SSC) signals obtained with FCM (bottom line). Values of samples from three time-points of 1 day (A), 2.9 days (B), and 7.3 days (C) are depicted.

DHM provided additional information such as the circularity and phase homogeneity. The circularity is negatively affected by lipid droplet accumulation (Fig. 3C). Formation of lipid droplets leads to deformation of the cell wall because they are not distributed evenly inside the cell. The circularity is also decreased during growth compared to that of the cells at the onset of the fed-batch phase as likely maturation also leads to cell deformation. Therefore, the circularity itself can be used as a parameter to identify phases of rather high metabolic activity. Phase homogeneity is distinctly lower when cells accumulate DHA (time-point c in Fig. 3 D), which is in contrast to the time-point when DHA production ceased (time-point d in Fig. 3 D). The degree of phase homogeneity seems to be a good indicator for a high DHA synthesis period because lipid droplets are not evenly distributed inside the cell. If they were evenly distributed, they will occupy the cell volume, and maximum lipid accumulation is achieved.

One major advantage of DHM is the assumption of the optical height of the cells. While the size of spherical cells increases, their 'thickness' also increases. Three-dimensional images of the cells show the increase in diameter and optical height. The optical height is greater at the onset of the fed-batch phase (time-point a, Fig. 5A) and at the end of the production phase (time-point d, Fig. 5 D) than that between the two phases (Fig. 5B and C). It is the greatest in comparison to the cell diameter at time-point d. Moreover, the optical height as measured inside the cell is very diverse at this time-point. Lipid droplet formation exposes different optical features at the edges of the droplets.

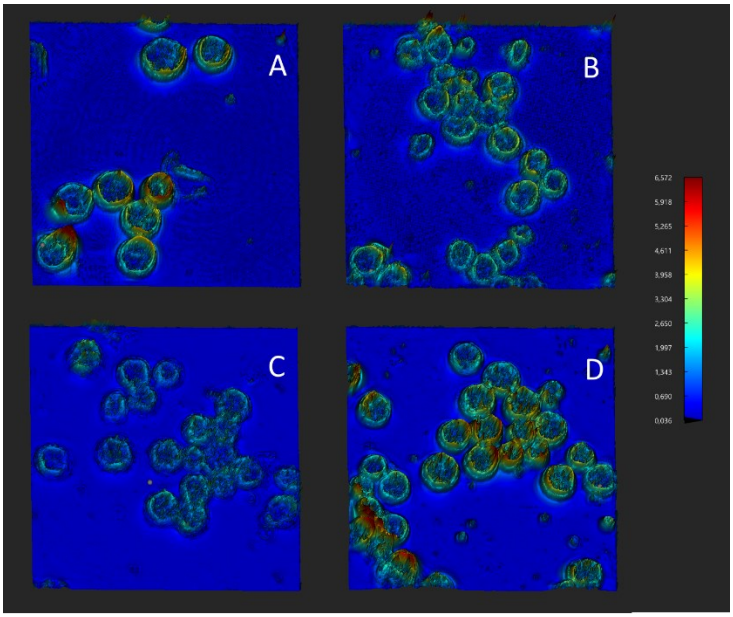

Figure 5. Optical volume of *C. cohnii* cells as measured in samples of heterotrophic 1 L fed-batch cultivations with the DHM. Time-points of 1 day (A), 2.9 days (B), 5.2 days (C) and 7.3 days (D) are depicted.

The actual correlation between the average single-cell size and DHA content was finally quantified using a regression analysis. A linear regression resulted in coefficients (R) of 0.835 (Nile red), 0.825 (BOX), 0.791 (SSC) andn0.632 (DHM). A maximum coefficient (R) of 0.983 (Fig. 6) was obtained using the data obtained from ISM and a second-order equation:

$$DHA_{pred} = -1459.5 + 157.5 * D_C - 4.2\, D_C^2 \quad (3)$$

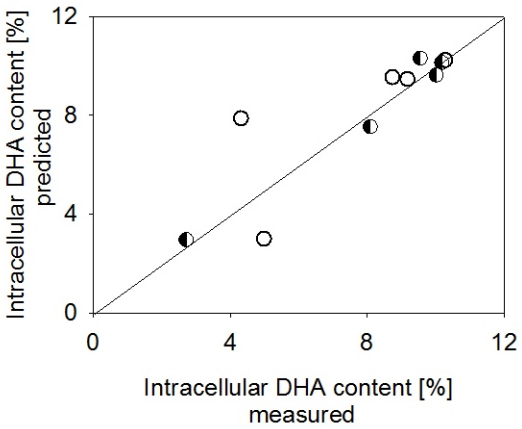

Figure 6. Second order correlation between DHA content measured *off line* (GC-FID) and predicted based on the average of the Sauter mean diameter (d_{32}) as detected *on line* with ISM and cross-calibration. Values used for calibration (●) and for prediction (○).

Eq. (3) represents a nonlinear correlation as the change in the cell size is related not only to the DHA formation but also to the cellular protein content. The cellular protein content most likely decreases if a high DHA content is obtained, thus decelerating the increase in the cell size until a maximal size and consequently the maximal capacity of DHA storage is achieved. However, this should be a reproducible effect. The accuracy of the prediction increases with an increase in DHA content. This underlines the

relationship between DHA accumulation (lipid droplet formation) and the increase in the cell size. The lower the DHA content (the smaller the cells), the weaker is the dependence between the cell size and the DHA content. Thus, cells with high and low DHA content can be clearly separated.

3.2. Screening experiments

Among the two common grades of stainless steel typically used in bioprocesses, 304-stainless steel is susceptible to corrosion if the chloride level exceeds 300 ppm (0.3 g L^{-1}) and 316-stainless steel is susceptible to corrosion if the chloride level exceeds 1000 ppm (1 g L^{-1}). Other grades of stainless steel that exhibit a higher resistance to chloride corrosion are usually not used because of high investment costs and a lack of approval for food processes and sterilization procedures. Therefore, to avoid corrosion problems, a reduction of the chloride ion content in media is useful for the industrial application of marine processes. As an example, in this study, different chloride ion substitutes were tested with respect to the cell growth and lipid accumulation in *C. cohnii*. Investigations included the analysis of the single-cell size distribution within the culture by ISM. Data were compared with *off line* analysis results. Fig. 7A shows that the concentration of Cl^- ions affects the growth and DHA accumulation. At least a 2.5-fold higher cell concentration was obtained in the presence of sufficient NaCl (4.10^6 cells mL^{-1}) after 72 h of cultivation; cell titres were similar to those reported previously (Hillig, et al., 2013). DHA concentration was three-fold higher using Cl^- ions than that using Cl^- ion substitutes. In the case of $K_2S_2O_8$ addition, no DHA was detected and almost no growth was observed; the number of cells increased only by 5% in 3 days, in contrast to 48% or 40% if $NaNO_3$ or NaH_2PO_4, respectively, were used or even 90% in the control culture. Almost no glucose was present in the control cultivation (with NaCl) after 72 h, whereas only 7 g L^{-1} and 1 g L^{-1} of glucose was consumed with $NaNO_3$ and NaH_2PO_4 supplementation, respectively. Barely any consumption was observed with $K_2S_2O_8$ addition. Osmotic effects and different growth rates may have led to a large variation in the obtained cell size. The different cell sizes also resulted in a larger deviation between the values of the DCW concentration and cell counts. Larger cells were obtained when $NaNO_3$, NaH_2PO_4 and $K_2S_2O_8$ were added (Fig. 7 B). The maximum difference in comparison to the control culture was detected when NaH_2PO_4 was added. The d_{32} reached 19.5 (±0.1) µm compared to 14.6 (±0.1) µm in the control culture.

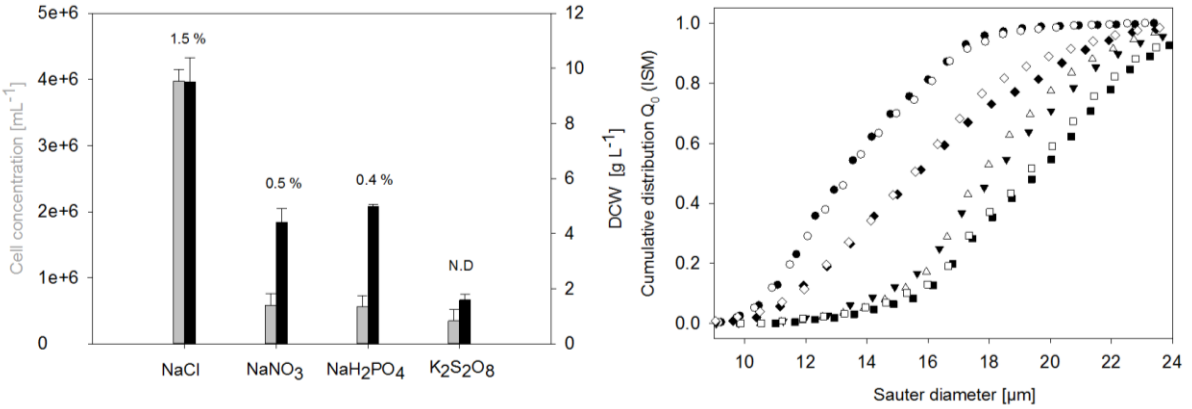

Figure 7. Cell concentration (grey columns) and dry cell weight concentration (black columns) obtained after 72 h in shake flask cultivations of *C. cohnii* when NaCl or replacements of it were applied. Numbers above columns indicate the intracellular DHA content (A). Cumulative single-cell size distribution as measured with ISM with different media compositions, containing either NaCl (○,●) or $NaNO_3$ (△,▼), NaH_2PO_4 (□,■) or $K_2S_2O_8$ (◇,◆) (B).

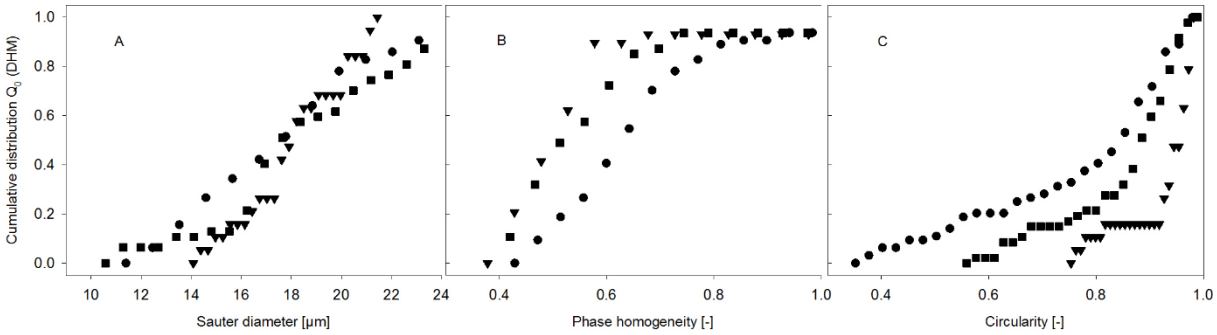

Figure 8. Cumulative single-cell size distribution (A), cumulative phase homogeneity (B), cumulative cell circularity (C) in shake flask cultivations of *C. cohnii* with different media compositions, containing either NaCl (●) or $NaNO_3$ (▼) or NaH_2PO_4 (■), as measured with DHM.

The addition of $NaNO_3$ and $K_2S_2O_8$ also resulted in a higher d_{32} of 18.7 (±0.1) and 17.0 (±0.3) µm, respectively, than that obtained in the control. When $K_2S_2O_8$ was added, a broader distribution was obtained, possibly because of severely unfavourable growth conditions. The higher cell diameter most likely reflects a cell state similar to that at the onset of the fed-batch cultivations in the bioreactor (Fig. 3 A, time-point a). This state is represented by a high substrate availability and very slow or no maturation. In contrast, the cell size distribution as measured in the control culture reflects a state similar to that at the end of the growth phase of the fed-batch cultivations (Fig. 3A, time-point b). The distribution is comparably narrow, and the cells are significantly smaller. A positive skewness can be observed in this control culture that mainly consists of cells that had matured throughout the cultivation and did not accumulate high amounts of DHA. A negative skewness on $NaNO_3$ or NaH_2PO_4 addition seems to be related to a retarded growth (Fig. S4). The diameters of the cells were also determined by DHM. Although similar trends were obtained in comparison to ISM, like those seen in

the measurements of samples from the bioreactor cultivation, the absolute values differed between both the methods. Interestingly, cells of the control culture had a higher phase homogeneity probably because of growth retardation and a lower circularity (Fig. 8B and C). This is in conformity with the observations in the bioreactor cultivation: a higher degree of homogeneity achieved after growth retardation, and a lower degree of circularity indicated a higher content of lipid droplets. Both assumed correlations seem to fit for the shake-flask experiments in which the control culture exhibited a higher growth and lipid accumulation inside the cells.

In summary, if the cell size distribution distinguished between the conditions in which growth (at a low C/N ratio) and DHA production (at a high C/N ratio) is favoured, the growth state of cells and DHA productivity can be determined. Population heterogeneity is usually increased in environmental conditions that cause cell stress such as oscillatory conditions. As observed at the onset of the fed-batch phase compared with later time points, growth under favourable conditions decreases the heterogeneity in the cell size distribution. Thus, it can be assumed that a narrow distribution is favourable for a good growth and production performance of the culture.

3.3. Statistical relevance

Differences in the cell sizes measured in screening experiments and throughout the course of the bioreactor cultivations are significant because the deviance between two replicates is much lower (usually 0.1–0.2 µm) than those obtained between experiments, i.e. a few µm (Figs. 2 and 7). Moreover, the technical error is 0.4 µm, as obtained from triplicate measurements of the same sample and three different image sets with at least 1000 recognized cells. This number of cells (events) is of statistical relevance and thus representative of the population from which they were extracted under the consideration of an infinite or unknown population. This assumption can be made when the population is larger than 100,000 cells, which was the case for all experiments (10^6 cells mL^{-1} in 100 mL in the shake-flask experiments and 107 cells mL^{-1} in 1-L bioreactor cultivations). The variability (σ), which can be obtained from previous data; accuracy, which is the amplitude of the confidence interval (1− α); and the admitted error (e) are the factors that affect the determination of the sample size. The maximal deviance in the cell size between measurements of the same sample was considered to be less than 0.4 µm, the desired accuracy was considered to be 0.02 µm and the admitted error was considered to be 5% or lower ($z_{1-\alpha/2}$ = 1.96). Then, the number of cells that should be analysed (n) was determined to be 945 (Eq. (4)).

$$n = \left(\frac{\sigma\, z_{1-\alpha/2}}{e}\right)^2 \qquad (4)$$

This number of events can be easily achieved by ISM. In contrast, when DHM is used, the number of cells is restricted to the number of analysed slides and practical handling issues. Nevertheless, the

maximal deviance of the holographic microscopy is in the range of 0.1 µm; thus, the accuracy is increased (up to 0.005 µm) if the same sample size was applied. When the same restriction that the maximal error should not exceed 5% is maintained, the necessary cell counts are 59. This allows a practical application of DHM, although it not operated in a bypass. However, the results of the bioreactor cultivation indicated that DHM is more suitable to monitor a higher number of cells because the media, the change in optical features of cells and other factors may affect the accuracy. Thus, *at line* or *in situ* application is favourable as replacement of established methods. Both DHM and ISM can be operated so that a sufficient number of cells can be detected within a reasonable time.

4. Conclusions

In general, there is a need for rapid detection methods, particularly for parallel and automated state-of-the-art process optimization (Neubauer, et al., 2013); otherwise, the bottleneck of time is shifted away from the cultivation itself to the analysis. Usually, the bioreactor variables that are monitored *on line* and/or controlled are physical and chemical parameters rather than physiological ones. This study describes two commercially available novel tools for a faster and *in situ* monitoring of the cell size distribution. They were successfully used to monitor population heterogeneity and, indirectly, fatty acid accumulation in heterotrophic algae. The cell status can be distinctly differentiated using the cell size and broadness of the size distribution under growth conditions. Under conditions of fatty acid accumulation (high C/N ratio), the cell size kept concomitantly changing. The phase heterogeneity as measured by DHM changed simultaneously with the DHA synthesis. The amount of information obtained by DHM is similar to that by FCM but with much lesser effort. Advantages such as a high measurement frequency and the possibility of obtaining a tool for process control when applied *in situ* have to be compared with the disadvantages such as a loss of accuracy and higher detection limit with respect to the size of structures. Therefore, the application of any method must be oriented towards the final purpose and acceptable minimal data quality. Both microscopy methods, DHM and ISM, are suitable alternatives to other well-established *off line* methods. As traditional microscopic techniques are not sufficient to achieve the same valuable information, further developments for commercially available bypass or *in situ* monitoring tools are required for application in cultivations with smaller cells, e.g. yeast or bacteria.

Abbreviations

DHA: docosahexaenoic acid, DHM: digital holographic microscopy, ISM: *in situ* microscopy, FCM: flow cytometry, *C. cohnii: Cryptecodinium cohnii*, DO: dissolved oxygen, BOX: Bis-(1.3-dibutylbarbituric acid) trimethine-oxonol, NR: Nile-Red, ID: inner diameter, DF: film thickness, Rs : substrate uptake rate in a time interval, Δ_{cs}: difference in substrate concentration in a time interval, c_{s0}: feed substrate concentration, c_{sm}: average substrate concentration in a time interval, V_l: average working volume in a time interval, Δt: time interval, F: feed rate, R_p: production rate , Δc_p: difference of the product concentration in a time interval, C/N ratio: ratio in between carbon and nitrogen concentration, FPIA: flow particle image analysis, GC-FID: gas phase chromatograph equipped with a flame ionization detector, R^2: correlation coefficient of determination, FSC: forward side scatter, SSC: side scattered light, DHA_{pred}: DHA predicted with a non-linear correlation, D_c: cell diameter measured with the photo-optical microscopy probe, DCW: dry cell weight, σ: variability, e: admitted error, 1-α: amplitude of the confidence interval, n: sample size.

Acknowledgements

The work was partially supported by the German Federal Ministry of Food and Agriculture within the innovation program coordinated by the federal office for agriculture and food (project: FENA - fishmeal and –oil feed substitutes for a sustainable aquaculture, project no.: 511-06.01-28-1-73.026-10).

We thank the company Ovizio Imaging Systems NV/SA for the kind support for adjusting the algorithms for the automated algae detection.

Appendix A. Supplementary data

Supplementary data associated with this article can be found, in the online version, at http://dx.doi.org/10.1016/j.procbio.2016.11.003.

4.2. Sterol synthesis and cell size distribution under oscillatory growth conditions in *Saccharomyces cerevisiae* scale-down cultivations

Anna-Maria Marbà-Ardébol, Anika Bockisch, Peter Neubauer, Stefan Junne

Abstract

Physiological responses of yeast to oscillatory environments as they appear in the liquid phase in large−scale bioreactors have been the subject of past studies. So far, however, the impact on the sterol content and intracellular regulation remains to be investigated. Since oxygen is a cofactor in several reaction steps within sterol metabolism, changes in oxygen availability, as occurs in production-scale aerated bioreactors, might have an influence on the regulation and incorporation of free sterols into the cell lipid layer. Therefore, sterol and fatty acid synthesis in two- and three-compartment scale-down *Saccharomyces cerevisiae* cultivation were studied and compared with typical values obtained in homogeneous lab-scale cultivations. While cells were exposed to oscillating substrate and oxygen availability in the scale-down cultivations, growth was reduced and accumulation of carboxylic acids was increased. Sterol synthesis was elevated to ergosterol at the same time. The higher fluxes led to increased concentrations of esterified sterols. The cells thus seem to utilize the increased availability of precursors to fill their sterol reservoirs; however, this seems to be limited in the three-compartment reactor cultivation due to a prolonged exposure to oxygen limitation. Besides, a larger heterogeneity within the single-cell size distribution was observed under oscillatory growth conditions with three-dimensional holographic microscopy. Hence the impact of gradients is also observable at the morphological level. The consideration of such a single-cell-based analysis provides useful information about the homogeneity of responses among the population.

Keywords: oxygen limitation, *S. cerevisiae*, scale-down, single-cell size distribution, squalene, sterols

1. Introduction

Sterols are essential compounds of yeasts. They become strictly sterol auxotrophic under anaerobic conditions (Daum, et al., 1998; Klug and Daum, 2014). The sterol content has an influence on the fluidity and permeability of the cell membrane, and thus on the transport through the membrane. The first intermediate of the sterol pathway, squalene, is a triterpene, which is converted to lanosterol. Squalene itself is synthesized from acetoacetyl-CoA. This synthesis is active under both aerobic and oxygen−limiting conditions. Nevertheless, several further reactions require oxygen in the post-squalene metabolism. It was shown that the production of ergosterol decreased strongly under anaerobic conditions in the continuous absence of oxygen, while squalene accumulated (Jahnke and Klein, 1983), if ergosterol concentrations themselves were low (Garaiova, et al., 2014). Under these conditions, growth is not only reduced but ceases. When such an anaerobic culture is suddenly aerated, growth starts again and squalene is further converted to sterols (Maczek, et al., 2006). In order to maintain sterol homeostasis, cells are able to esterify free sterols. This step does not require any oxygen. Cells are also able to downregulate the sterol biosynthesis or acetylate the sterols in order to secrete excess amounts of them into the media (Ploier, et al., 2014).

A relation between sterol regulation and growth was published earlier (Arnezeder and Hampel, 1990). Interestingly, a recent study proved that the de novo sterol biosynthesis is essential for cell polarization, and therefore for the initiation of growth (Makushok, et al., 2016). Sterols are partially synthesized in the cell wall, transferred to the cell surface and allocated to cell poles. Growth retardation and a loss of cell polarizability were observed when the conversion of squalene to lanosterol was blocked with ketoconazole. If zymosterol synthesis itself was blocked by repression of the ERG24 gene, which encodes a sterol C-14 reductase, cells were not viable unless sterols were added extracellularly (Daum, et al., 1998; Klug and Daum, 2014).

Inhomogeneities of dissolved oxygen and substrate concentrations appear in the liquid phase of large-scale nutrient-limited fed-batch bioprocesses at high cell densities (Neubauer and Junne, 2010). The specific oxygen uptake rate (qO_2) depends on the consumption rate of carbohydrates in aerobic cultivations. Thus, cells cope with oxygen limitation or even depletion close to the feed zone. The high substrate consumption rate leads to a volumetric oxygen demand of the culture that exceeds the oxygen transfer to the liquid phase in this zone. While cells are changing in between these zones due to the turbulent flow, they experience oscillating environmental conditions between high and low substrate and oxygen availability.

In order to investigate the consequences of these heterogeneities on cell physiology, multi-compartment scale-down reactor systems have been applied to mimic such gradients at the lab-scale (Heins, et al., 2015; Neubauer and Junne, 2010; Takors, 2012). Such scale-down reactors are based on

the principle that a certain portion of cells is exposed to oscillating (partially random) fluctuations. These will reproduce the flow conditions encountered at a large-scale, in which the stirred tank reactor simulates the bulk zone, in which oxygen and substrate availability is sufficient.

Previously, scale-down experiments with baker's yeast have been performed and compared to an industrial cultivation of a 215 m^3 scaled bubble column reactor (George, et al., 1998). A similar growth reduction and gassing behaviour in doughs were observed as if the culture was grown at a production scale. Current attempts on scale-down approaches foster the consideration of theoretical computational fluid dynamics studies for the experimental design. Several scenarios were simulated based on the appearance of the Crabtree effect in yeast (Haringa, et al., 2017) so that scalability becomes feasible.

In contrast to previous studies, not only a two-, but also a three-compartment reactor (two-CR and three-CR) was applied as a scale-down system in this study. These reactors consist of one typical stirred tank reactor coupled to one or two plug flow reactors, which were applied to mimic both the feed zone with substrate excess and a zone with strong starvation far away from it (Junne, et al., 2011; Marba-Ardebol, et al., 2016). It has been shown that a three-CR most likely reflects better the situation in a large-scale process (Lemoine, et al., 2015). Bacterial scale-down studies proved that the scale-down set-up has a significant impact on the cellular response. Additionally, big changes are seen if complex media are used rather than mineral salt media (Lemoine, et al., 2016). Thus complex media were used throughout this study in order to match production conditions closely.

The present study aims to investigate the impacts of oscillating substrate and oxygen supply on sterol and fatty acid synthesis in yeast, as it occurs in large-scale fed-batch bioreactor cultivations. Potential reasons for the observable growth reduction are discussed. Since cell morphology in yeast is often coupled to the growth state e.g. (Lencastre Fernandes, et al., 2013), the single-cell size distribution was monitored to investigate the heterogeneity of the population. Various methods have been used to measure the cell size in yeast (Turner, et al., 2012). In this study, size based population heterogeneity was quantified with three-dimensional digital holographic microscopy (DHM).

2. Materials and Methods

2.1. Yeast strain

The yeast strain *Saccharomyces cerevisiae* AH22 (MATa leu2-3 leu2-12 its4-519 can1) (Maczek, et al., 2006) was used throughout all cultivations.

2.2. Media and cultivation conditions

Cells were grown in buffered YPD medium, which consists of yeast extract, peptone and dextrose, as described previously (Maczek et al., 2006). A glucose concentration of 2% (w/w) was applied in pre-cultures and batch phases of all bioreactor cultivations. Pre−cultures were grown aerobically in Ultra Yield™ flasks (Thomson Instrument Co., USA) at 25°C and 250 rpm. 1% (v/v) of antifoam 204 (Sigma, Germany) was added prior to cultivation.

5 mL of antifoam 204 (Sigma, Germany) was also added to each bioreactor cultivation. The temperature was set to 27 °C, the aeration rate to 0.5 vvm and the stirrer speed to 500 rpm. After a lag-phase of approx. 4 h, the aeration rate was increased to 0.7 vvm and the stirrer speed to 650 rpm. In order to ensure aerobic conditions in the stirred tank reactor (STR) compartment of the scale-down bioreactor or in the single-CR, the stirrer speed was changed to 800 rpm when an OD_{600} of 30 was reached. Bioreactor cultivations were inoculated with 2% v/v of pre-culture, so that an initial OD_{600} of 0.2 was obtained. The process started as batch mode in the STR compartment or the single-CR until an OD_{600} of 24 was reached (after ~20 h), followed by a substrate-limited fed-batch mode. The pH-value was adjusted to pH=5.5 and controlled automatically by the addition of 30% (v/v) NaOH during the fed-batch phase. Prior to feed start, plug flow reactor (PFR) modules were connected to the STR in case of scale-down cultivations. The glucose feed (YPD medium with a content of 40% (w/w) of glucose) was added exponentially at a specific growth rate (μ) of 0.12 h^{-1} according to eq. (1).

$$F\,(t) = 0.00318\ V_F\ e^{0.12t} \qquad (1)$$

where V_F is the working volume and t the fed−batch cultivation time.

The feed was added to the top gas phase of the STR for the single-CR cultivation or at the bottom of one PFR module at scale-down cultivations, denoted as PFR-F in the following. The PFR module without feed addition is denoted as PFR-S. Bioreactor cultivations were performed in biological duplicates. Unless otherwise stated, all data were obtained from samples taken from the STR compartment.

2.3. Cultivation systems

A Techfors-S stirred tank bioreactor (Infors, Switzerland) equipped with three Rushton turbines was used for the single−compartment reactor (single-CR) cultivations. The initial liquid volume was 10 litres

and decreased merely during the feed phase, while sampling for sterol analysis required more volume than that gained during feed addition. The STR was connected to one or two PFR modules at the scale–down cultivations. The PFR units consisted of four static mixer modules and five evenly distributed sampling ports. The liquid volume of each PFR module was 1.8 litres (including the transfer from the STR to the PFR (0.15 litres) and backwards (0.45 litres)). A detailed description of the two–CR system and residence times at a current flow rate of 1.78 ml min^{-1} has been published previously (Junne, et al., 2011). The setup of the three-CR has also been described (Lemoine, et al., 2015; Marba-Ardebol, et al., 2016). Briefly, in the two-CR system two parts of the spatial segregation of the large–scale bioreactors are represented: (i) a bulk zone, in which the substrate concentration is limited, but not the dissolved oxygen (STR compartment); and (ii) a zone of high substrate availability but oxygen limitation (PFR–F). In a second PFR without feed addition (PFR–S), a third zone is simulated, in which the availability of both, substrate and oxygen is very low. These gradients are represented schematically in Figure 1.

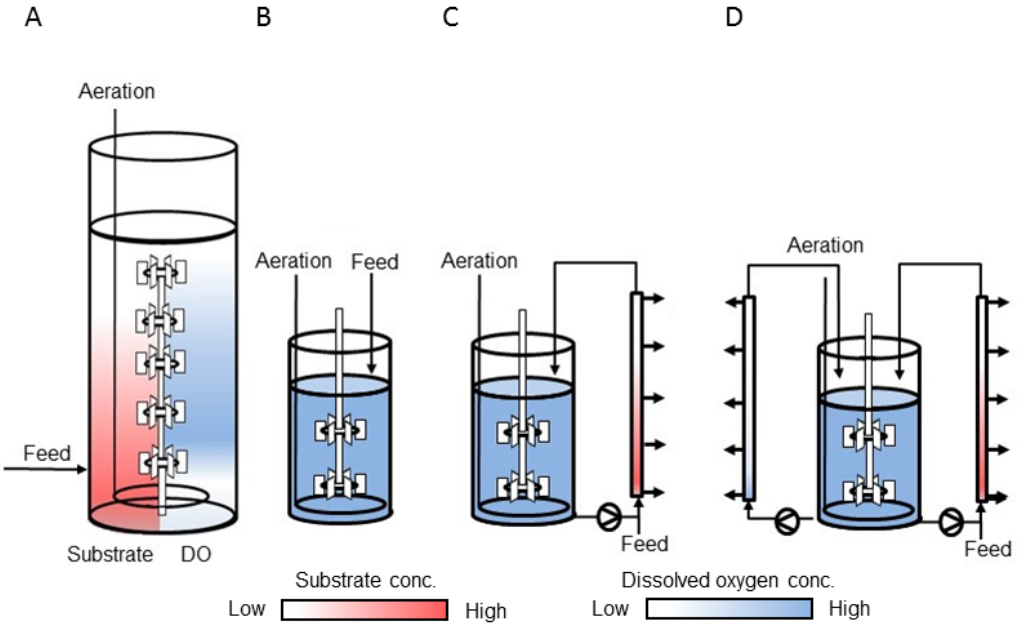

Figure 1. Distribution of substrate and dissolved oxygen concentrations as expected in an industrial scale nutrient-limited fed-batch cultivation, when the feed is added at the bottom part of the liquid phase. Next to it, the different reactors set-ups used in this study with the gradients that each one simulate: A (single-CR), B (two-CR) and C (three-CR).

2.4. Analysis

2.4.1. Cell growth and metabolites determination

Cell growth was quantified throughout the cultivation by measurement of the optical density at a wavelength of 600 nm with a spectrophotometer (Ultraspec 3000, GE Healthcare, CT, USA). For the analysis of the dry cell weight, 2 mL of culture were centrifuged for 10 min at 4 °C and 21,500 x g in previously weighted 2 mL Eppendorf tubes, then washed with 2 mL of 0.9 g L^{-1} NaCl solution and centrifuged again under the same conditions. Then the Eppendorf tubes were stored in a drying oven (75 °C) for at least 48 h and weighted.

Samples for extracellular metabolite determination were filtered through a membrane filter with a pore size of 0.8 µm (Carl Roth, Karlsruhe, Germany) directly at the sampling port of the STR bioreactor. The supernatant was transferred to 1.5 mL Eppendorf tubes and immediately stored at -80 °C.

Organic acids were quantified with an Agilent 1200 system, which was equipped with a refractive index detector and a HyperRez XP Carbohydrate H^+ column (300 × 7.7 mm, 8 µm; Fisher Scientific, Schwerte, Germany). A 5 mM H_2SO_4 solution as eluent was applied at a flow rate of 0.5 mL min^{-1} and a column temperature of 15 °C.

2.4.2. Lipid analysis

Sterol analysis was performed as it was described previously (Maczek, et al., 2006). All samples contained 70 mg of dry biomass. Cell membranes were disrupted with thermal treatment followed by saponification after base as well as methanol and pyrogallol addition for quantification of the total sterol content. If the non−esterified fraction of sterols was determined, cells were broken through mechanical treatment with glass beads. The content of esterified sterols was determined by the difference of the content of free (non-esterified sterols) and total sterols. Quantification of sterols was conducted by gas chromatography with flame ionization detector (GC-FID). Samples were analysed with a CP-Sil 5 CB capillary column with dimensions 25 m × 0.25 mm and a film thickness of 0.12 µm (Varian, Germany). Briefly, conditions were as follows: 150 °C was maintained for 2 min before heating at a rate of 15 °C min^{-1} to a temperature of 250 °C. After 37 min, the column was heated to a final temperature of 290 °C at a rate of 5 °C min^{-1}, which was maintained for 7 min. The injector and detector temperatures were set to 290 °C and 300 °C, respectively. Samples were analysed in splitless mode using an autosampler AOC-20i. The injection volume was 0.5 µl. Cholesterol was used as internal standard (Sigma, Germany). The sterol composition was determined on the basis of retention times of known sterol standards: cholesterol, ergosterol, lanosterol, squalene (Sigma, Germany), and zymosterol (Avanti Polar Lipids, AL), respectively. Quantification of sterols was performed by the integration of peak areas with the software package GC solution, version 2.2 (Shimadzu, Germany).

Fatty acid concentration measurements were conducted in a GC-FID and analysed as published previously for docosahexaenoic acid quantification (Hillig, et al., 2014a). Samples were analysed with the same capillary column as for sterols. Conditions were as follows: 150 °C was maintained for 2 min before heating at a rate of 15 °C min^{-1} to a temperature of 250 °C. After 37 min, the column was heated to a final temperature of 280 °C at a rate of 5 °C min^{-1}, which was maintained for 7 min. The injector and detector temperatures were set to 290 °C and 300 °C, respectively. The injection volume was 0.3 µl and was performed in splitless mode. Nonadecanoic acid (Sigma, Germany) was used as internal standard. The fatty acid composition was determined on the basis of retention times of known mixed fatty acid methyl ester (FAME) standard solutions (GLC-10, GLC-50 and GLC-100, Sigma, Germany). Quantification was conducted based on peak area integration with the software package GC solution, version 2.2 (Shimadzu, Germany).

2.4.3.Single-cell size distribution

The three-dimensional digital holographic microscope oLine-OT40GA (Ovizio, Belgium) was used to monitor the single-cell size distribution. Samples were diluted to an OD_{600} of 2 and measured on a microscope slide. Several images were acquired in order to obtain at least 200 cells at each time point (Marbà-Ardébol, et al., 2017). This number is representative if the maximal deviance of the cell size measurements (σ), the desired accuracy (1-α) and the admitted error (e) are considered. The average technical error was 0.05 µm (0.02 µm in the best case and 0.12 µm in the worst case), as obtained from triplicate measurements of the same sample with 200 cells. The desired accuracy was chosen as 0.005 µm and the admitted error should not exceed 5% ($z_{1-\alpha/2}$ = 1.96). Then, the minimum amount of cells that needed to be analysed according to eq. (2) is 123:

$$n = \left(\frac{\sigma\, z_{1-\alpha/2}}{e}\right)^2 \qquad (2)$$

However, since the media and the change of optical features can affect the accuracy, a higher number of cells was monitored.

The variance of the single-cell size distribution (σ^2) was calculated according to eq. (3) in order to evaluate quantitatively the population heterogeneity:

$$\sigma^2 = \sum d^2\ p(d) - \left(\sum d\ p(d)\right)^2 \qquad (3)$$

where *d* is the cell diameter and p(d) is the frequency of the cell diameter in a distribution.

Several settings such as size boundaries and the applied algorithms were adjusted for automated yeast cell detection. Parameters of this detection are summarized in Table 1.

Table 1. Parameters for the detection of yeast cells in the OsOne software version 4.3 (Ovizio).

Parameter	OsOne
Background	2.67609
Median cell size (d_{50}) [µm]	9.00363
Background detection algorithm	Phase variance
Cell detection algorithm	Local maximum
Apply refocus	yes
Detect invalid areas	yes
Cell minimum size [µm]	50
Cell maximum size [µm]	10
Remove image defects	9
Split neighbor cells	6
Invalid area- sensitivity	4

2.5. Further determination of process parameters

The specific substrate uptake rate (q_s) was calculated within a time interval as described in eq. (4). Glucose was measured with an enzymatic assay (r-biopharm, Germany) according to the manufacturer's instructions:

$$q_s = \frac{\left[\frac{\Delta c_S}{\Delta t} + \frac{F}{V_l}\left(c_{S_0} - c_{S_m}\right)\right]}{X} \qquad (4)$$

where c_S is the difference in substrate concentration in a time interval, t is the time interval, F is the feed rate, c_{S0} is the feed substrate concentration, c_{Sm} is the average substrate concentration in a time interval and X is the average of the biomass concentration in a time interval.

The specific oxygen uptake rate (q_{O_2}) and the specific carbon dioxide production rate (q_{CO_2}) were calculated based on equations (5) and (6). The volumetric parameters (Q_{O_2} and Q_{CO_2}) were divided by the cell dry weight concentration to obtain the specific ones (q_{O_2} and q_{CO_2}). The respiratory coefficient (RQ) was determined by the division of eq. (6) through eq. (5):

$$Q_{O_2} = \frac{V_G^{\propto}}{V_F 22.4}\left[Y_{O_2}^{\propto} - \frac{1 - Y_{O_2}^{\propto} - Y_{CO_2}^{\propto}}{1 - Y_{O_2}^{\omega} - Y_{CO_2}^{\omega}}\, Y_{O_2}^{\omega}\right] \qquad (5)$$

$$Q_{CO_2} = \frac{V_G^{\propto}}{V_F 22.4}\left[Y_{CO_2}^{\omega}\frac{1 - Y_{O_2}^{\propto} - Y_{CO_2}^{\propto}}{1 - Y_{O_2}^{\omega} - Y_{CO_2}^{\omega}} - Y_{CO_2}^{\alpha}\right] \qquad (6)$$

where $V^{\propto}_G$ is the volumetric gas flow rate, V_F is working volume, $Y^{\propto}_{O2}$ is the molar fraction of oxygen at the entrance of the gas phase, $Y^{\propto}_{CO2}$ is the molar fraction of carbon dioxide at the entrance of the gas phase. Y^{ω}_{CO2} is the molar fraction of oxygen in the exhaust gas and Y^{ω}_{CO2} is the molar fraction of carbon dioxide in the exhaust gas.

3. Results and discussion

3.1. Growth and main carbon metabolism

Two scale-down reactor systems have been applied to mimic different substrate and oxygen gradient scenarios. Results were compared to homogenous conditions in the single-CR system. The dissolved oxygen tension (DO) remained above 40% for all cultivations in the STR compartment. Oxygen limitation was observed in the PFR modules of scale-down cultivations 3 h after the feed started at the PFR-F in the two-CR and three-CR, and 4 h after the feed started at the PFR-S in the three-CR (Fig. 2A and B). The glucose gradients created in the PFR-F were in a range from 1 g L^{-1} at the first port of the feeding module to 0.6 g L^{-1} at the last port (fifth port), whereas gradients were in a lower range from 0.2 to 0.1 g L^{-1} in the PFR-S (Fig. 2C). A direct influence of oscillatory oxygen availability was observed at growth, which was reduced after oxygen availability became limited in the PFR modules (Fig. 3A). A reduction of growth was also observed in a *S. cerevisiae* cultivation in a two-STR system, which was operated in continuous mode at a dilution rate of 0.2 h^{-1}, and in which the time of exposure to oxygen limitation was increased steadily (Sweere, et al., 1988a).

The substrate uptake rate (q_s) was in the same range as already observed for *S. cerevisiae* cultures under substrate-limited steady-state conditions at a growth rate of μ= 0.1 h^{-1} (Van Urk, et al., 1989). Oxygen limitation in the PFR-F module occurred at the same time at which q_s rather increased (Fig. 3B). The increment of q_s is probably related to the well-known Pasteur effect, as described, for example, in (Sarris and Papanikolaou, 2016; Sonnleitner and Kappeli, 1986). The increase in q_s is similar to what was observed in other scale-down studies conducted with *E. coli* (Neubauer, et al., 1995; Sandoval-Basurto, et al., 2005). In the latter study, q_s increased with the residence time of cells in a non-aerated PFR until cells were not able to cope with the increasing gradients. *S. cerevisiae* cells seem to be robust against oxygen limitation, since their uptake capacity was even undisturbed in the three-CR system, in which the time of exposure to oxygen limitation was doubled (in comparison with the two-CR).

The oscillating environment supported the synthesis of lactate and other carboxylic acids (Fig. 4). A reassimilation of these intermediates in the stirred tank compartment was not observed. The accumulation of these metabolites follows the same tendency in both scale-down systems, except that acetate accumulation started 2 h earlier in the three-CR.

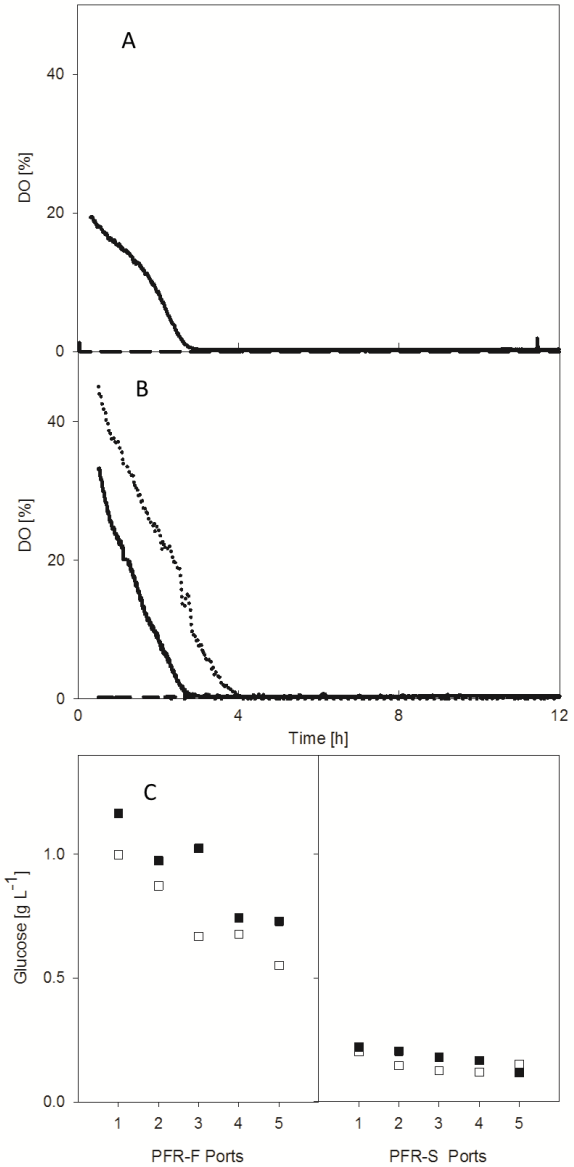

Figure 2. (Left) DO concentrations in the PFR modules of the two-CR and three-CR during fed-batch cultivations. (A) DO concentration measured at port 1 (straight line) and port 5(dashed line) of the PFR-F of the two-CR, which correspond to residence time 26 s and 62 s, (B) DO concentration measured at port 1(straight line) and port 5 (dashed line) of the PFR-F and port 1 (dotted line) and port 5 (dashed line) of the PFR-S of the three-CR, corresponding to the same residence time as the PFR ports of the two-CR. (C) Glucose gradients along the PFR-F and PFR-S at two time points: 10 h (□) and 12 h after feed started (■) of the three-CR. Samples where measured along the PFR in 5 points corresponding to the residence time: τ_{port1}= 26 s, τ_{port2}=35 s, τ_{port3}=45 s, τ_{port4}=56 s, τ_{port5}=62 s

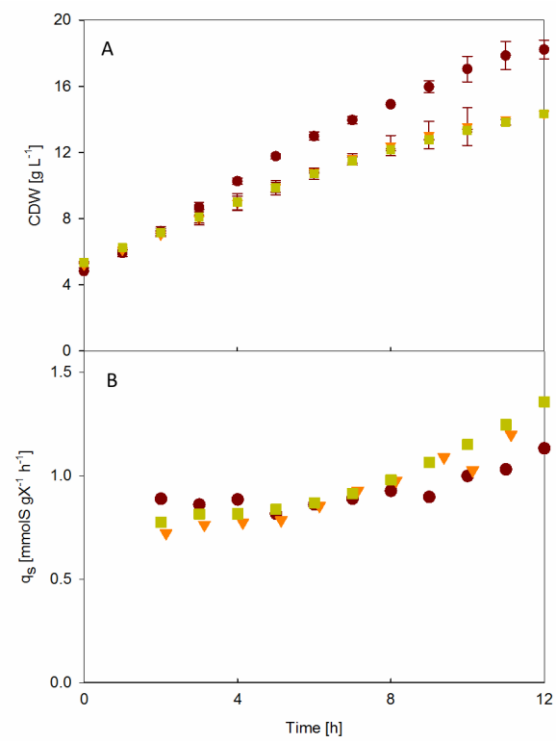

Figure 3. (Right) (A) Dry cell weight concentration and (B) specific substrate uptake rate of the single-CR (●), two-CR (▼) and three-CR ■) fed-batch cultivations.

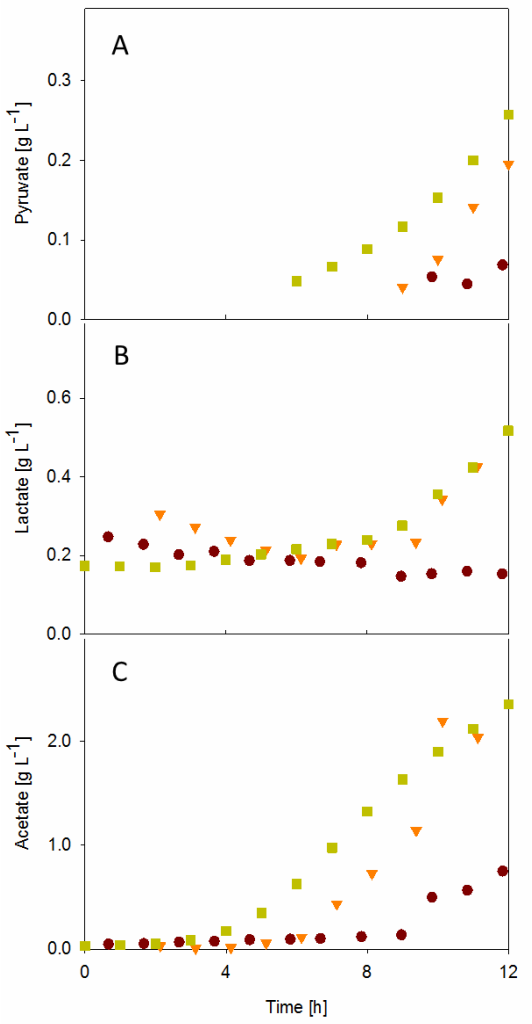

No accumulation of TCA intermediates or of ethanol was observed in any of the cultivations. The oxygen consumption and the carbon dioxide production rates (q_{O2} and q_{CO2}, respectively) remained more or less constant during the first 5 h of the fed-batch phase in the scale-down cultivations. RQ started to increase after 6 h due to the fermentative co-metabolism under oxygen limitation (Fig. 5). The increase in RQ is most likely due to depletion of some amino acid sources in the media in the single-CR cultivation after 9 h. A depletion of valine, leucine, isoleucine, phenylalanine and histidine was detected by high-performance liquid chromatography at this time (data not shown).

Figure 4. Extracellular concentrations of (A) pyruvate, (B) lactate and (C) acetate of the single-CR ( ), two-CR ( ) and three-CR ( ) fed-batch cultivations.

3.2. Sterol synthesis

In contrast to expectations, sterol formation was not influenced negatively but positively by oscillating conditions. While almost no difference was seen in the free sterol concentrations (see Supporting information), the esterified form of the end product ergosterol was increased by 75% (Fig. 6F). The accumulation of esterified intermediates initiated a higher flux through the sterol pathway under scale-down cultivation conditions. Only the squalene accumulation indicated potential limitations to achieve higher fluxes towards ergosterol, if more oxygen would have been available. An increase in the portion of the esterified fraction of sterols was observed. The conversion of free sterols to the corresponding esterified forms does not require any oxygen, and thus will not be affected by oscillatory oxygen availability anyway.

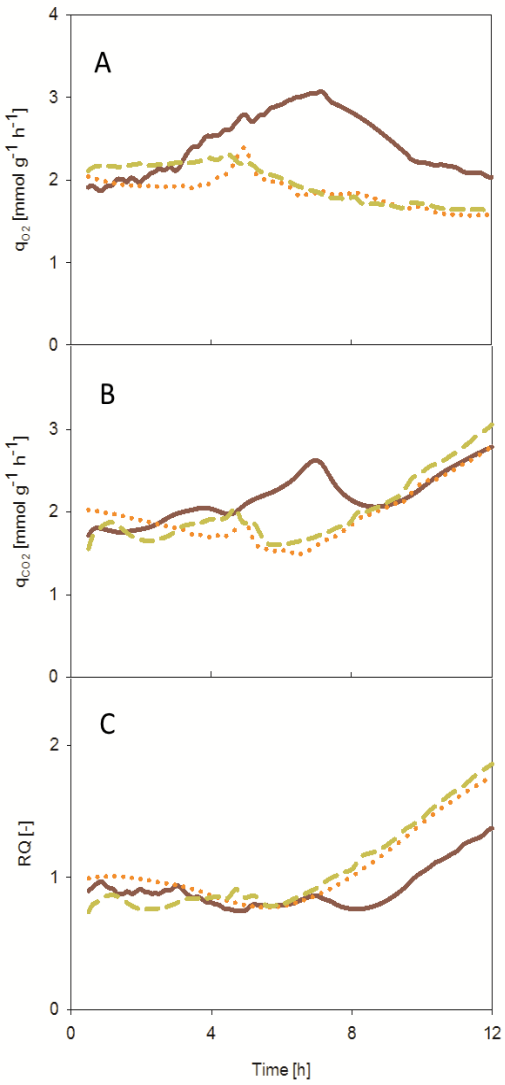

Zymosterol is the first intermediate within the sterol pathway that maintains growth rates of yeasts and accumulates after a sudden shift to aeration (Maczek, et al., 2006). The esterified form of zymosterol was doubled in the two-CR cultivation in comparison to the control in the present study. The concentration of the zymosterol ester was still increased by 50% in the three-CR cultivation in comparison to the control (Fig. 6C). Zymosterol already enables the cells to cover most of the functionality they would have if sufficient amounts of ergosterol were present, as other studies described (Klug and Daum, 2014). Nevertheless, from 12 mol of oxygen that are required until ergosterol is formed, the major portion of oxygen (10 mol) is required to form zymosterol (the exact requirement for oxygen might be higher as several conversions have not yet been fully examined).

Figure 5. q_{O2} (a), q_{CO2} (b) and RQ(c) in THE STR module of the reference and scale-down cultivations: single-CR ( ), two-CR ( ) and three-CR ( ).

Although a similar accumulation of ergosterol ester was seen in scale-down cultivations after 10 h, accumulation started earlier in the two-CR (Fig. 6F). Probably, the higher oxygen availability promoted a higher carbon flux through the post-squalene pathway in comparison to the three-CR, in which a 10–fold accumulation of squalene was observable in comparison to the control. While ergosterol ester is the first one to be accumulated in the two-CR, zymosterol ester is the first one in the three-CR.

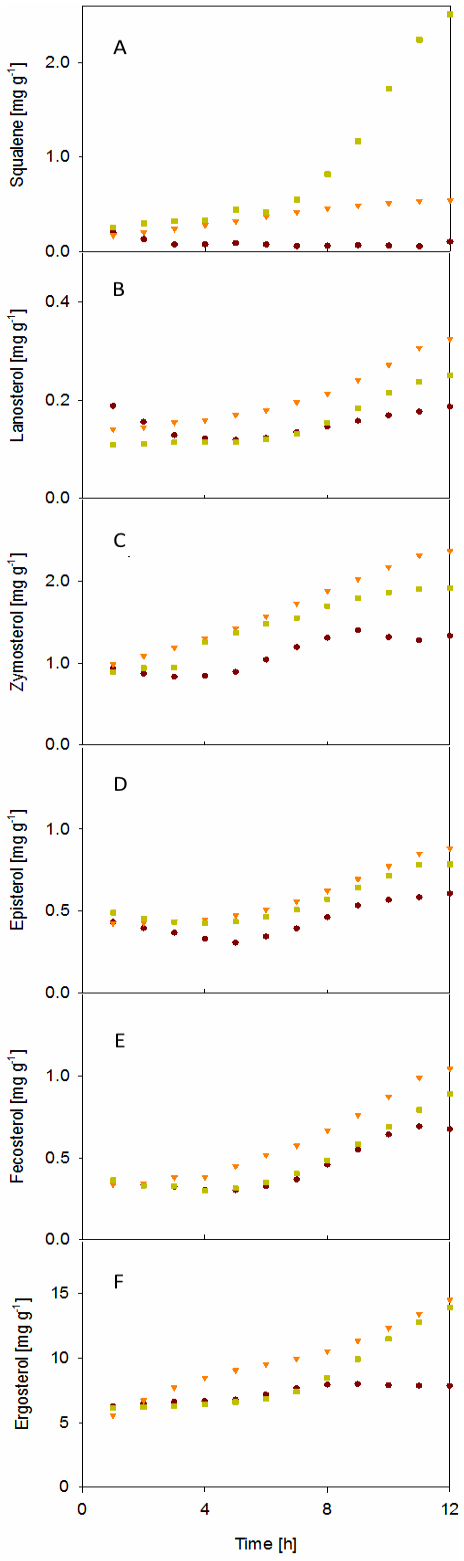

Figure 6. Course of (A) Squalene and esterified sterols concentrations: (B) Lanosterol, (C) Zymosterol, (D) Episterol, (E) Fecosterol, (F) Ergosterol of the single-CR ( ), two-CR (▼) and three-CR (■) fed-batch cultivations.

The concentration of enzymes that catalyse esterification, Are1p and Are2p, are underlying mechanisms which regulate the sterol content itself. Arthington-Skaggs et al. (1996) described that Are1p is present at higher concentration if sterol pre-cursors accumulated in the cell. A reduced ergosterol concentration led to a higher concentration of both Are1p and Are2p. The two enzymes are not influenced by the ergosterol concentration itself (no product inhibition). Moreover, studies have shown that an enhanced capacity to esterify sterols, in this case by the overexpression of ARE2, which is localized directly at sterol-rich microdomains (Gulati, et al., 2015), can enrich the sterol content in yeast (Polakowski, et al., 1999). In the study of (Rintala, et al., 2009), the concentration of enzymes of ergosterol biosynthesis including Are1p, was high anaerobic conditions in comparison to various degrees of oxygen availability. Although, in the case of oxygen depletion, yeast does not benefit from this upregulation, it is certainly an advantage in situations in which small amounts of oxygen are available. It was observed that pulses of dissolved oxygen increased yeast survival under an otherwise anaerobic environment (Rosenfeld, et al., 2003).

The authors proposed that this accelerated de novo sterol synthesis increased the fermentation yield. Thus it might be that the oscillating conditions trigger this response. In combination with precursor accumulation, higher fluxes occur whenever sufficient oxygen as cofactor is available.

Sterols are esterified with fatty acids. Unsaturated fatty acids, like C16:1 and C18:1, represent about 80% of the fatty acids under homogeneous cultivation conditions (Figure 7C, D). This is in good accordance with previous studies (Tehlivets, et al., 2007). They serve predominantly as precursors in sterol ester formation (Athenstaedt, et al., 1999), while the saturated fatty acids are usually used in smaller amounts (Mullner and Daum, 2004). Nevertheless, under oscillating conditions, the percentage of unsaturated fatty acids went down to 74% in the two−CR and to 70% in the three−CR in comparison to the control. This is mainly due to an increase in saturated fatty acids (Figure 7A, B). It is unlikely that this change has an influence on the esterification of sterols.

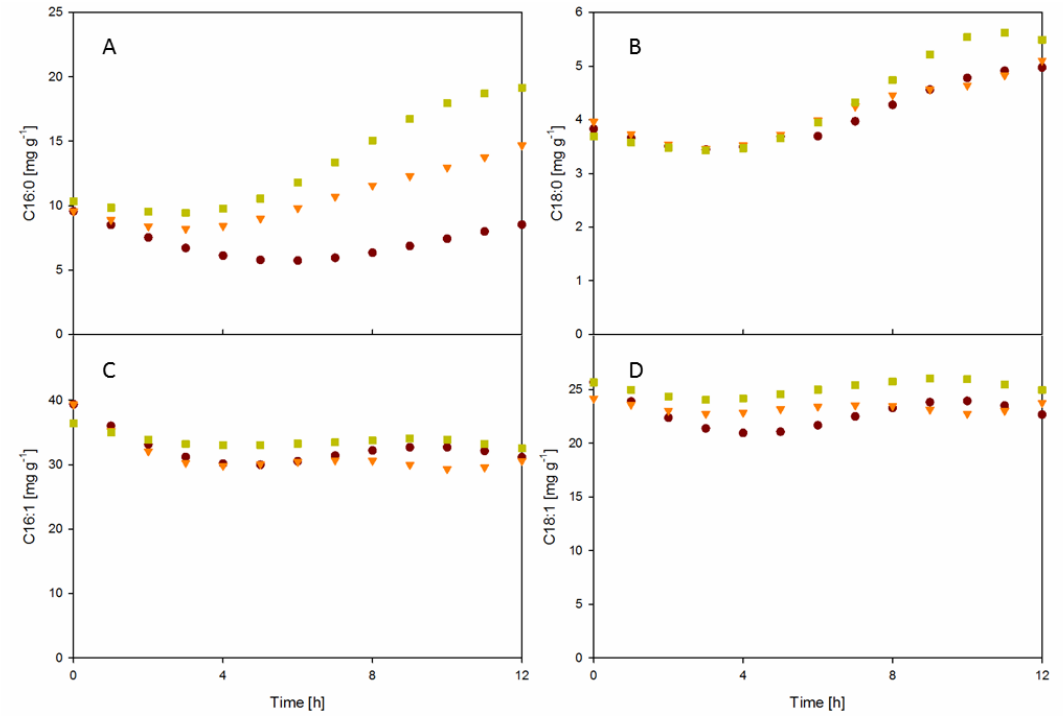

Figure 7. Course of the fatty acids concentrations: (A) C16:00 (palmitic acid), (B) C18:00 (stearic acid), (C) C16:1 (palmitoleic acid), (D) C18:1 (*oleic acid)* of the single-CR ( ), two-CR ( ) and three-CR ( ) fed-batch cultivations.

Fermentable sugars are converted to pyruvate in the mitochondrion and by the cytosolic pyruvate-acetaldehyde-acetate pathway (Beopoulos, et al., 2011); thus a bottleneck in the further synthesis towards TCA leads to acetyl−CoA accumulation in parallel with elevated pyruvate and acetate concentrations inside the cell. Since acetyl−CoA is a precursor of the long−chain fatty acid synthesis itself, an accumulation of acetyl−CoA increases their synthesis.

3.3. Single-cell size distribution

It was investigated whether oscillating cultivations conditions have an impact on the cell population homogeneity. Therefore, the cell size was determined with DHM (Fig. 8 and Table 2). Results showed that growth and the single-cell size distribution remained similar within 3 h after feed start among all experiments ($\mu = 0.16 \pm 0.032\ h^{-1}$). During this time cells were not yet exposed to oxygen limitation in the PFR compartments. Subsequently, cells were exposed to strong oxygen limitation (no dissolved O_2 detectable in the liquid phase along the PFR compartments). Growth rate was higher under homogeneous conditions ($\mu = 0.15 \pm 0.041\ h^{-1}$) in comparison to scale-down conditions ($\mu=0.10 \pm 0.017\ h^{-1}$). Nevertheless, no relevant changes were seen in the cell size distribution. Hence there is only a weak impact of cell growth on the population heterogeneity, if any. In the following, cell growth became similar after 7 h of feeding among all cultivations ($\mu = 0.05 \pm 0.005\ h^{-1}$). Nevertheless, heterogeneity developed differently in the reactors. It was strongly increased in the three-CR cultivations, which was observable at the increment of the variance between 7 and 10 h (Table 2); however, the mean value of the cell diameter remained unchanged. Only a maximum change of 0.4 µm among all cultivations conditions was determined. The change within the same cultivation did not exceed 0.1 µm.

Table 2. Variance of the single-cell size frequency distribution for the time points showed at Figure 8.

Time [h]	Variance [µm²]		
	single-CR	two-CR	three-CR
3	0.93	1.12	0.89
7	1.26	1.11	1.09
10	0.97	1.05	1.87
12	1.03	1.13	1.70

The time at which a noticeable increase in population heterogeneity occurred was the same time at which an accumulation of several metabolites, including several sterols, was detected in the three-CR. Population heterogeneity may be due to unsynchronized cell cycle phases (Müller, et al., 2010; Turner, et al., 2012). Hence the impact of oscillating conditions is likely uneven, probably based on the individual cell age. A prolonged maturation state will also lead to a higher proportion of large cells. A population with larger cells was observed in both scale-down cultivations in comparison to the control. Pereira and co−authors described qualitatively an increase in cell size in high−gravity cultivations when sterols were accumulated (between a two−and fivefold increase during cultivation). The authors proposed that the industrial strain is able to channel a higher fraction of the limited amount of available oxygen at the beginning of the fermentation for the synthesis of essential lipids (Pereira, et al., 2011). Other studies showed a relation between cell heterogeneity and growth status. In the study of (Lencastre Fernandes, et al., 2013), flow cytometry was used to measure the total protein content and

DNA during batch cultivation with *S. cerevisiae*. During growth on glucose (μ = 0.41 ± 0.001 h^{-1}), a unimodal distribution was observed, while a bimodal distribution was obtained after a diauxic shift with ethanol as carbon source (μ = 0.10 ± 0.02 h^{-1}).

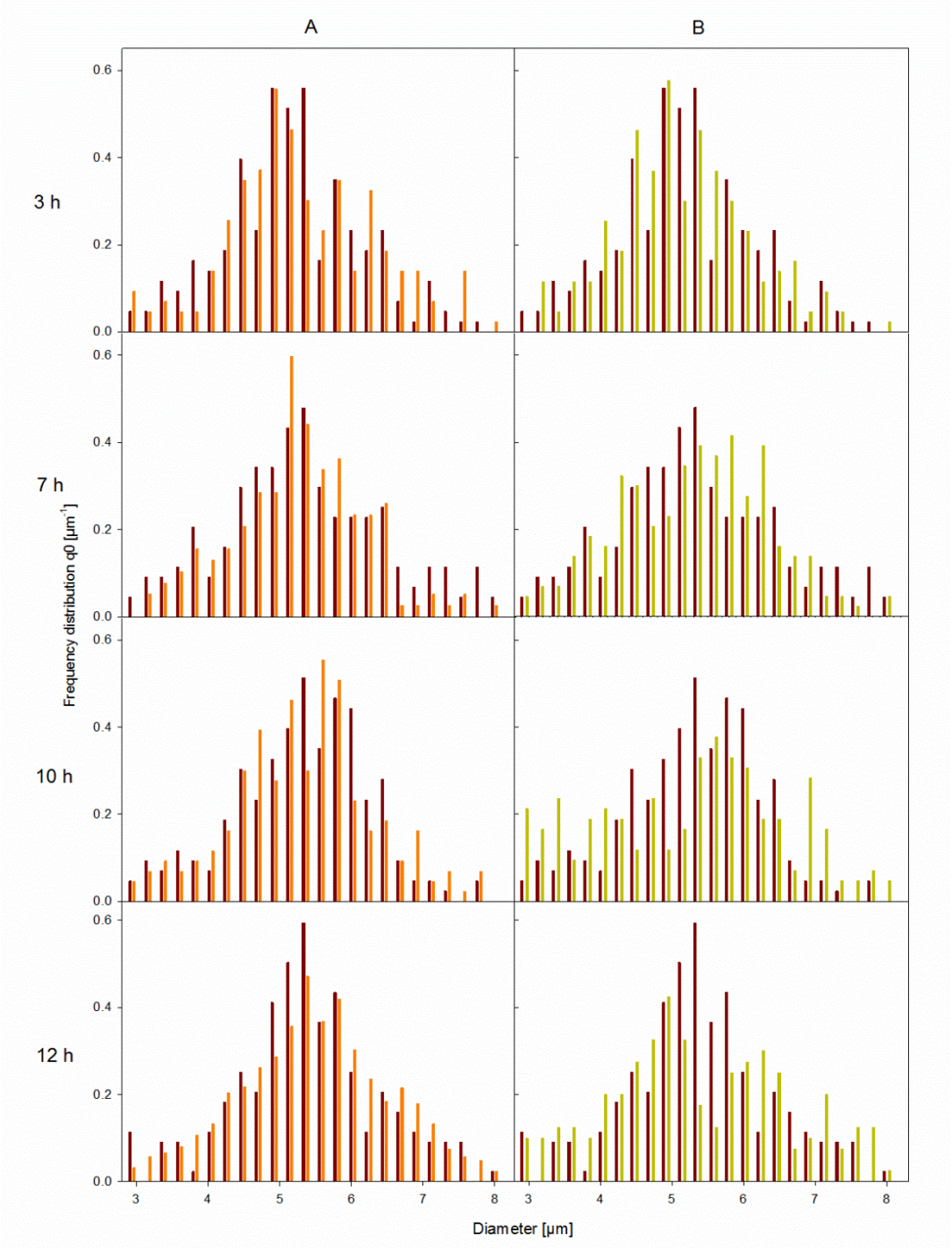

Figure 8. Single-cell frequency distribution as measured with the DHM for the single-CR (■), two-CR (■) and three-CR (■) cultivations, for the times 3 hours, 7 hours, 10 hours and 12 of the fed-batch cultivation. Column A shows single-CR and two-CR together, meanwhile column B shows single-CR and three-CR together.

Another flow cytometry study was performed in order to gain information about the population heterogeneity in a scale−down reactor set−up of two connected stirred tank reactors in a continuous cultivation mode. One reactor represented conditions existing near the feed addition on a large-scale, while the other reactor represented conditions in the bulk of the liquid phase. When the culture was exposed to a low dilution rate of μ = 0.05 h^{-1} and a circulation rate of 0.1 litre h^{-1}, a high degree of homogeneity was achieved in comparison to a dilution rate of 0.2 h^{-1} and a circulation rate of 0.3 litre h^{-1}. Hence a faster exchange between compartments at higher growth supported cell heterogeneity (Heins, et al., 2015).

4. Conclusions

An oscillating oxygen availability, as present in industrial-scale nutrient-limited fed-batch cultivations, has in contrast to continuous oxygen depletion in anaerobic fermentations, no negative influence on sterol availability. It becomes obvious that the mechanism used to maintain sterol homeostasis was raising sterol esterification in all scale−down cultivations. Specific esterified sterol concentrations kept increasing throughout the observation period. A higher degree of heterogeneity during the scale−down experiments was observable with analyses of the single-cell size distribution; however, it was not directly related to growth reduction but rather to the presence of a zone of strong substrate limitation. Deficiencies that might occur in cells led to larger cell particles, likely due to disturbed maturation. In order to investigate this further, *in situ* single-cell-based analysis methods will be applied in future experiments.

The described approach is able to reflect large-scale effects and provides insight into the response within the sterol metabolism under oscillatory conditions. Although yeast is robust enough to maintain free sterol levels under oscillatory conditions, cell growth changed severely. The detailed regulation mechanisms behind this phenomenon remain to be investigated. Results of this study are significant for processes, in which the product is based on sterol precursors or affects sterol synthesis, as for applications in the food and pharmaceutical industry (Du, et al., 2016; Garaiova, et al., 2014).

SUPPORTING INFORMATION

Additional Supporting Information may be found online in the supporting information tab for this article.

.

4.3. Real-time monitoring of the budding index in *Saccharomyces cerevisiae* batch cultivations with *in situ* microscopy

Anna-Maria Marbà-Ardébol, Jörn Emmerich, Michael Muthig, Peter Neubauer, Stefan Junne

Abstract

Background

The morphology of yeast cells changes during budding, depending on the growth rate and cultivation conditions. A photo-optical microscope was adapted and used to observe such morphological changes of individual cells directly in the cell suspension. In order to obtain statistically representative samples of the population without the influence of sampling, *in situ* microscopy (ISM) was applied in the different phases of a *Saccharomyces cerevisiae* batch cultivation. The real-time measurement was performed by coupling a photo-optical probe to an automated image analysis based on a neural network approach.

Results

Automatic cell recognition and classification of budding and non-budding cells was conducted successfully. Deviations between automated and manual counting were considerably low. A differentiation of growth activity across all process stages of a batch cultivation in complex media became feasible. An increased homogeneity among the population during the growth phase was well observable. At growth retardation, the portion of smaller cells increased due to a reduced bud formation. The maturation state of the cells was monitored by determining the budding index as a ratio between the number of cells, which were detected with buds and the total number of cells. A linear correlation between the budding index as monitored with ISM and the growth rate was found.

Conclusion

It is shown that ISM is a meaningful analytical tool, as the budding index can provide valuable information about the growth activity of a yeast cell, e.g. in seed breeding or during any other cultivation process. The determination of the single-cell size and shape distributions provided information on the morphological heterogeneity among the populations. The ability to track changes in cell morphology directly *on line* enables new perspectives for monitoring and control, both in process development and on a production scale.

Key words: *in situ* microscopy, *Saccharomyces cerevisiae*, image detection, budding index, monitoring, cell size, morphology, growth activity.

1. *Introduction*

The morphology of single cells is traditionally measured with microscopy. Due to a certain relationship between form and function, the growth state of cells, and even the production performance can be investigated on the basis of cell size and other morphological features. As such features are determined *off line* or *at lin*e, they cannot be measured in real-time for the purpose of process monitoring.

Among the mostly applied methods to determine the growth activity is plating on solid media followed by incubation for several hours up to several days, or cell staining (Davey, 2011). Microscopy is usually not connected to automated sampling, the achievement of a sufficient number of cells is time-consuming. Consequently, neither a representative sample is obtained, since only a few cells are counted at certain specific time points, nor the heterogeneity of the cell population is considered. If conventional microscopy is coupled to a sampling tube and flow cell, the sample is either affected by the conditions in the sample tube or the device has to be located very close to the reactor. This is often not applicable in daily laboratory practice.

Among automated methods for the characterization of a yeast population, flow cytometry (FCM) or cell counting is often applied. The morphological heterogeneity in a population can be measured as well with these methods. Moreover, FCM can provide further information beyond morphological features at the same time, e.g. total protein and DNA content measurements (Lencastre Fernandes, et al., 2013). FCM was successfully applied to brewing yeast for the determination of the physiological state during propagation (Novak, et al., 2007), and for the quantification of the vitality of cells before fermentation (Lodolo and Cantrell, 2007). Partial least squares regression models were created using data from fluorescent propidium iodide staining microscopy and Coulter counter cell size distributions when cells were exposed to different stresses (temperature shift, acetate or furfural addition) (Tibayrenc, et al., 2010). Such methods are usually used for quality assessment, but have not become widely applied tools for process monitoring.

Other authors have used imaging microscopy (Coelho, et al., 2004; Tibayrenc, et al., 2010) or image cytometry of shake flask cultures (Laverty, et al., 2013; Saldi, et al., 2014) for assessing the morphology of yeast cells. The acquisition of the images is conducted *off line*, but the particle recognition is usually automated. The cells are assumed to be elliptical, then the equivalent major and minor axes are determined. Further parameters such as cell size or volume are derived from this information. Image cytometry is a combination of image microscopy and the observation of light scattering data from cells that have been stained in order to directly assess viability. These methods are less time-consuming and avoid some of the typical errors of completely manual procedures, but certainly not all (Thomson, et al., 2015). Sampling (automatic or manual) and staining is still required, when fluorescent markers cannot be applied, e.g. whenever targeted genetically modification is not possible.

If the morphology can be correlated with certain features of a culture, the single-cell size distribution can be used to investigate these without any further cell treatment. For example, morphological heterogeneity is affected by the age of cells and the status of the cell cycle (Müller, et al., 2010). Due to asymmetric division (Turner, et al., 2012), budding of yeast cells can increase the morphological heterogeneity of a population. The usual variation of the composition and quality of complex media compounds (Kirdar, et al., 2010) alters growth activity and population heterogeneity from batch to batch as well (Kasprow, et al., 1998; Van Nierop, et al., 2006). Cultivation conditions influence this heterogeneity, since individual cells can react differently to them, e.g. at substrate limitation or during the accumulation of secondary metabolites. Single-cell monitoring, which generates statistically valid data, can therefore provide appropriate information on the status of a culture and contributes to improved process and quality control.

The present study aims to achieve a further development stage by monitoring the maturation state of the budding yeast *Saccharomyces cerevisiae* with *in situ* microscopy (ISM) on a single-cell level. In the case of the budding yeast, the proportion of cells that are in the maturation state at a time (represented with the budding index, BI), can provide information about the growth vitality (Brauer, et al., 2008; Porro, et al., 2009).

An evolved version of a photo-optical probe, which was formerly applied in cultures of larger microbial cells like the heterotrophic microalgae *Cryptecodinium cohnii* (Marbà-Ardébol, et al., 2017), was used in yeast batch bioreactor cultivations for the first time. Automated image recognition was applied to differentiate between budding and non-budding cells on the basis of machine learning algorithms, and a correlation analysis was conducted in order to prove that data of ISM reflected well data of growth measurements throughout all process stages.

2. Materials and Method***s***

Yeast strain

The yeast strain *Saccharomyces cerevisiae* AH22 (MATa leu2-3 leu2-12 its4-519 can1) (Maczek, et al., 2006) was used for all experiments.

Cultivation conditions

Cells were grown in buffered YPD medium at a pH-value of 5.5. The medium contained 2 % of glucose, 1 % of yeast extract, 2 % of peptone, 1.4 % of KH_2PO_4, 0.1 % NH_4Cl (all w/w) as described previously (Maczek, et al., 2006). This complex medium was chosen rather than mineral salt medium in order to achieve conditions closer to industrial application.

Pre-cultures were grown aerobically in Ultra Yield™ Flasks (Thomson Instrument Company, VA, USA) at 25 °C and 250 rpm with 1 % (v/v) of antifoam 204 (Sigma-Aldrich, Germany). Batch cultivations were conducted in a Biostat® B plus stirred tank bioreactor (Sartorius AG, Germany). The temperature was set to 27 °C, the aeration rate to 1 vvm, and the stirrer speed to 400 rpm, respectively.

Cell growth was determined with the optical density at a wavelength of 600 nm (OD_{600}) with a spectrophotometer (Ultraspec 3000, GE Healthcare, CT). Batch cultivations were inoculated so that the initial OD_{600} reached 0.3. The pre-culture was in the early log phase (OD_{600}=4) at the time of inoculation. Baffled 250 mL shake flasks with non-invasive pH and DO sensors were used to record pre-culture conditions (PreSens-Precision Sensing, Germany). Alternatively, cell growth can be determined through the dry cell weight (DCW). 2 mL of culture were centrifuged for 10 min at 4°C and 21,500 × g in previously weighted 2 mL Eppendorf tubes, then washed with 2 mL of 0.9 g L^{-1} NaCl solution and centrifuged again under the same conditions as before. Then, the Eppendorf tubes were stored in a drying oven (75°C) for 48 h and weighted.

The biological reproducibility of the three bioreactor cultivations was quantified with the standard deviation (σ) obtained between the values of the curve fit and of each experiment.

Off line analysis

Every hour, a sample was taken for the measurement of cell growth and the quantification of extracellular metabolites. Cell growth was determined with the OD_{600} as described in the previous section. Samples for extracellular metabolite determination were filtered through a membrane filter with a pore size of 0.8 µm (Carl Roth, Germany). The supernatant was transferred to 1.5 mL Eppendorf tubes and immediately stored at -80 °C.

Organic acids were quantified with an Agilent 1200 system, which was equipped with a refractive index detector and a HyperRez XP Carbohydrate H^+ column (Fisher Scientific, Germany) as previously described (Marbà-Ardébol, et al., 2017).

In situ microscopy

Cells were monitored *in situ* with the photo-optical probe SOPAT MM-Ho (SOPAT, Germany), which was installed directly in the bioreactor and dipped into the cell suspension. Another probe with stronger magnification, the SOPAT MM 2.1, was used through a bypass. The bypass was connected 2 hours after inoculation.

Table 1 provides an overview of the main characteristics of both microscopic probes, Fig. 1 provides a schematic view of the devices. Both sensors used the same light sources, but different optics and camera systems. The illumination is achieved by transmission, therefore the light source is located at

the opposite side of the camera (Panckow, et al., 2017). The light passes an adjustable distance (measuring gap) through the cell suspension. A short distance leads to the effect that light with a higher energy density re-enters the optical unit on the opposite side. More important is the decrease of obscuration due to overlapped cells within the measuring gap, especially at a high cell concentration. This results in images of higher contrast and an improved differentiation between objects and the background.

Table 1. Overview of the main characteristics of the MM-Ho and MM 2.1 probes.

Parameter	MM-Ho	MM 2.1
Field Depth [µm]	2.32	1
Camera	2750 × 2200 CCD with 19fps, 1”	2048 × 2048 CMOS with 26fps, 1”
Conversion factor [µm pix^{-1}]	0.166	0.087
Interface	GigE Vision	GigE Vision
Magnification	26.6 ×	40 ×
Numeric aperture	0.1	0.55
Illumination	Transmission, Xenon flash lamp, 2.6 J, pulse duration 8µs	Transmission, Xenon flash lamp, 2.6 J, pulse duration 8µs
Measuring Gap [µm]	40	50
Probe length [mm]	270	266
Probe diameter [mm]	24.5	50.0
Software Version	SOPAT v1R.002.0053	SOPAT v1R.003.0092

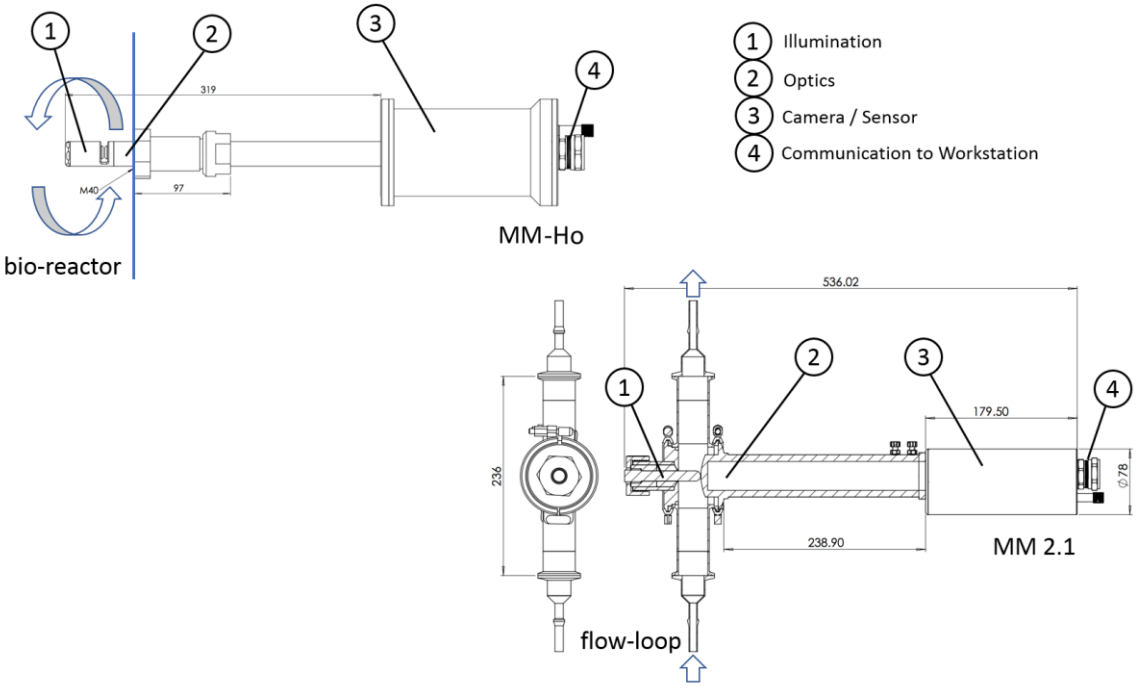

Fig. 1. Sketch of the ISM devices: the probe MM-Ho was installed directly in the bioreactor, whereas the probe MM 2.1 was used in a bypass. The culture broth circulation is marked with arrows in each picture.

Table 2 summarizes parameters of the image acquisition. As a result of the different optical configurations between the probes MM-Ho and MM 2.1, a number of settings were adjusted. Due to the different light transmission characteristics of the optics, the exposure time of the light needed to be increased by a factor of 10 for measurements with the MM 2.1 probe. The rate of captures were increased in parallel to a reduced field of view in order to obtain a sufficient amount of cells that were captured at each time point.

Table 2. Parameters of the image acquisition of the MM-Ho and MM 2.1 probe.

Acquisition parameter	MM-Ho	MM 2.1
Image acquisition rate [min]	each 3	each 5
Exposure time [µs]	15	150
Stroboscope intensity [%]	5	5-12
Frames per trigger [-]	150	200

Automated cell identification

An artificial neural network (ANN) was trained for automated cell recognition. The first step was the annotation of the objects of interest, which were divided in two classes, budding and non-budding (including daughter) cells. As soon as a cell had a visible bud attached to the mother cell, it was considered as a budding cell. This large variability of automated recognizable particle sizes within the class of budding cells was feasible due to a flexible boundary detection. This was enabled through training the machine learning algorithm with annotated samples that covered the entire variability of the cell culture. Various examples of budding and non-budding cells are shown in Fig. 2.

Agglomerates, and cells that were partly or completely out of focus were classified as background.

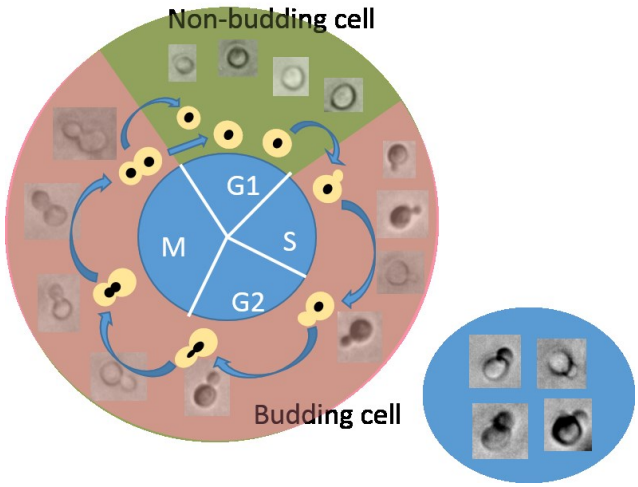

Fig. 2. Classification of cells: non-budding (G1) states are depicted in front of a green background, budding cells (S, G2 and M) are depicted in front of a red background. Examples of overlapping cells that were excluded from the identification are shown in the blue ellipse.

The annotated images served as training data for the ANN as previously described by Ronneberger *et. al.* (Ronneberger, et al., 2015). Afterwards, in order to exclude the falsely identified events, the detected and categorized objects, which were obtained from the ANN, were classified again. A normal Bayes classifier was trained with the labeled particles, from which a feature vector was created. This vector was a function of the area, convex area, eccentricity, equivalent diameter, perimeter and solidity.

Examples of the particle identification and classification are shown in the supplements (Additional file 1: Figure S1). The portion of false positive (particles erroneously detected as cells) and false negative (cells that were not recognized as such) was approx. 5 % of the sum of correctly recognized and false negative counts as determined by manual annotation for the captures of the probe MM-Ho (Additional file 1: Table S1) and slightly higher for captures of the probe MM 2.1 (Additional file 1: Table S2). The budding index (BI) was automatically calculated based on the classification of budding and non-budding cells.

Reliability of the automatic cell identification.

In order to proof the reliability of the cell detection, a manual counting of budding and non-budding cells was performed with captures of the two probes. The automated cell detection has a lower standard deviation than the manual detection, both recognition methods yield similar results (Fig. 3.a and 3.b). The correlation between the BI derived from data of automated and manual cell detection was R = 0.98 for the MM-Ho probe (Fig. 3.c) and R =0.99 for the MM 2.1 probe (Fig. 3.d). In case a sample was measured three times, a coefficient of variation of less than 0.15 % was achieved. The divergence in the BI of captures from the probes MM-Ho and MM 2.1 is seen in both manual and automated cell detection. This divergence might be due to differences of the pre-culture (biological divergence), but also due to the differences in the bypass unit (technical divergence). Due to the setup of the bypass, it is considered to be unlikely that yeast cells are affected in such a short time of 60 s at the given concentration. The impact is lower than at off line microscopy anyway, which is the only reliable reference method. Therefore, any influence would be hardly detectable, if it is less than at the sample treatment for *off line* measurements. In any case, the same dynamics of metabolic concentrations and morphologic cell features were observed.

A certain portion of budding cells are identified as non-budding cells, if (i) either the bud is hidden by its mother cell (optical shadow), or (ii) if the bud is situated directly in front of it. This percentage can be approximated under consideration of the portion of the surface area of the mother cell, in which a daughter cell (bud) is completely hidden (A_{hd}). Finally, the relation between the total surface (S_m) and the A_{hd} multiplied by two will provide the probability of false positive detections in non-budding cells (X_{Fnb}). If X_{Fnb} is derived as explained in the supplementary materials (Additional file 1: Figure S2), a

maximum of 4 % of all cells will be classified as non-budding, although they should actually be classified as budding cells. An even distribution of cells towards the optical plane is assumed.

However, it is likely that cells are oriented towards the direction of flow. In this case, the bud will likely be located in orthogonal direction towards the optical plane. Thus, the proportion of buds in the optical shadow or directly in front of the mother cell is lower than assumed under a normal distribution of the buds. Since the error is systemic and similar across all cultivations and also occurs with the usual *off line* light microscopy, it is considered to be negligible for the further discussion.

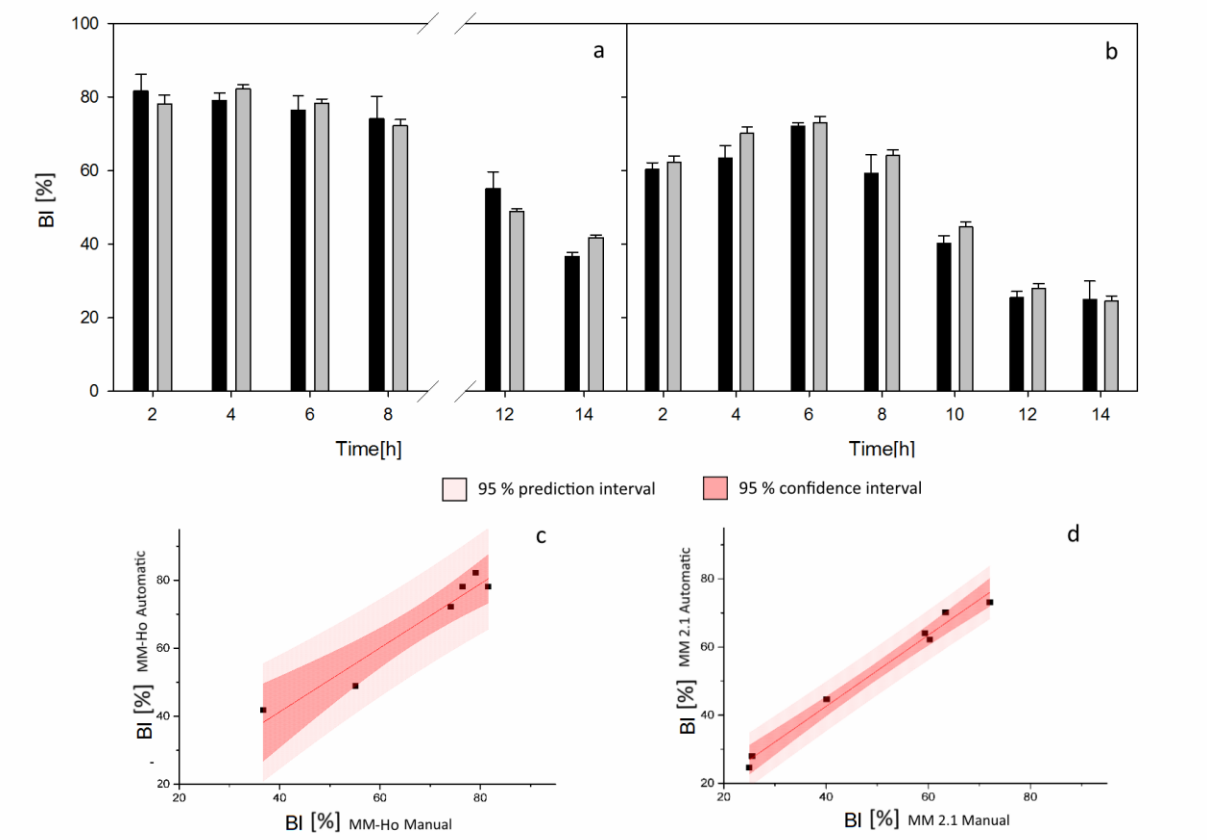

Fig. 3. Comparison between the budding indices obtained with ISM (black bars) and with manual counting (gray bars) with the respective standard deviations for the probe MM-Ho (a) and the probe MM 2.1 (b). The standard deviation of the manual counting was obtained from two mean values from a sample size of between 100 and 200 cells. The standard deviation of the automated cell detection is calculated as difference from a fit (spline function) with the values of single time points. Linear correlation between the manual and automatic recognition for the probe MM Ho (c) and the probe MM 2.1 (d).

Sample size and sample concentration

In order to ensure that a representative sample of the cell population was measured, a sensitivity analysis from each cell class (budding and non-budding) was performed, as both classes had a different grade of heterogeneity (data not shown). A certain heterogeneity is obtained, because budding particles vary in size due to the ongoing budding process. A higher heterogeneity requires more data

for training. It was taken care that the number of cells that are identified at each time point exceeded the required number to gain a reproducible value of the mean cell Feret diameter and the Dv90 (the cell size, which encounters 90 % of the detected cell sizes), as described elsewhere (Marba-Ardebol, et al., 2018a).

Morphological parameters

The morphological parameters that were obtained from the ISM were cell Feret diameter (d_F) and the aspect ratio (AR). A certain d_F of a particle is calculated as the difference between the maximum and the minimum length of the particle projection on a unit vector with a certain rotation. The minimum, maximum and mean d_F are estimated by rotating the unit vector from 0° to 180° by 16 steps. Then, the smallest, largest and mean diameters are determined according to ISO norms. The aspect ratio is obtained by dividing the minimum through the maximum d_F.

In order to reduce the influence of outliers, the median of the minimum, maximum or mean d_F of all cells is shown in the manuscript. Moreover, the interquartile range (IQR), which is the difference between the 75^{th} percentile, also denoted as third quartile (Q3), and the 25^{th} percentile, also denoted as first quartile (Q1), is provided to indicate the variability around the median.

3. *Results*

In situ monitoring of the budding index

Three glucose-limited aerobic batch cultivations of *S. cerevisiae* were conducted. In addition to the standard *off line* sampling for the investigation of cell proliferation and the metabolite concentration profile (Fig. 4.a and b), ISM was used to obtain information on the growth vitality of yeast cells. Two cultivations were monitored with the probe MM-Ho, and one with the probe MM 2.1.

The increment of the cell concentration over time of either OD_{600}= 6.2 or 2.8 g L^{-1} of DCW exceeded the threshold value for a suitable cell identification due to numerous overlapping objects. For an *in situ* application, however, the probe must cover a common concentration range. In order to achieve this objective, two parameters were tested for their robustness: (i) the modification of the focus plane, and (ii) the stroboscope intensity. The first one influenced the sharpness of the separation of a cell from the background, which has an influence on the determination of the cell size. It must therefore remain constant during an application. However, it has been demonstrated that adjusting the stroboscope intensity did not affect the results. Although captures were gained at different stroboscope intensities, neither the BI nor the cell size of budding and non-budding cells were affected (Fig. 5). A further development to automate the adjustment of the stroboscope intensity to the increase of the cell concentration is in progress.

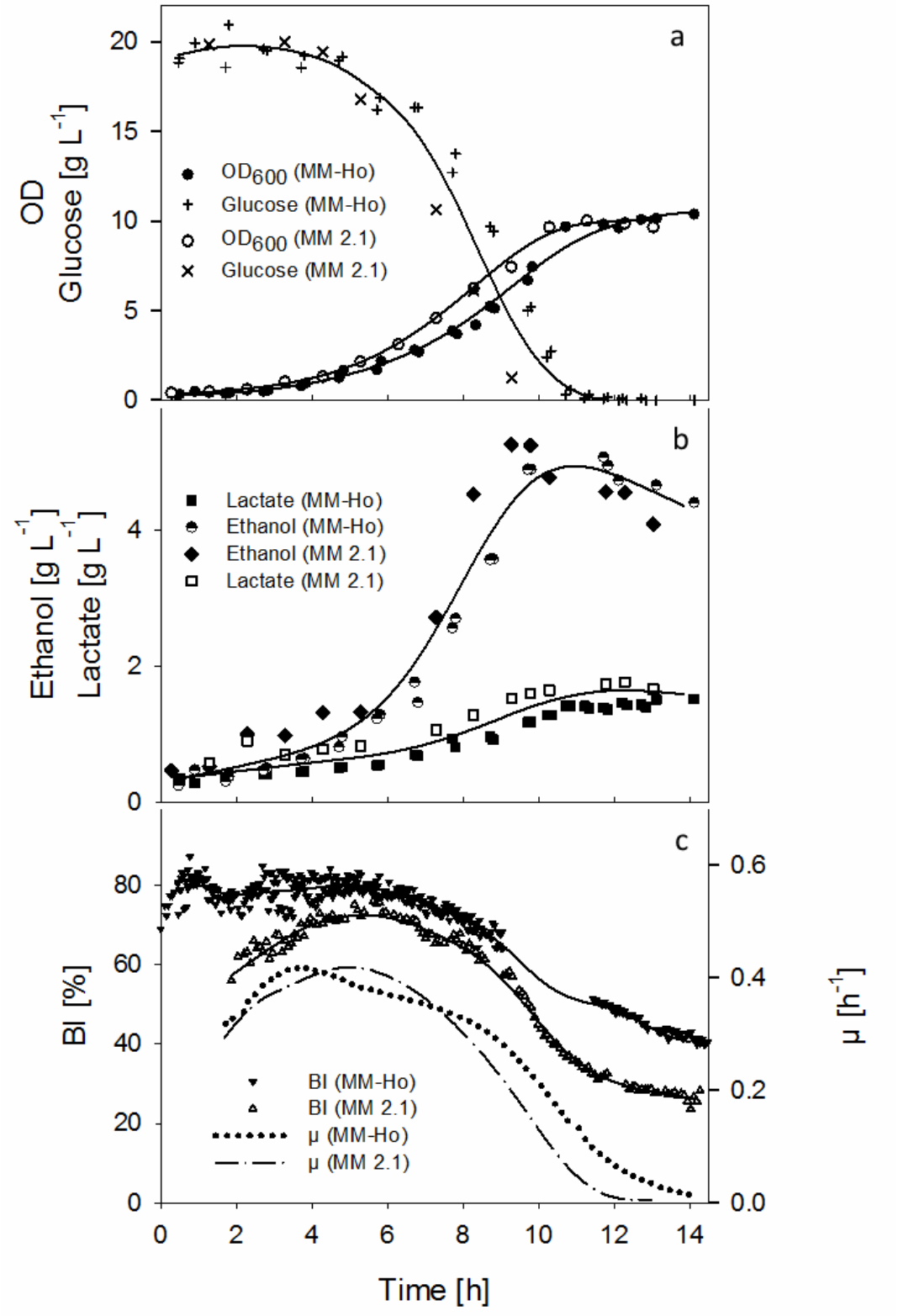

Fig. 4. Performance of *S. cerevisiae* batch cultivations: (a) OD_{600} of cultures monitored with the probe MM-Ho and MM 2.1 and the respective glucose concentration, as well as in (b) ethanol and lactate concentrations. The standard deviation between experimental points and curve fits (spline function) are 0.46 (OD_{600}), 1.2 g L^{-1} (glucose), 0.3 g L^{-1} (ethanol), and 0.2 g L^{-1} (lactic acid concentrations). (c) Budding index as determined with the probe MM-Ho and MM 2.1, and the respective growth rate. Experimental data is represented with dots, curve fits with straight lines.

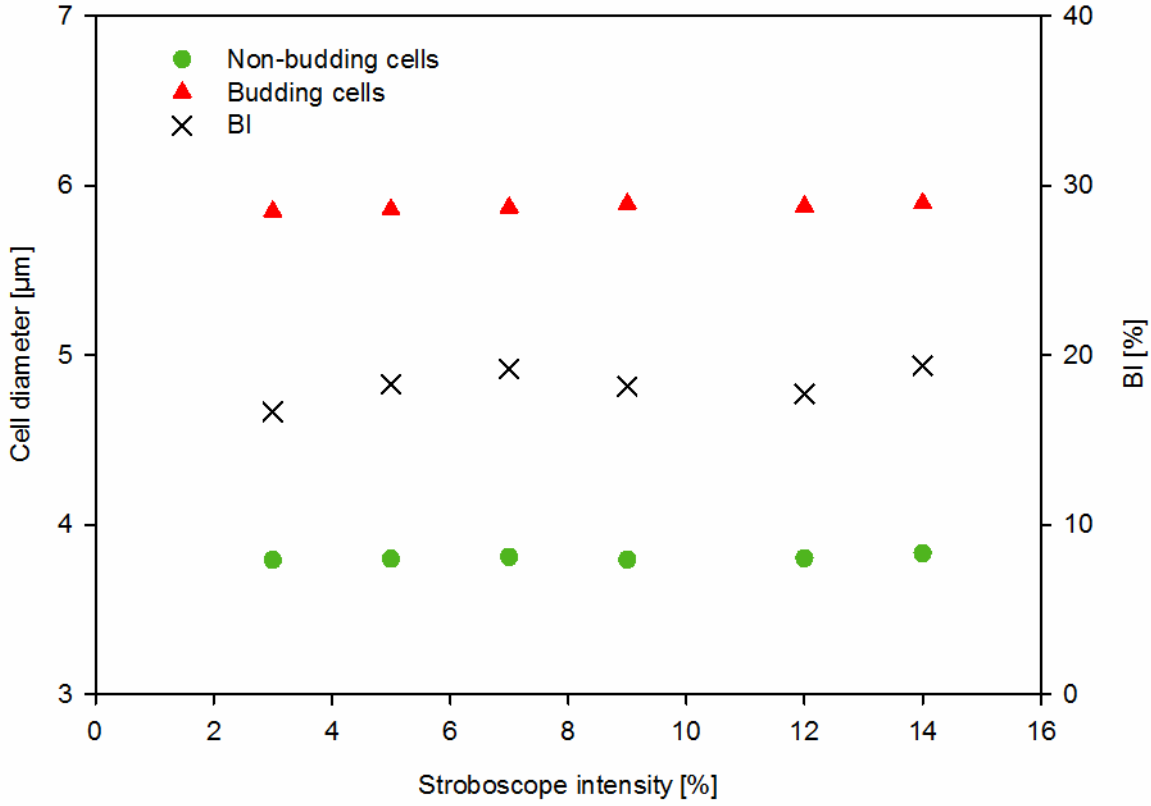

Fig. 5. Yeast cells of the stationary phase measured with six different stroboscope intensities. The median of the mean d_F of budding and non-budding cells, and the budding index is depicted.

Monitoring with the MM 2.1 probe (with a higher magnification) was performed with an adjusted stroboscope intensity. In parallel to the increasing cell concentration, the intensity was increased from 5 % to 12 % after 9 hours. This allowed a proper cell detection throughout the entire process.

All cultures performed similarly in terms of growth, production and consumption rates as well as cell morphology (Fig. 4). The two cultivations, in which monitoring was conducted directly *in line* in the cell suspension, were almost uniform, and a third cultivation, in which ISM was applied in a bypass, showed only minor deviations from the previous experiments (values of the standard deviation are listed in the legend of Fig. 4).

The patterns were typical for aerobic cultivations with yeast. By using a pre-culture that was inoculated during its early exponential phase, a growth rate of 0.3 h^{-1} after one hour of bioreactor cultivation was achieved, followed by an exponential growth phase, in which a maximum rate of 0.42 h^{-1} was reached (Fig. 4.c).

In each of the growth phases, a different BI was obtained. The BI increased to a maximum of 80 % in the first hour after inoculation. Afterwards, a reduction in the BI was observed, which can be attributed to mitosis, as the proportion of daughter cells from freshly saturated cells increases.

As soon as the culture entered the exponential phase, the BI began to decline due to an accelerated proportion of mature daughter cells. It decreased linearly at a rate of -4.4 ± 0.13 % h^{-1} up to about 9 hours after inoculation. The trend in the BI decreased to 22 % when the glucose concentration was close to limitation (measured with the probe MM 2.1). After the shift to ethanol consumption, the proportion of budding cells decreased, while maturation slowed down and only a few cells entered the S-phase. While the development of the BI is uniform among the different probes, which were applied, the absolute value differs. This is most likely due to an improved recognition of cells, which belong to the class of small non-budding cells due to improved optics of probe MM 2.1. This can be seen in Fig. 7.

The BI is well correlated with the growth activity of cells, as demonstrated by a cross-calibration correlation analysis (provided in the supplementary material). This correlation applies to more or less all growth stages with a coefficient of determination of R = 0.99 (Additional file 1: Figure S3).

A maximum DCW of 5 g L^{-1} was achieved during batch experiments. No more than 12 % of the light capacity of the stroboscope was used. Therefore, there is a potential to monitor higher concentrated cell suspensions. A concentration range of 3 gL^{-1} to 65 g L^{-1} was tested by adjusting the stroboscope light intensity. Then, the images were processed as follows: first, a Laplace filter was applied to the original image. Then, the output was normalized with the average image brightness at the adjusted stroboscope intensities. Afterwards, the predicted concentration was calculated with the most suitable feature combination for the best fit of true concentrations. The correlation between the measured DCW and the predicted DCW was R = 0.97 (Fig. 6). Nevertheless, in order to achieve reliable results of the BI at higher cell densities, a further annotation and training of the ANN is suggested.

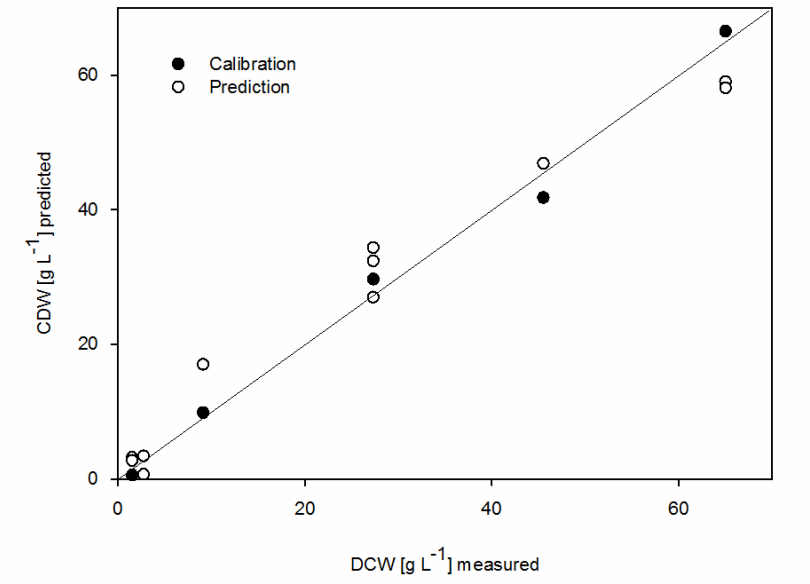

Fig. 6. Linear correlation between the DCW as measured *off line,* and the DCW as predicted with ISM. Depicted are the values used for calibration and prediction.

Growth dynamics and population heterogeneity

The heterogeneity of the population can be studied using the morphological parameters determined by the ISM. The sample was divided into two populations, budding and non-budding cells. This resulted in a bimodal distribution. Fig. 7 shows the unicellular size distribution in relation to the max. d_F of some selected time points during the batch cultivations. The distribution was wider in the early stage of the exponential phase (3 h). The portion of small cells increased after 9 h of cultivation, when cells reached the post-diauxic phase, while the distribution between small and large cells remained rather constant between 3 and 7 h of cultivation. There existed a similar size distribution over a certain time period, when the change of substrate availability, byproduct formation and other changing factors do not have an impact on growth and vitality.

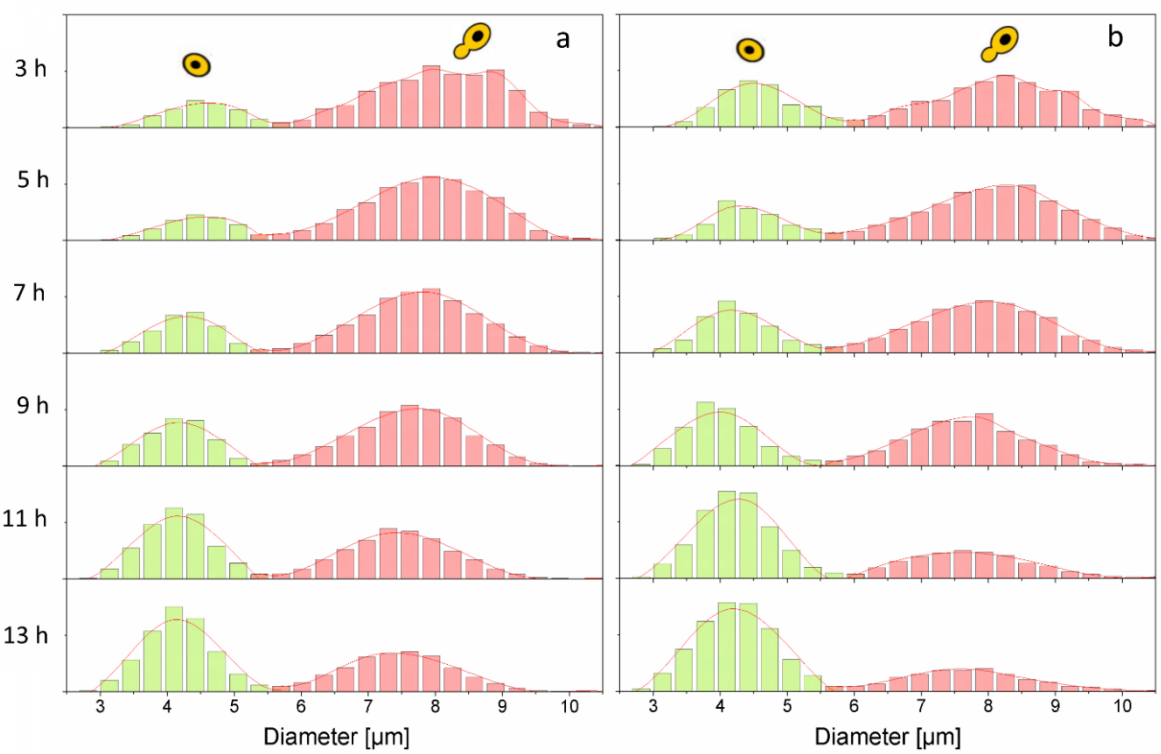

Fig. 7. Single-cell size frequency distribution of the max. d_F for cells classified as budding (red) and non-budding (green) measured with the probe MM-Ho (a) or MM 2.1 (b).

The size development during a cultivation is shown in Fig. 8. Since the daughter cell is always smaller than its mother cell, the difference of the minimum and maximum d_F of budding cells provides information about the bud size. The mother cell usually remains almost invariably large during the budding phase, the d_F of mother cells is rather a value between the minimum d_F of budding cells and the maximum d_F of the non-budding cell fraction. The maximum d_F of the non-budding cells remains almost constant during the growth phase, while the minimum cell size of budding cells decreases in parallel to a decreasing growth rate. The cell size is affected by many parameters, among them are

internal metabolite and ion concentrations, lipid, protein and RNA contents. These are steadily changing while growth decelerates. The appearance of smaller budding cells might thus be an early indicator for growth retardation. The heterogeneity in the lag phase is greater than in the post-diauxic phase, as a broader cell-to-cell variation is probably due to the stress response after transfer and inoculation than during glucose starvation, in which cells likely respond in a similar manor. The homogeneity of budding cells increased during cultivation (Additional file 1: Figure S4).

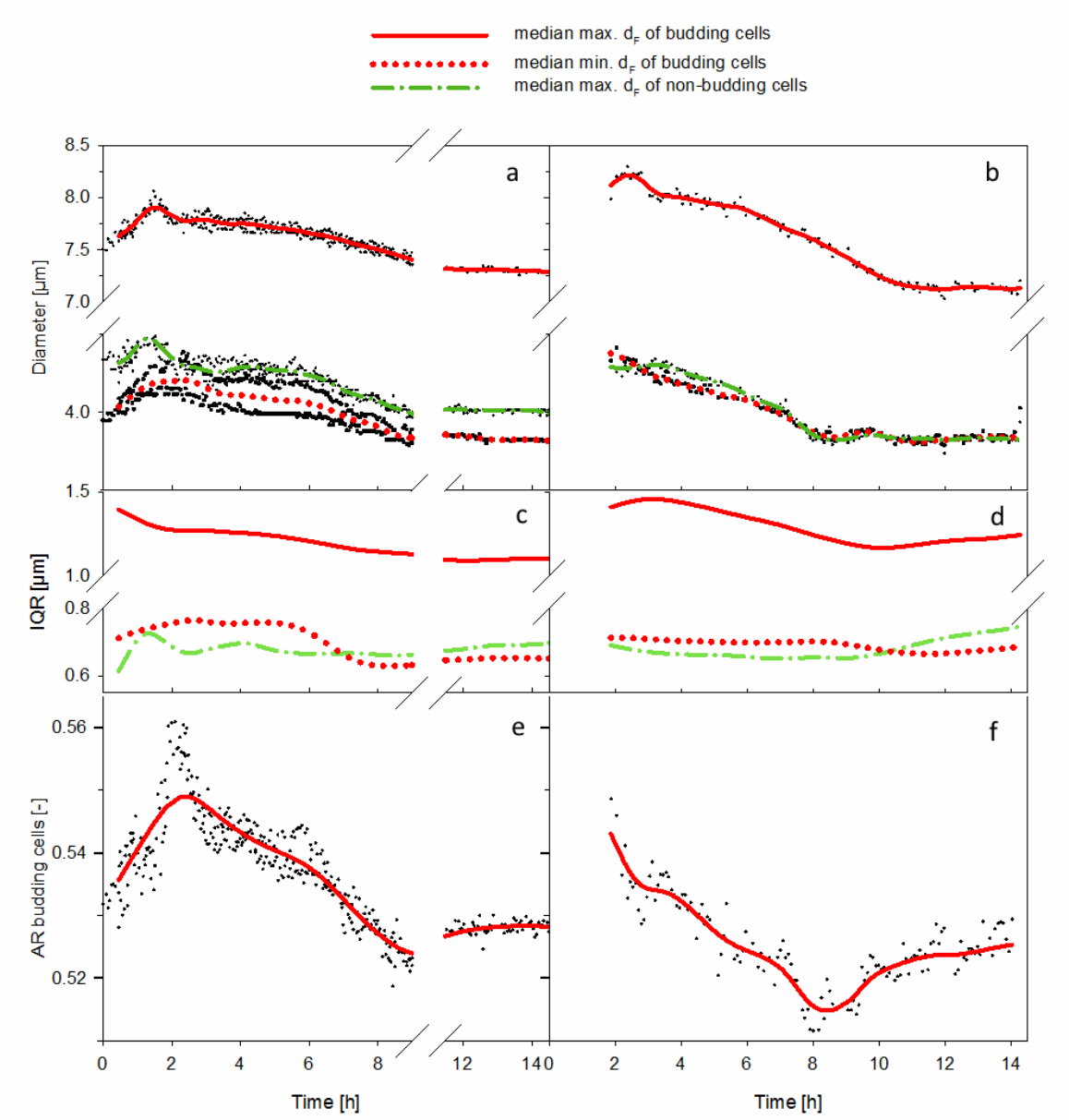

Fig. 8. Variation of morphological parameters. Values in the left column were obtained with the MM-Ho probe, values at the right column with the MM 2.1 probe. (a) and (b) Evolution of the median of the max. d_F and the min. d_F . (c) and (d) Variation of the interquartile range (IQR) of the median of the max. d_F and the min. d_F. (e) and (f) Evolution of the aspect ratio (AR) for budding cells, that is the ratio between the median of the min. d_F and the median of the max. d_F.

The AR of the non-budding cells remained almost constant (~0.9), since these cells are preserved as almost perfect spheres. From the moment on when the cells entered the exponential phase, the AR of budding cells probably decreased due to an increase in cell size during the maturation phase under elevated growth (Soifer and Barkai, 2014). When diauxic growth occurred, the AR increased due to a reduced bud size due to the retardation of bud growth. It seems that the cell cycle stagnated at the same time, while the BI changed only slightly. All other morphological parameters remained constant, so that hardly any cell entered the S-phase. Multi-budding yeast cells were hardly observable among all cultivations and therefore neglected during cell recognition.

4. Discussion

Many efforts have been made to develop *in situ* microscopes for the application in bioprocessing (Belini, et al., 2013; Suhr and Herkommer, 2015). Initially, probes (Type III XTF, Sartorius and Hannover Univ.) required mechanical sampling, or a bypass measurement (Havlik, et al., 2013b). Previous studies used ISM without mechanical sampling techniques for the determination of the biomass concentration and the cells' volume. The cell concentration was examined with a further developed version of ISM type XTF. The biomass concentration of the yeast *Pichia pastoris* was monitored up to a concentration of almost 80 g L^{-1} with a standard deviation of less than 12 % (Marquard, et al., 2016) (in the same concentration range as shown in the present paper, 65 ± 4 g L^{-1}). The cell size variation, which was influenced by osmotic stress responses, was assessed (Camisard, et al., 2002). Cell identification was conducted with template matching and the resembling of circles. Aggregates were ignored like in our study. The volume of cells (38-30 µm^3 during the batch phase) indicate that the detection was restricted to non-budding cells.

In order to distinguish between budding and non-budding cells as performed in this study, it was assumed that the cell projection is an ellipse and the relationship between the major axis and minor axis can be used to classify the maturation state (the aspect ratio, as shown in the Results section, or vice versa, the elongation). Thus, it yields an approximation of the BI (Coelho, et al., 2004). Therefore, the AR or elongation value need to be set to discriminate both maturation states. Consequently, budding cells may be considered as non-budding cells at the beginning of the S-phase. However, the value selected by Coelho, et al. (extension=1.5) correlates well with the data presented in this study.

ISM was not affected negatively by agitation as long as the power input was sufficient to generate a certain flow through the measurement gap. Then the image acquisition frame rate was adjusted in order to guarantee that cells from a previous frame will not appear in the following frame. Captures including bubbles were ignored for further image analysis. Undissolved particles of complex media are not influencing cell detection since the ANN approach will recognize those particles as background. This was applied in this study as complex media with yeast extract and peptone was used. However,

threshold concentrations will exist, which does not allow for a precise measurement anymore, but this depends on many factors and has to be evaluated in each specific case. One benefit of any automated cell detection method is the consideration of a large number of cells within a short time. The minimum sample size, which is required to obtain a representative cell size distribution (n) of a population (N), can be determined with eq. 1. This approximation is based on the assumption that N is much larger than n, and that n is normally distributed (Kauermann and Kuechenhoff, 2010). The desired accuracy (e) was set to 5% of the variance of the max. d_F of budding and non-budding yeast. The admitted error was assumed to be $\alpha = 5\%$ among the number of annotated cells n. A Gaussian distribution of the cell size of each class ($z_{1-\alpha/2}=1.96$) was considered. The amount of cells that needed to be identified from each class at each sample point under the assumptions described above is shown in table 3.

$$n = \left(\frac{\sigma\, z_{1-\alpha/2}}{e}\right)^2 \quad (1)$$

The recognized amount of cells exceeded these cell numbers at all analyses.

Table 3. Sample size to obtain representative data of a population with the probes MM-Ho and MM 2.1.

	MM-Ho		**MM 2.1**	
	Non-budding	Budding	Non-budding	Budding
Variability (σ)	0.55	0.89	0.52	0.95
Accuracy (1-α)	0.05	0.06	0.04	0.07
Sample size (n)	502	768	633	794

The processing of captures lasted about 16 s with the probe MM-Ho. Hence, the estimated total process time for a sample point with 150 images was approx. 40 min. The higher magnification reduced the time of image post-processing with the probe MM 2.1. Only 2.5 s were required to process an image, in total approx. 8 min for a sample point of 200 captures. Consequently, the method is assumed to be suitable for real-time monitoring and control of a bioprocess.

In order to validate automatic image recognition, the study by Rupes et al. observed a systematic error (Rupes, 2002), as the deviation between manual and automatic detection increased when large quantities of buds were analyzed. No systematic error was observed in the present study. Although the divergence between manual and automatic detection at some points in time is up to 14 %, it remained under 8 % on average (Additional file 1: Tables S1and S2).

Population heterogeneity can make a difference in the performance of a culture. Therefore, monitoring of the heterogeneity is crucial as it can influence the robustness and productivity of a bioprocess (Delvigne and Goffin, 2014). A certain cell size have to be reached for the initiation of budding and DNA replication (Porro, et al., 2009). The same critical cell size applies to all daughter cells, while in parent cells it increases with age. The heterogeneity of budding cells was reduced during the growth phase,

while it was higher in the lag phase. As recent studies have shown, bet-hedging mechanisms may be the reason for prolonged delay periods due to the formation of subpopulations with different phenotypes when cells cope with environmental stress, as it occurs after inoculation (Rosenthal, et al., 2017).

The determination of yeast quality was often determined by the viability and vitality of cells. However, vitality is not clearly defined and can be seen as a continuum of cell activity, from very active to very inactive cells, which is unacceptable for cultivation (Lodolo and Cantrell, 2007). Real-time monitoring of growth activity on a single-cell basis is achieved with ISM, so that it does not rely on an average value, but provides the possibility for a continuous observability of the process. Until now only animal cells structure, as detected with ISM, were related to cell viability (Wiedemann, et al., 2011a). The proper detection of smaller cells like many bacteria remains still a challenge and clearly limits currently ISM for the application in such bioprocesses. Although some studies have investigated the cell concentration of bacteria like *Escherichia coli* (Marquard, et al., 2017), the determination of the dried biomass concentration was only recently performed on the basis of a grayscale intensity measurement of captures. Single-cell analysis as described for cell line cultivation, algae or yeast has not been conducted yet for bacteria. Further experiments are required to investigate the limits of application at high cell densities at various complex media compositions.

5. Conclusions

ISM was applied successfully to monitor growth and budding activity in yeast batch cultures. In addition to growth information, the heterogeneity among the population of budding yeast cells can be quantified as well. The measurement can be performed directly in the reactor during the cultivation period by means of a photo-optical sensor in conjunction with an automated image analysis. Although other techniques can also provide data about cell size distributions, imaging microscopy gain data about the shape and any potential structural segregation of individual cells. In addition, the use of accelerated image recognition for process control is conceivable. In order to further improve applicability to differentiate cell structures, e.g. at intracellular product accumulation, the application of a higher resolution and the consideration of overlapping cells are currently under development.

List of abbreviations

artificial neural network (ANN), aspect ratio (AR), budding index (BI), cell Feret diameter (d_F), dissolved oxygen (DO), dry cell weight (DCW), flow cytometry (FCM), *in situ* microscopy (ISM), interquartile range (IQR).

Additional Supporting Information may be found online in the supporting information tab for this article.

5. **Summarizing discussion**

So far, mainly chemical and physical properties of the medium, like the pH-value and the dissolved oxygen concentration are monitored in bioprocesses. Consequently, neither the physiology of the cells nor the heterogeneity are considered. Moreover, the uneven spatial distribution in large-scale bioreactors, which is caused mainly due to a limited power input, can affect the performance of the process, as scale-down studies have shown. The aging of the cells and the cell cycle phases are a source of heterogeneity as well (Müller, et al., 2010). Alterations of raw material quality (Kirdar, et al., 2010) also affect the batch to batch reproducibility (Kasprow, et al., 1998).

The morphology of cells can be a suitable parameter to assess the growth state for different cultivation conditions, as the size and shape changes accordingly (Tibayrenc, et al., 2010). Consequently, there is a relationship between form and function in microbial processes (Gao, et al., 2014; Gonzalez, et al., 2008): the physiological state is related with the morphological state.

Until recently, there existed a limitation to rapidly assess cell morphological data due to a lack of suitable measurement technology. The application of movable parts, the required sterilizability, stability, maintenance and the short response time for image detection represented huge challenges (Beutel and Henkel, 2011). The time needed for processing a statistically reliable amount of data was exceeding the time of cell dynamics in microbial cultivations (cell cycle, growth rate and production rate), hence many microscopy technologies were not suitable for real-time applications, especially not *in situ*.

The present work contributed to resolve some of the challenges towards a fast and reliable microscopic measurement of eukaryotic single cells. *At line* and *in situ* measurements were conducted with (i) 3-D holographic interferometric microscopy (DHM) and (ii) photo-optical *in situ* microscopy (ISM). Relevant industrial processes, namely the budding yeast *S. cerevisiae* during batch cultivations and scale-down experiments, as well as the two-stage cultivation for DHA production with the heterotrophic algae *C. cohnii* were investigated.

A sufficient resolution is the key for a successful cell identification for both microscopic techniques, since it is affecting the sharpness of the delimitation of the cell with the background, and hence the cell recognition and cell size estimation (Marba-Ardebol, et al., 2018a). Finding an appropriate focus plane is not trivial and it depends on the object itself and on the matrix. Additionally, it depends on the preview (intensity picture or hologram for DHM and the bright field for ISM) and the time of light exposure, which influences the subjective impression of a correct focus plane. In contrast to ISM, DHM offers the possibility to refocus *off line.* Although refocusing is not an option for ISM, the image can be pre-processed for improving its quality before any particle identification (e.g. particles that are

appearing repeatedly in several images can be deleted by the application of filters or the brightness of the images can be normalized).

The cell diameter of algae cells was computed directly from the surface of each cell. Both techniques (ISM and DHM) used the approximation of the Sauter mean diameter (d_{32}). It was assumed that the cell is a perfect sphere, and its diameter was equivalent to the diameter of a circle that has the same area as the cell. The Sauter mean diameter, which was measured at different growth states, differ by 4% on average and by 8% at maximum between ISM and DHM measurements. The single-cell size distribution dynamics obtained with both techniques were in agreement to each other (Marbà-Ardébol, et al., 2017).

Budding yeast cells represent a bigger challenge for automated image detection, as cells during budding are not of a spherical shape. So far, budding cell sizes have been calculated assuming that all cells were a perfect sphere or at best an ellipsoid in captures of ISM measurements. If the first option was applied, no differentiation between the maturation state of the cells could be made (Camisard, et al., 2002). If it was assumed that the cell is an ellipse, the ratio between the major and the minor axis was used to classify the maturation state (Coelho, et al., 2004).

The present study achieved a further development stage. The differentiation between budding and non-budding cells was feasible, because of the flexible boundary detection enabled through machine learning algorithms, in particular through the training of an artificial neural network (ANN). A neural network is a type of machine learning algorithm based on pattern recognition. This approach has reduced the time needed for processing a statistically reliable amount of data, which was the major limitation until now for the applicability of imaging systems in real-time applications.

The yeast cells maturation state became trackable through the BI determination, as a ratio between cells with buds and the total amount of cells (Marba-Ardebol, et al., 2018b). However, annotation procedure for training the ANN is time consuming, if accurate results should be obtained (Marba-Ardebol, et al., 2018a). Otherwise, a simplified annotation can consist in labelling cells into different classes, without tracing their edges. This can reduce the time and man power to be invested, when obtaining the ratio between classes is already a valuable process parameter (as it is the BI) and not the size evolution of the cells.

In contrast, DHM cell recognition algorithm was not able to detect budding cells as such (**Figure 8**), but rather only the mother cell was detected. DHM cell size was approximated through the Sauter mean diameter, as it has been explained above, whereas ISM approximated the cell size by the Feret diameter (d_F). A certain d_F of a particle is calculated with the particle projection on a unit vector with a certain rotation (0° to 180° by 16 steps) according to ISO norms. Therefore, if results of DHM and ISM

should be comparable, the diameter distribution of DHM would be equivalent to the distribution of the maximum diameter of the non-budding cells plus the minimum diameter of the budding cells. The ranges of the single-cell size distributions were: DHM 3 to 8 µm (mean value was 5.3 ± 0.1 µm) and ISM for max. $d_{F,\,n\text{-}b}$ and min. $d_{F,\,b}$ 2.5 to 6.5 µm (mean value was 4.1 ± 0.1 µm).

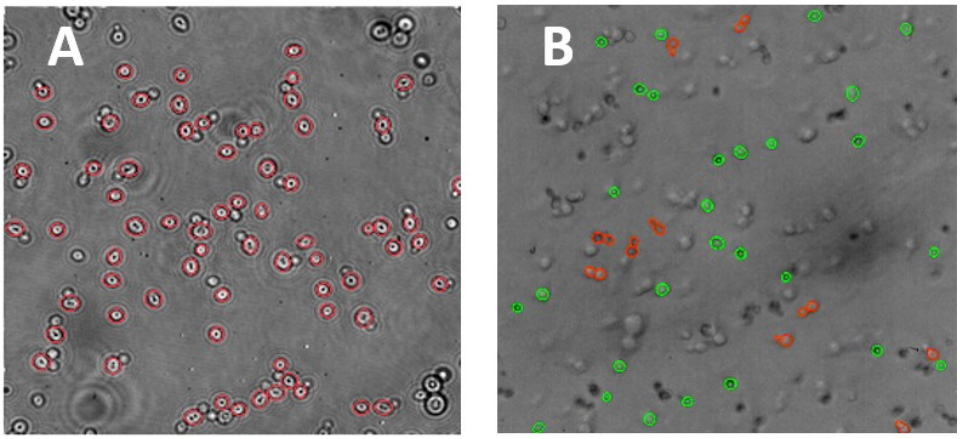

Figure 8. Microscopic pictures of *S. cerevisiae* cell detection as obtained with DHM (A) and ISM (B).

Both microscopic techniques allowed the measurement of a representative sample of the cell population. No sampling was needed for ISM measurements. They were performed directly in the suspension, or through a bypass line. Although the possibility of measuring through a bypass is also feasible for DHM measurements, sampling was needed for the approach as used in the experiments.

Favorable and unfavorable growth and DHA production conditions were identified in *Crypthecodinium cohnii* cultivations. Size, circularity and phase homogeneity were affected depending on the C/N ratio, but also due to the effect of different media on growth and lipid accumulation. **The intracellular accumulation of DHA was predicted non-invasively and in real-time by means of DHM and ISM** (Marbà-Ardébol, et al., 2017). A correlation between the DHA content measured *off line* (using gas phase chromatograph equipped with a flame ionization detector) and predicted using the average d_{32} as detected *on line* by ISM through cross-calibration was found. Former studies detected already the connection between cell size and DHA accumulation. A relation between cell biomass concentration and cell density indicated that cell size almost tripled during the course of fermentation when the marine algae *Schizochytrium limacinum* produced DHA (Chi, et al., 2009).

The influence of gradients, as they appear in large-scale, on the morphological heterogeneity of yeast cultures was investigated (Marbà-Ardébol, et al., 2017). Large-scale cultivation conditions, which were mimicked in a three-CR scale-down system (with an exposure to oxygen limitation for about 2 min) increased the degree of cell heterogeneity, which was revealed by means of the single-cell size distribution. Yeast cells were robust enough to maintain free sterol concentrations under scale-down cultivation conditions, but their morphological variability increased under severe exposure to oxygen

limitation (three-CR). This was probably because not all cells could trigger the enzymatic response necessary for obtaining higher fluxes whenever sufficient oxygen as cofactor was available. Population heterogeneity studies have been performed also for a scale-down reactor set-up consisting of two interconnected stirred tank reactors, operated in continuous cultivation mode. A reporter strain of *S. cerevisiae* showed that growth on ethanol increased the population heterogeneity as well (Heins, et al., 2015).

The increment of the morphological heterogeneity in the three-CR was not directly related to a growth reduction, but rather to the presence of a zone of strong substrate limitation. If the exposure to oxygen limitation was reduced to about 1 min in a two-CR scale-down reactor, the homogeneity of the cell size was comparable to cultivations in homogeneous conditions. **Surprisingly, sterol formation was not influenced negatively but positively by oscillating conditions.** The post-squalene pathway was altered in both scale-down systems (two-CR and three-CR). The mechanism used to maintain free sterol homeostasis was raising the sterol esterification. Higher fluxes led to increased concentrations of all esterified sterols. The esterified form of the end product ergosterol increased the most (75% in comparison to homogeneous conditions). Under more severe oxygen limitation, as it occurred in the three-CR system, even an accumulation of the precursor squalene was observed (a 10-fold accumulation in comparison to homogeneous conditions). Therefore, ergosterol or squalene production can be enhanced when cells cope with oscillating oxygen limitation. A positive effect of the large-scale conditions with baker's yeast was already presented by George *et al*. when the quality of the cells (gassing power of the yeast in a dough) was better than from homogeneous lab-scale experiments (George, et al., 1998). Nevertheless, the final biomass concentration was lower when cells cope with gradients in both studies.

Morphological changes appeared in dependence of the growth status for the budding yeast *S. cerevisiae* during a batch cultivation. The maturation state of the cells was monitored *in situ* for the first time (either directly *in line* or in a bypass system) and was used to evaluate the metabolic activity of the cells. The BI was well correlated with the cell growth rate. The determination of the single-cell size and shape distributions provided information about the morphological population heterogeneity as well.

This study proofs that both the DHM and the photo-optical ISM are well-suited process analytical tools to assess population status in eukaryotic cell cultivations. The evaluation of the subpopulations phenotype dynamics (through the single-cell morphological analysis) allows the estimation of the macroscopic cell population response. The photo-optical sensor, when applied *in situ*, and the DHM applied as a bypass can be suitable for process monitoring, if the time response remains shorter than the cells' dynamics.

6. **Outlook**

Challenges and limitations of the *in situ* microscopy in industrial bioprocesses

The application of single-cell analysis in industry can help to identify unsuitable cultivation conditions regarding cell response. So far, it was demonstrated that phenotypic heterogeneity can increase the population fitness or survival rates upon environmental changes, whereas it also can reduce the overall productivity due to low performance subpopulations. However, the measurement of heterogeneity has not yet been used technically for optimizing microbial cultivations. In order to do so, acquisition of reliable data with heterogenic information in the large-scale production is required; and the relation of these signals with the cell physiology and the environmental conditions has to be investigated.

Until now, in order to avoid limitations of growth-coupled processes, which are dependent on the metabolic pathway chosen, two-stage cultivations have been applied mostly to increase productivity. Although its effectiveness was demonstrated, the second stage of the process is usually induced when sufficient biomass is produced, independently from the physiology of the cells. Nevertheless, if process environmental conditions and/or growth status along the first phase influence cell morphology, the shift from the growth phase to the production phase could be monitored on an individual cell basis. E.g. when taking into account the homogeneity of the culture, and a culture with similar production rates could be obtained. As it is shown in the present study, the heterogeneity of the culture can increase with prolonged exposure to oscillating oxygen limitation. Consequently, the shift to the second stage could be initiated before the segregation of the population is not any longer tolerable.

Engineered cells, which are able to cope with stress conditions of large-scale bioreactors are an option to reach higher yields and productivities, and therefore dynamic metabolic control (DMC) should be highlighted (Brockman and Prather, 2015). Cells operating by DMC should be able to redistribute metabolic fluxes through controllable gene expression or protein activity in response to an internal or external signal. When using this regulation in large-scale cultivations, cells could be able to readjust their metabolic fluxes according to the oscillating environmental conditions coped within the reactor space. Cells should sense and respond in order not to compromise the cell integrity e.g. by deciding when it is the right time to be productive, and hence avoiding a critical accumulation of undesired side products. These adaptations should be conducted in a pre-defined manner and they should have fast response times and be reversible. However, this approach is challenging since it requires an understanding of cell fluxes dynamics. In this case, the membrane integrity has a fundamental role for the tolerance against by-products accumulations, limitations or excess of some metabolites. In order to achieve these goals, there is a necessity for better and more inexpensive methods for high-throughput screening. ISM could be the appropriated tool for monitoring cell membrane integrity in

microfluidic systems undergoing these screenings. More information could be gained with fluorescent biosensors, if the engineered cells response is connected with fluorescent markers, as already used for heterogeneity inspection in FCM studies. For this purpose a further adaptation of ISM in terms of light source and detectors is needed.

As already shown in this work, process optimization and development can be assisted by scale-down systems. However, approaches that truly reflect cells interactions with cultivation conditions are challenging, since often only engineering parameters are taken into account. Moreover, engineering parameters in industrial bioreactors are usually measurements at a single position. This can be crucial if gradient formation appears, since this one sensor spot is eventually not located in representative conditions. In order to investigate gradients, multi-position sensors have been applied. The application of such systems is very limited until now, due to sterility concerns and regulations. Cell-based measurement methods, especially if they rely on the morphological state of a cell, are rather independent of their location, since changes of these parameters usually exceed mixing and residence times. Thus, gradient formation does not disturb the measurements. The feasibility to apply the same technology (ISM) from the lab-scale to the production scale will facilitate its success. Moreover, optical methods can avoid false interpretations and technical bias, which is sometimes difficult to detect when measuring other indirect variables. E.g. when measuring the backscattering laser light, only the cell size distribution is obtained, and the user have to interpret its shape.

Morphological information might be used also for synthetic biology approaches. The successful implementation of models, depends not only on the models used, but also on the measurement technology. The possibility to monitor changes in morphology directly *on line* enables to link morphological changes with –omics levels and feed models with real-time data and gain new parameters for monitoring and control.

The generation of data in real-time allows a better way of process monitoring, development and optimization. Nevertheless, there is a challenge in processing and interpreting the vast amount of data also in real time of the images acquired. The interpretation can be simplified by multiparametric data analysis, where not only imaging data will be encountered in 2 or 3-D, but also fluorescence or color information, and the time scale.

Despite the recent progresses, ISM has still some limitations that should be addressed. Beyond the industrial applications showed in the present study, other relevant industrial processes, where the morphology is affected along the cultivation time, can be a future application of the ISM (Lemoine, et al., 2017). Cell agglomeration in bacteria, chain elongation of lactic acid bacteria or clumping of filaments of *Streptomyces* have shown to be related to the process cultivation conditions applied, such

as oxygen and substrate limitation in large-scale bioreactors, or pH-gradients due to growth. In this study, only eukaryotic cells have been considered, but a lot of industrial relevant microorganisms are smaller prokaryotic organisms, or have a more complex morphological structure. Nevertheless, there is still a limitation in image resolution, which might be circumvented with respective hardware and software developments. An insufficient resolution also can be an obstacle in industrial-scale bioreactors with high cell densities cultivations, which can lead to overlapping events that can difficult or even prevent the cell recognition. Overlapping events are still under investigation, and so far overlapping cells cannot yet be differentiated with technologies here applied.

Since all microscopy analysis steps (image acquisition, particle identification and data analysis) need to be adapted to the organism of study, the application of ISM for the detection of a contamination, e.g. in cell culture, has to consider the size and shape of the contaminant, which can vary a lot from the resident cell line (e.g. bacteria). The focus is adjusted regarding the cell size of the organism of interest. Therefore, there is the possibility that other cells stay out of focus and remain invisible for particle identification. The cell recognition algorithm is based on a training set. Consequently, the learning machine has to have learnt, which events represent a contamination. Otherwise, the foreign cells may be focused, but they will be identified as background.

Although many challenges remain for practical applications, ISM has proven to be a reliable tool for relevant and interesting cases, in which no alternative monitoring methods can provide the same information in such a short time and low effort for sample preparation.

7. Conclusions

- Relevant statistical information from morphological features of the heterotrophic algae *C. cohnii* was obtained by the application of three-dimensional digital holographic microcopy and photo-optical *in situ* microscopy. Comparable measurements regarding the single-cell size distribution dynamics, as well as absolute sizes were obtained with both techniques.
- Relevant statistical information from morphological features of budding yeast *S. cerevisiae* on a single-cell basis was obtained by the application of three-dimensional digital holographic microscopy and photo-optical *in situ* microscopy.
- On the basis of the measurement of morphological parameters (size, circularity and phase homogeneity), it could be concluded whether the growth was favored or the DHA production was favored in *C. cohnii* cultivations.
- The intracellular accumulation of DHA could be predicted non-invasively and in real-time by single-cell size distribution measurements.
- Budding yeast cells were robust enough to maintain free sterol homeostasis under scale-down cultivation conditions.
- Sterol synthesis of the budding yeast was positively affected by oscillatory oxygen availability. The esterified form of the end product ergosterol increased by 75% under scale-down conditions in comparison to homogeneous conditions.
- Microbial growth slowed down in scale-down conditions and side-product formation occurred. After 12 hours under fed-batch scale-down conditions the final biomass was reduced by 20% in comparison to homogeneous conditions.
- Cell size and population heterogeneity were changed under oscillatory cultivation conditions. Morphological variability increased under severe exposure to oxygen limitation.
- The growth status of yeast cultivations could be distinguished with *in situ* microscopy during a glucose limited fed-batch cultivation.
- Maturation of yeast became trackable through the budding index (BI), ratio between cells with buds and total cells. The BI was well correlated with the cell growth rate (R^2=0.99).

8. **References**

Ackermann, M. (2015). A functional perspective on phenotypic heterogeneity in microorganisms. *Nature Reviews Microbiology* **13,** 497-508.

Albertin, W., Marullo, P., Aigle, M., Dillmann, C., de Vienne, D., Bely, M. and Sicard, D. (2011). Population size drives industrial *Saccharomyces cerevisiae* alcoholic fermentation and is under genetic control. *Applied and environmental microbiology* **77,** 2772-2784.

Amanullah, A., McFarlane, C. M., Emery, A. N. and Nienow, A. W. (2001). Scale-down model to simulate spatial pH variations in large-scale bioreactors. *Biotechnology and bioengineering* **73,** 390-399.

Arnezeder, C. and Hampel, W. (1990). Influence of growth rate on the accumulation of ergosterol in yeast-cells. *Biotechnology letters* **12,** 277-282.

Arthington-Skaggs, B., Crowell, D., Yang, H., Sturley, S. and Bard, M. (1996). Positive and negative regulation of a sterol biosynthetic gene (ERG3) in the post-squalene portion of the yeast ergosterol pathway. *FEBS letters* **392,** 161-165.

Athenstaedt, K., Zweytick, D., Jandrositz, A., Kohlwein, S. D. and Daum, G. (1999). Identification and characterization of major lipid particle proteins of the yeast Saccharomyces cerevisiae. *Journal of bacteriology* **181,** 6441-8.

Back, A., Krier, F., Nicaud, J.-M., Dhulster, P. and Rossignol, T. (2016). High-throughput fermentation screening for the yeast *Yarrowia lipolytica* with real-time monitoring of biomass and lipid production. *Microbial cell factories* **15,** 147.

Baeshen, N. A., Baeshen, M. N., Sheikh, A., Bora, R. S., Ahmed, M. M. M., Ramadan, H. A., Saini, K. S. and Redwan, E. M. (2014). Cell factories for insulin production. *Microbial cell factories* **13,** 141.

Baez, A., Flores, N., Bolívar, F. and Ramírez, O. T. (2011). Simulation of dissolved CO2 gradients in a scale-down system: A metabolic and transcriptional study of recombinant *Escherichia coli*. *Biotechnology journal* **6,** 959-967.

Baicu, L., Ifrim, G., Frangu, L. and Caraman, S. (2015). Viability diagnosis in biotechnological cultures through image processing. *System Theory, Control and Computing (ICSTCC), 2015 19th International Conference on*, pp. 770-775.

Bailey, J. E. and Ollis, D. F. (1977). *Biochemical engineering fundamentals*. McGraw-Hill.

Barrick, J. E. and Lenski, R. E. (2013). Genome dynamics during experimental evolution. *Nature Reviews Genetics* **14,** 827-839.

Belini, V. L., Wiedemann, P. and Suhr, H. (2013). *In situ* microscopy: A perspective for industrial bioethanol production monitoring. *Journal of microbiological methods* **93,** 224-232.

Bellgardt, K. H. (1998). Proces models for production of β-lactam antibiotics In Schügerl, K. (Ed), *Relation Between Morphology and Process Performances*, Springer Berlin Heidelberg: Berlin, Heidelberg, pp. 153-194.

Beopoulos, A., Nicaud, J. M. and Gaillardin, C. (2011). An overview of lipid metabolism in yeasts and its impact on biotechnological processes. *Applied microbiology and biotechnology* **90,** 1193-206.

Besmer, M. D., Weissbrodt, D. G., Kratochvil, B. E., Sigrist, J. A., Weyland, M. S. and Hammes, F. (2014). The feasibility of automated online flow cytometry for in-situ monitoring of microbial dynamics in aquatic ecosystems. *Frontiers in microbiology* **5**.

Beutel, S. and Henkel, S. (2011). *In situ* sensor techniques in modern bioprocess monitoring. *Applied microbiology and biotechnology* **91,** 1493.

Binder, D., Drepper, T., Jaeger, K.-E., Delvigne, F., Wiechert, W., Kohlheyer, D. and Grünberger, A. (2017). Homogenizing bacterial cell factories: analysis and engineering of phenotypic heterogeneity. *Metabolic engineering* **42,** 145-156.

Bisova, K. and Zachleder, V. (2014). Cell-cycle regulation in green algae dividing by multiple fission. *Journal of experimental botany* **65,** 2585-602.

Blasi, T., Hennig, H., Summers, H. D., Theis, F. J., Cerveira, J., Patterson, J. O., Davies, D., Filby, A., Carpenter, A. E. and Rees, P. (2016). Label-free cell cycle analysis for high-throughput imaging flow cytometry. *Nature communications* **7,** 10256.

Bluma, A., Höpfner, T., Lindner, P., Rehbock, C., Beutel, S., Riechers, D., Hitzmann, B. and Scheper, T. (2010). *In-situ* imaging sensors for bioprocess monitoring: state of the art. *Analytical and bioanalytical chemistry* **398,** 2429-2438.

Bonk, S., Sandor, M., Rudinger, F., Tscheschke, B., Prediger, A., Babitzky, A., Solle, D., Beutel, S. and Scheper, T. (2011). *In-situ* microscopy and 2D fluorescence spectroscopy as online methods for monitoring CHO cells during cultivation. *BMC Proc* **5 Suppl 8,** P76.

Bouix, M. and Ghorbal, S. (2015). Rapid assessment of *Oenococcus oeni* activity by measuring intracellular pH and membrane potential by flow cytometry, and its application to the more effective control of malolactic fermentation. *International journal of food microbiology* **193,** 139-146.

Brauer, M. J., Huttenhower, C., Airoldi, E. M., Rosenstein, R., Matese, J. C., Gresham, D., Boer, V. M., Troyanskaya, O. G. and Botstein, D. (2008). Coordination of growth rate, cell cycle, stress response, and metabolic activity in yeast. *Molecular biology of the cell* **19,** 352-67.

Brockman, I. M. and Prather, K. L. (2015). Dynamic metabolic engineering: new strategies for developing responsive cell factories. *Biotechnology journal* **10,** 1360-1369.

Brognaux, A., Han, S., Sørensen, S. J., Lebeau, F., Thonart, P. and Delvigne, F. (2013a). A low-cost, multiplexable, automated flow cytometry procedure for the characterization of microbial stress dynamics in bioreactors. *Microbial cell factories* **12,** 100.

Brognaux, A., Thonart, P., Delvigne, F., Neubauer, P., Twizere, J. C., Francis, F. and Gorret, N. (2013b). Direct and indirect use of GFP whole cell biosensors for the assessment of bioprocess performances: Design of milliliter scale-down bioreactors. *Biotechnology progress* **29,** 48-59.

Brunner, M., Braun, P., Doppler, P., Posch, C., Behrens, D., Herwig, C. and Fricke, J. (2017). The impact of pH inhomogeneities on CHO cell physiology and fed-batch process performance–two-compartment scale-down modelling and intracellular pH excursion. *Biotechnology journal* **12**.

Bryan, A. K., Engler, A., Gulati, A. and Manalis, S. R. (2012). Continuous and long-term volume measurements with a commercial Coulter counter. *PLoS One* **7,** e29866.

Bryan, A. K., Goranov, A., Amon, A. and Manalis, S. R. (2010). Measurement of mass, density, and volume during the cell cycle of yeast. *Proceedings of the National Academy of Sciences* **107,** 999-1004.

Budde, C. F., Riedel, S. L., Willis, L. B., Rha, C. and Sinskey, A. J. (2011). Production of poly(3-hydroxybutyrate-co-3-hydroxyhexanoate) from plant oil by engineered *Ralstonia eutropha* strains. *Applied and environmental microbiology* **77,** 2847-54.

Bühligen, F., Lindner, P., Fetzer, I., Stahl, F., Scheper, T., Harms, H. and Müller, S. (2014). Analysis of aging in lager brewing yeast during serial repitching. *Journal of biotechnology* **187,** 60-70.

Buysschaert, B., Byloos, B., Leys, N., Van Houdt, R. and Boon, N. (2016). Reevaluating multicolor flow cytometry to assess microbial viability. *Applied microbiology and biotechnology* **100,** 9037-9051.

Bylund, F., Collet, E., Enfors, S.-O. and Larsson, G. (1998). Substrate gradient formation in the large-scale bioreactor lowers cell yield and increases by-product formation. *Bioprocess Engineering* **18,** 171-180.

Bylund, F., Guillard, F., Enfors, S.-O., Trägårdh, C. and Larsson, G. (1999). Scale down of recombinant protein production: a comparative study of scaling performance. *Bioprocess Engineering* **20,** 377-389.

Camisard, V., Brienne, J., Baussart, H., Hammann, J. and Suhr, H. (2002). Inline characterization of cell concentration and cell volume in agitated bioreactors using in situ microscopy: application to volume variation induced by osmotic stress. *Biotechnology and bioengineering* **78,** 73-80.

Carbó, R., Ginovart, M., Carta, A., Portell, X. and Del Valle, L. J. (2015). Effect of aerobic and microaerophilic culture in the growth dynamics of *Saccharomyces cerevisiae* and in training of quiescent and non-quiescent subpopulations. *Archives of microbiology* **197,** 991-999.

Carlquist, M., Fernandes, R. L., Helmark, S., Heins, A.-L., Lundin, L., Sørensen, S. J., Gernaey, K. V. and Lantz, A. E. (2012). Physiological heterogeneities in microbial populations and implications for physical stress tolerance. *Microbial cell factories* **11,** 94.

Caspeta, L., Flores, N., Pérez, N. O., Bolívar, F. and Ramírez, O. T. (2009). The effect of heating rate on *Escherichia coli* metabolism, physiological stress, transcriptional response, and production of temperature-induced recombinant protein: A scale-down study. *Biotechnology and bioengineering* **102,** 468-482.

Chan, Y.-H. M. and Marshall, W. F. (2010). Scaling properties of cell and organelle size. *Organogenesis* **6,** 88-96.

Chi, Z., Liu, Y., Frear, C. and Chen, S. (2009). Study of a two-stage growth of DHA-producing marine algae *Schizochytrium limacinum* SR21 with shifting dissolved oxygen level. *Applied microbiology and biotechnology* **81,** 1141-1148.

Coelho, M. A., Belo, I., Pinheiro, R., Amaral, A. L., Mota, M., Coutinho, J. A. and Ferreira, E. C. (2004). Effect of hyperbaric stress on yeast morphology: study by automated image analysis. *Applied microbiology and biotechnology* **66,** 318-24.

Cook, M. and Tyers, M. (2007). Size control goes global. *Current opinion in biotechnology* **18,** 341-350.

Cooksey, K. E., Guckert, J. B., Williams, S. A. and Callis, P. R. (1987). Fluorometric-Determination of the Neutral Lipid-Content of Microalgal Cells Using Nile Red. *Journal of Microbiological Methods* **6,** 333-345.

Croughan, M. S., Konstantinov, K. B. and Cooney, C. (2015). The future of industrial bioprocessing: Batch or continuous? *Biotechnology and bioengineering* **112,** 648-651.

Daum, G., Lees, N. D., Bard, M. and Dickson, R. (1998). Biochemistry, cell biology and molecular biology of lipids of *Saccharomyces cerevisiae*. *Yeast* **14,** 1471-1510.

Davey, H. M. (2011). Life, Death, and In-Between: Meanings and Methods in Microbiology. *Applied and environmental microbiology* **77,** 5571-5576.

de la Jara, A., Mendoza, H., Martel, A., Molina, C., Nordstron, L., de la Rosa, V. and Diaz, R. (2003). Flow cytometric determination of lipid content in a marine dinoflagellate, *Crypthecodinium cohnii. Journal of Applied Phycology* **15,** 433-438.

De Swaaf, M. E., Sijtsma, L. and Pronk, J. T. (2003). High-cell-density fed-batch cultivation of the docosahexaenoic acid producing marine alga *Crypthecodinium cohnii*. *Biotechnol Bioeng* **81,** 666-72.

Delvigne, F., Boxus, M., Ingels, S. and Thonart, P. (2009). Bioreactor mixing efficiency modulates the activity of a prpoS:: GFP reporter gene in *E. coli*. *Microb Cell Fact* **8,** 15.

Delvigne, F. and Goffin, P. (2014). Microbial heterogeneity affects bioprocess robustness: dynamic single-cell analysis contributes to understanding of microbial populations. *Biotechnology journal* **9,** 61-72.

Delvigne, F., Takors, R., Mudde, R., van Gulik, W. and Noorman, H. (2017). Bioprocess scale-up/down as integrative enabling technology: from fluid mechanics to systems biology and beyond. *Microbial biotechnology* **10,** 1267-1274.

Demain, A. L. and Martens, E. (2017). Production of valuable compounds by molds and yeasts. *The Journal of antibiotics* **70,** 347.

Desai, S. G. (2015). Continuous and semi-continuous cell culture for production of blood clotting factors. *Journal of biotechnology* **213,** 20-27.

Di Talia, S., Skotheim, J. M., Bean, J. M., Siggia, E. D. and Cross, F. R. (2007). The effects of molecular noise and size control on variability in the budding yeast cell cycle. *Nature* **448,** 947-51.

Di Talia, S., Wang, H., Skotheim, J. M., Rosebrock, A. P., Futcher, B. and Cross, F. R. (2009). Daughter-specific transcription factors regulate cell size control in budding yeast. *PLoS biology* **7,** e1000221.

Du, H. X., Xiao, W. H., Wang, Y., Zhou, X., Zhang, Y., Liu, D. and Yuan, Y. J. (2016). Engineering *Yarrowia lipolytica* for Campesterol Overproduction. *Plos One* **11,** 14.

Eggeling, L. and Bott, M. (2015). A giant market and a powerful metabolism: l-lysine provided by *Corynebacterium glutamicum*. *Applied microbiology and biotechnology* **99,** 3387-3394.

Enfors, S. O., Jahic, M., Rozkov, A., Xu, B., Hecker, M., Jurgen, B., Kruger, E., Schweder, T., Hamer, G., O'Beirne, D., Noisommit-Rizzi, N., Reuss, M., Boone, L., Hewitt, C., McFarlane, C., Nienow, A., Kovacs, T., Tragardh, C., Fuchs, L., Revstedt, J., Friberg, P. C., Hjertager, B., Blomsten, G., Skogman, H., Hjort, S., Hoeks, F., Lin, H. Y., Neubauer, P., van der Lans, R., Luyben, K., Vrabel, P. and Manelius, A. (2001). Physiological responses to mixing in large scale bioreactors. *Journal of biotechnology* **85,** 175-85.

Feng, C. and Johns, M. R. (1991). Effect of C/N Ratio and Aeration on the Fatty-Acid Composition of Heterotrophic *Chlorella-Sorokiniana*. *Journal of Applied Phycology* **3,** 203-209.

Fernandes, R. L., Nierychlo, M., Lundin, L., Pedersen, A. E., Tellez, P. P., Dutta, A., Carlquist, M., Bolic, A., Schäpper, D. and Brunetti, A. C. (2011). Experimental methods and modeling techniques for description of cell population heterogeneity. *Biotechnology advances* **29,** 575-599.

Food, U. and Administration, D. (2004). PAT guidance for industry–a framework for innovative pharmaceutical development, manufacturing and quality assurance. US Department of Health and Human Services. *Food and Drug Administration, Center for drug evaluation and research, Center for veterinary medicine, Office of regulatory affairs, Rockville, MD*.

Gao, D., Zeng, J., Yu, X., Dong, T. and Chen, S. (2014). Improved lipid accumulation by morphology engineering of oleaginous fungus *Mortierella isabellina*. *Biotechnology and bioengineering* **111,** 1758-66.

Garaiova, M., Zambojova, V., Simova, Z., Griac, P. and Hapala, I. (2014). Squalene epoxidase as a target for manipulation of squalene levels in the yeast *Saccharomyces cerevisiae*. *Fems Yeast Research* **14,** 310-323.

Garcia-Ochoa, F. and Gomez, E. (2009). Bioreactor scale-up and oxygen transfer rate in microbial processes: an overview. *Biotechnology advances* **27,** 153-176.

Ge, X., Zhao, X. and Bai, F. (2005). Online monitoring and characterization of flocculating yeast cell flocs during continuous ethanol fermentation. *Biotechnology and bioengineering* **90,** 523-531.

Geiler-Samerotte, K., Bauer, C., Li, S., Ziv, N., Gresham, D. and Siegal, M. (2013). The details in the distributions: why and how to study phenotypic variability. *Current opinion in biotechnology* **24,** 752-759.

George, S., Larsson, G. and Enfors, S.-O. (1993). A scale-down two-compartment reactor with controlled substrate oscillations: metabolic response of *Saccharomyces cerevisiae*. *Bioprocess and biosystems engineering* **9,** 249-257.

George, S., Larsson, G., Olsson, K. and Enfors, S.-O. (1998). Comparison of the Baker's yeast process performance in laboratory and production scale. *Bioprocess and biosystems engineering* **18,** 135-142.

Godin, M., Delgado, F. F., Son, S., Grover, W. H., Bryan, A. K., Tzur, A., Jorgensen, P., Payer, K., Grossman, A. D. and Kirschner, M. W. (2010). Using buoyant mass to measure the growth of single cells. *Nature methods* **7,** 387-390.

Gomes, J., Chopda, V. R. and Rathore, A. S. (2015). Integrating systems analysis and control for implementing process analytical technology in bioprocess development. *Journal of Chemical Technology and Biotechnology* **90,** 583-589.

González-Cabaleiro, R., Mitchell, A. M., Smith, W., Wipat, A. and Ofiţeru, I. D. (2017). Heterogeneity in Pure Microbial Systems: Experimental Measurements and Modeling. *Frontiers in microbiology* **8,** 1813.

Gonzalez, R., Vian, A. and Carrascosa, A. V. (2008). Note. Morphological Changes in *Saccharomyces cerevisiae* during the Second Fermentation of Sparkling Wines. *Food Science and Technology International* **14,** 393-398.

Guan, N., Li, J., Shin, H.-d., Du, G., Chen, J. and Liu, L. (2017). Microbial response to environmental stresses: from fundamental mechanisms to practical applications. *Applied microbiology and biotechnology* **101,** 3991-4008.

Guez, J. S., Cassar, J. P., Wartelle, F., Dhulster, P. and Suhr, H. (2004). Real time in situ microscopy for animal cell-concentration monitoring during high density culture in bioreactor. *J Biotechnol* **111,** 335-43.

Gulati, S., Balderes, D., Kim, C., Guo, Z. M. A., Wilcox, L., Area-Gomez, E., Snider, J., Wolinski, H., Stagljar, I., Granato, J. T., Ruggles, K. V., DeGiorgis, J. A., Kohlwein, S. D., Schon, E. A. and Sturley, S. L. (2015). ATP-binding cassette transporters and sterol O-acyltransferases interact at membrane microdomains to modulate sterol uptake and esterification. *Faseb Journal* **29,** 4682-4694.

Hammes, F., Broger, T., Weilenmann, H. U., Vital, M., Helbing, J., Bosshart, U., Huber, P., Peter Odermatt, R. and Sonnleitner, B. (2012). Development and laboratory-scale testing of a fully automated online flow cytometer for drinking water analysis. *Cytometry Part A* **81,** 508-516.

Han, Y., Gu, Y., Zhang, A. C. and Lo, Y.-H. (2016). imaging technologies for flow cytometry. *Lab on a chip* **16,** 4639-4647.

Hansen, A. S., Hao, N. and O'shea, E. K. (2015). High-throughput microfluidics to control and measure signaling dynamics in single yeast cells. *Nature protocols* **10,** 1181-1197.

Haringa, C., Deshmukh, A. T., Mudde, R. F. and Noorman, H. J. (2017). Euler-Lagrange analysis towards representative down-scaling of a 22m 3 aerobic *S. cerevisiae* fermentation. *Chemical Engineering Science*.

Havlik, I., Lindner, P., Scheper, T. and Reardon, K. F. (2013a). On-line monitoring of large cultivations of microalgae and cyanobacteria. *Trends Biotechnol* **31,** 406-14.

Havlik, I., Reardon, K. F., Ünal, M., Lindner, P., Prediger, A., Babitzky, A., Beutel, S. and Scheper, T. (2013b). Monitoring of microalgal cultivations with on-line, flow-through microscopy. *Algal Research* **2,** 253-257.

Heins, A. L., Lencastre Fernandes, R., Gernaey, K. V. and Lantz, A. E. (2015). Experimental and in silico investigation of population heterogeneity in continuous *Saccharomyces cerevisiae* scale-down fermentation in a two-compartment setup. *Journal of Chemical Technology and Biotechnology* **90,** 324-340.

Hewitt, C. J. and Nebe-Von-Caron, G. (2001). An industrial application of multiparameter flow cytometry: assessment of cell physiological state and its application to the study of microbial fermentations. *Cytometry* **44,** 179-187.

Hewitt, C. J. and Nienow, A. W. (2007). The scale-up of microbial batch and fed-batch fermentation processes. *Advances in applied microbiology* **62,** 105-35.

Hillig, F. (2014). Impact of cultivation conditions and bioreactor design on docosahexaenoic acid production by a heterotrophic marine microalga - A scale up study, *Faculty of Process Sciences*, TU Berlin: City, pp. 163.

Hillig, F., Annemüller, S., Chmielewska, M., Pilarek, M., Junne, S. and Neubauer, P. (2013). Bioprocess Development in Single-Use Systems for Heterotrophic Marine Microalgae. *Chemie Ingenieur Technik* **85,** 153-161.

Hillig, F., Pilarek, M., Junne, S. and Neubauer, P. (2014a). Cultivation of Marine Microorganisms in Single-Use Systems. *Disposable Bioreactors Ii* **138,** 179-206.

Hillig, F., Porscha, N., Junne, S. and Neubauer, P. (2014b). Growth and docosahexaenoic acid production performance of the heterotrophic marine microalgae *Crypthecodinium cohnii* in the wave-mixed single-use reactor CELL-tainer. *Engineering in Life Sciences* **14,** 254-263.

Huang, G. H., Chen, G. and Chen, F. (2009). Rapid screening method for lipid production in alga based on Nile red fluorescence. *Biomass & Bioenergy* **33,** 1386-1392.

Jahnke, L. and Klein, H. P. (1983). Oxygen requirements for formation and activity of the squalene epoxidase in *Saccharomyces cerevisiae*. *Journal of bacteriology* **155,** 488-492.

Jenzsch, M., Gnoth, S., Kleinschmidt, M., Simutis, R. and Lübbert, A. (2006). Improving the batch-to-batch reproducibility in microbial cultures during recombinant protein production by guiding the process along a predefined total biomass profile. *Bioprocess and biosystems engineering* **29,** 315-321.

Jin, M., Slininger, P. J., Dien, B. S., Waghmode, S., Moser, B. R., Orjuela, A., da Costa Sousa, L. and Balan, V. (2015). Microbial lipid-based lignocellulosic biorefinery: feasibility and challenges. *Trends in Biotechnology* **33,** 43-54.

Junker, B. H. (2004). Scale-up methodologies for *Escherichia coli* and yeast fermentation processes. *Journal of Bioscience and Bioengineering* **97,** 347-364.

Junne, S., Klingner, A., Kabisch, J., Schweder, T. and Neubauer, P. (2011). A two-compartment bioreactor system made of commercial parts for bioprocess scale-down studies: Impact of oscillations on *Bacillus subtilis* fed-batch cultivations. *Biotechnology Journal* **6,** 1009-1017.

Kan, A. (2017). Machine learning applications in cell image analysis. *Immunology and Cell Biology*.

Kasprow, R. P., Lange, A. J. and Kirwan, D. J. (1998). Correlation of fermentation yield with yeast extract composition as characterized by near-infrared spectroscopy. *Biotechnol Prog* **14,** 318-25.

Kauermann, G. and Kuechenhoff, H. (2010). *Stichproben: Methoden und praktische Umsetzung mit R*. Springer-Verlag.

Khona, D. K., Shirolikar, S. M., Gawde, K. K., Hom, E., Deodhar, M. A. and D'Souza, J. S. (2016). Characterization of salt stress-induced palmelloids in the green alga, C*hlamydomonas reinhardtii*. *Algal Research* **16,** 434-448.

Kielhorn, E., Sachse, S., Moench-Tegeder, M., Naegele, H.-J., Haelsig, C., Oechsner, H., Vonau, W., Neubauer, P. and Junne, S. (2015). Multiposition sensor technology and lance-based sampling for improved monitoring of the liquid phase in biogas processes. *Energy & Fuels* **29,** 4038-4045.

Kirdar, A. O., Chen, G., Weidner, J. and Rathore, A. S. (2010). Application of near-infrared (NIR) spectroscopy for screening of raw materials used in the cell culture medium for the production of a recombinant therapeutic protein. *Biotechnology Progress* **26,** 527-531.

Klug, L. and Daum, G. (2014). Yeast lipid metabolism at a glance. *Fems Yeast Research* **14,** 369-388.

Konstantinov, K. B. and Cooney, C. L. (2015). White Paper on Continuous Bioprocessing. May 20–21, 2014 Continuous Manufacturing Symposium. *Journal of Pharmaceutical Sciences* **104,** 813-820.

Kothari, R., Pandey, A., Ahmad, S., Kumar, A., Pathak, V. V. and Tyagi, V. (2017). Microalgal cultivation for value-added products: a critical enviro-economical assessment. *3 Biotech* **7,** 243.

Kwok, A. C. and Wong, J. T. (2005). Lipid biosynthesis and its coordination with cell cycle progression. *Plant and cell physiology* **46,** 1973-1986.

Lange, J., Takors, R. and Blombach, B. (2017). Zero-growth bioprocesses: A challenge for microbial production strains and bioprocess engineering. *Engineering in Life Sciences* **17,** 27-35.

Lapin, A., Müller, D. and Reuss, M. (2004). Dynamic Behavior of Microbial Populations in Stirred Bioreactors Simulated with Euler−Lagrange Methods: Traveling along the Lifelines of Single Cells. *Industrial & Engineering Chemistry Research* **43,** 4647-4656.

Lapin, A., Schmid, J. and Reuss, M. (2006). Modeling the dynamics of *E. coli* populations in the three-dimensional turbulent field of a stirred-tank bioreactor—A structured–segregated approach. *Chemical Engineering Science* **61,** 4783-4797.

Larsson, G., Tornkvist, M., Wernersson, E. S., Tragardh, C., Noorman, H. and Enfors, S. O. (1996). Substrate gradients in bioreactors: Origin and consequences. *Bioprocess Engineering* **14,** 281-289.

Laverty, D. J., Kury, A. L., Kuksin, D., Pirani, A., Flanagan, K. and Chan, L. L. (2013). Automated quantification of budding *Saccharomyces cerevisiae* using a novel image cytometry method. *Journal of industrial microbiology & biotechnology* **40,** 581-8.

Leitao, R. (2017). The duration of mitosis and daughter cell size are modulated by nutrients in budding yeast, University of California, Santa Cruz: City.

Lemoine, A., Delvigne, F., Bockisch, A., Neubauer, P. and Junne, S. (2017). Tools for the determination of population heterogeneity caused by inhomogeneous cultivation conditions. *Journal of biotechnology*.

Lemoine, A., Limberg, M. H., Kästner, S., Oldiges, M., Neubauer, P. and Junne, S. (2016). Performance loss of *Corynebacterium glutamicum* cultivations under scale-down conditions using complex media. *Engineering in Life Sciences*.

Lemoine, A., Maya Martínez-Iturralde, N., Spann, R., Neubauer, P. and Junne, S. (2015). Response of *Corynebacterium glutamicum* exposed to oscillating cultivation conditions in a two-and a novel three-compartment scale-down bioreactor. *Biotechnology and bioengineering* **112,** 1220-1231.

Lencastre Fernandes, R., Carlquist, M., Lundin, L., Heins, A. L., Dutta, A., Sorensen, S. J., Jensen, A. D., Nopens, I., Lantz, A. E. and Gernaey, K. V. (2013). Cell mass and cell cycle dynamics of an asynchronous budding yeast population: experimental observations, flow cytometry data analysis, and multi-scale modeling. *Biotechnology and bioengineering* **110,** 812-26.

Leupold, M., Hindersin, S., Gust, G., Kerner, M. and Hanelt, D. (2013). Influence of mixing and shear stress on *Chlorella vulgaris*, Scenedesmus obliquus, and Chlamydomonas reinhardtii. *Journal of Applied Phycology* **25,** 485-495.

Lewis, C. L., Craig, C. C. and Senecal, A. G. (2014). Mass and density measurements of live and dead gram-negative and gram-positive bacterial populations. *Applied and environmental microbiology* **80,** 3622-3631.

Lewis, N. I., Xu, W., Jericho, S. K., Kreuzer, H. J., Jericho, M. H. and Cembella, A. D. (2006). Swimming speed of three species of Alexandrium (Dinophyceae) as determined by digital in-line holography. *Phycologia* **45,** 61-70.

Limberg, M. H., Joachim, M., Klein, B., Wiechert, W. and Oldiges, M. (2017). pH fluctuations imperil the robustness of *C. glutamicum* to short term oxygen limitation. *Journal of biotechnology* **259,** 248-260.

Lin, H., Wang, Q., Shen, Q., Zhan, J. and Zhao, Y. (2013). Genetic engineering of microorganisms for biodiesel production. *Bioengineered* **4,** 292-304.

Lindmeyer, M., Jahn, M., Vorpahl, C., Müller, S., Schmid, A. and Bühler, B. (2015). Variability in subpopulation formation propagates into biocatalytic variability of engineered Pseudomonas putida strains. *Frontiers in microbiology* **6**.

Lodolo, E. J. and Cantrell, I. C. (2007). Yeast Vitality-A Holistic Approach Toward an Integrated Solution to Predict Yeast Performance. *JOURNAL-AMERICAN SOCIETY OF BREWING CHEMISTS* **65,** 202.

Lorenz, E., Runge, D., Marba-Ardebol, A. M., Schmacht, M., Stahl, U. and Senz, M. (2017). Systematic development of a two-stage fed-batch process for lipid accumulation in Rhodotorula glutinis. *Journal of biotechnology* **246,** 4-15.

Maass, S., Rojahn, J., Haensch, R. and Kraume, M. (2012). Automated drop detection using image analysis for online particle size monitoring in multiphase systems. *Computers & Chemical Engineering* **45,** 27-37.

Machado, M. D. and Soares, E. V. (2014). Modification of cell volume and proliferative capacity of Pseudokirchneriella subcapitata cells exposed to metal stress. *Aquatic toxicology* **147,** 1-6.

Maczek, J., Junne, S., Nowak, P. and Goetz, P. (2006). Metabolic flux analysis of the sterol pathway in the yeast *Saccharomyces cerevisiae*. *Bioprocess and biosystems engineering* **29,** 241-252.

Makushok, T., Alves, P., Huisman, S. M., Kijowski, A. R. and Brunner, D. (2016). Sterol-rich membrane domains define fission yeast cell polarity. *Cell* **165,** 1182-1196.

Manfredini, R., Cavallera, V., Marini, L. and Donati, G. (1983). Mixing and oxygen transfer in conventional stirred fermentors. *Biotechnology and bioengineering* **25,** 3115-3131.

Marbà-Ardébol, A.-M., Emmerich, J., Neubauer, P. and Junne, S. (2017). Single-cell-based monitoring of fatty acid accumulation in *Crypthecodinium cohnii* with three-dimensional holographic and in situ microscopy. *Process Biochemistry* **52,** 223-232.

Marba-Ardebol, A. M., Emmerich, J., Muthig, M., Neubauer, P. and Junne, S. (2018a). In situ microscopy for real-time determination of single-cell morphology in bioprocesses. *Journal of visualized experiments : JoVE*.

Marba-Ardebol, A. M., Emmerich, J., Muthig, M., Neubauer, P. and Junne, S. (2018b). Real-time monitoring of the budding index in *Saccharomyces cerevisiae* batch cultivations with in situ microscopy. *Microbial Cell Factories* **submitted**.

Marba-Ardebol, A. M., Turon, X., Neubauer, P. and Junne, S. (2016). Application of flow cytometry analysis to elucidate the impact of scale-down conditions in *Escherichia coli* cultivations P. Gil Salvador 2013 Award in Bioengineering category.(November 22, 2013 in the Annual General Assembly of the AIQS). *Afinidad* **73**.

Marbà-Ardébol, A. M., Bockisch, A., Neubauer, P. and Junne, S. (2017). Sterol synthesis and cell size distribution under oscillatory growth conditions in *Saccharomyces cerevisiae* scale-down cultivations. *Yeast*.

Marquard, D., Enders, A., Roth, G., Rinas, U., Scheper, T. and Lindner, P. (2016). In situ microscopy for online monitoring of cell concentration in *Pichia pastoris* cultivations. *Journal of biotechnology* **234,** 90-8.

Marquard, D., Schneider-Barthold, C., Düsterloh, S., Scheper, T. and Lindner, P. (2017). Online monitoring of cell concentration in high cell density *Escherichia coli* cultivations using in situ Microscopy. *Journal of biotechnology* **259,** 83-85.

Martins, B. M. and Locke, J. C. (2015). Microbial individuality: how single-cell heterogeneity enables population level strategies. *Current opinion in microbiology* **24,** 104-112.

Maskell, D. L., Kennedy, A. I., Hodgson, J. A. and Smart, K. A. (2003). Chronological and replicative lifespan of polyploid *Saccharomyces cerevisiae* (syn. *S. pastorianus*). *FEMS yeast research* **3,** 201-209.

Mathuis, P. and Jooris, S. (2013). Digital holographic microscope with fluid systems, Google Patents: City.

Matos, J., Cardoso, C., Bandarra, N. M. and Afonso, C. (2017). Microalgae as healthy ingredients for functional food: a review. *Food & function* **8,** 2672-2685.

Mendes, A., Reis, A., Vasconcelos, R., Guerra, P. and da Silva, T. L. (2009). *Crypthecodinium cohnii* with emphasis on DHA production: a review. *Journal of Applied Phycology* **21,** 199-214.

Mittag, A. and Tárnok, A. (2009). Basics of standardization and calibration in cytometry–a review. *Journal of biophotonics* **2,** 470-481.

Müller, S., Harms, H. and Bley, T. (2010). Origin and analysis of microbial population heterogeneity in bioprocesses. *Current opinion in biotechnology* **21,** 100-113.

Mullner, H. and Daum, G. (2004). Dynamics of neutral lipid storage in yeast. *Acta biochimica Polonica* **51,** 323-47.

Nadeau, J. L., Cho, Y. B., Kühn, J. and Liewer, K. (2016). Improved tracking and resolution of bacteria in holographic microscopy using dye and fluorescent protein labeling. *Frontiers in chemistry* **4**.

Namdev, P. K., Thompson, B. G. and Gray, M. R. (1992). Effect of feed zone in fed-batch fermentations of Saccharomyces cerevisiae. *Biotechnol Bioeng* **40,** 235-46.

Navarro Llorens, J. M., Tormo, A. and Martínez-García, E. (2010). Stationary phase in gram-negative bacteria. *FEMS Microbiology Reviews* **34,** 476-495.

Neubauer, P., Cruz, N., Glauche, F., Junne, S., Knepper, A. and Raven, M. (2013). Consistent development of bioprocesses from microliter cultures to the industrial scale. *Engineering in Life Sciences* **13,** 224-238.

Neubauer, P., Haggstrom, L. and Enfors, S. O. (1995). Influence of substrate oscillations on acetate formation and growth yield in *Escherichia coli* glucose limited fed-batch cultivations. *Biotechnology and bioengineering* **47,** 139-46.

Neubauer, P. and Junne, S. (2010). Scale-down simulators for metabolic analysis of large-scale bioprocesses. *Current Opinion in Biotechnology* **21,** 114-121.

Neubauer, P. and Junne, S. (2016). Scale-Up and scaledown methodologies for bioreactors. Chichester: John Wiley & Sons.

Nguyen, K., Murray, S., Lewis, J. A. and Kumar, P. (2017). Morphology, cell division, and viability of *Saccharomyces cerevisiae* at high hydrostatic pressure. *arXiv preprint arXiv:1703.00547*.

Nielsen, J. (2013). Production of biopharmaceutical proteins by yeast: advances through metabolic engineering. *Bioengineered* **4,** 207-211.

Nielsen, J., Villadsen, J. and Lidén, G. (2003). Scale-up of bioprocesses, *Bioreaction Engineering Principles*, Springer, pp. 477-518.

Nienow, A. W., Nordkvist, M. and Boulton, C. A. (2011). Scale-down/scale-up studies leading to improved commercial beer fermentation. *Biotechnol J* **6,** 911-25.

Nienow, A. W., Scott, W. H., Hewitt, C. J., Thomas, C. R., Lewis, G., Amanullah, A., Kiss, R. and Meier, S. J. (2013). Scale-down studies for assessing the impact of different stress parameters on growth and product quality during animal cell culture. *Chemical Engineering Research and Design* **91,** 2265-2274.

Noorman, H. J. and Heijnen, J. J. (2017). Biochemical engineering's grand adventure. *Chemical Engineering Science* **170,** 677-693.

Novak, J., Basarova, G., Teixeira, J. and Vicente, A. (2007). Monitoring of brewing yeast propagation under aerobic and anaerobic conditions employing flow cytometry. *Journal of the Institute of Brewing* **113,** 249-255.

Ohnuki, S., Enomoto, K., Yoshimoto, H. and Ohya, Y. (2014). Dynamic changes in brewing yeast cells in culture revealed by statistical analyses of yeast morphological data. *Journal of bioscience and bioengineering* **117,** 278-84.

Okada, H., Ohnuki, S., Roncero, C., Konopka, J. B. and Ohya, Y. (2014). Distinct roles of cell wall biogenesis in yeast morphogenesis as revealed by multivariate analysis of high-dimensional morphometric data. *Molecular biology of the cell* **25,** 222-33.

Onyeaka, H., Nienow, A. W. and Hewitt, C. J. (2003). Further studies related to the scale-up of high cell density *escherichia coli* fed-batch fermentations. *Biotechnology and bioengineering* **84,** 474-484.

Oosterhuis, N. M., Kossen, N. W., Olivier, A. P. and Schenk, E. S. (1985). Scale-down and optimization studies of the gluconic acid fermentation by *Gluconobacter oxydans*. *Biotechnology and Bioengineering* **27,** 711-20.

Oosterhuis, N. M. G. (1984). Scale-down of bioreactors, Delft University of Technology.The Netherlands: City.

Ozturk, S. S. (2014). Opportunities and Challenges for the Implementation of Continuous Processing in Biomanufacturing. *Continuous Processing in Pharmaceutical Manufacturing*.

Panckow, R. P., Reinecke, L., Cuellar, M. C. and Maaß, S. (2017). Photo-Optical In-Situ Measurement of Drop Size Distributions: Applications in Research and Industry. *Oil Gas Sci. Technol. – Rev. IFP Energies nouvelles* **72,** 14.

Pereira, F. B., Guimarães, P. M., Teixeira, J. A. and Domingues, L. (2011). Robust industrial *Saccharomyces cerevisiae* strains for very high gravity bio-ethanol fermentations. *Journal of bioscience and bioengineering* **112,** 130-136.

Ploier, B., Daum, G. and Petrovič, U. (2014). Molecular Mechanisms in Yeast Carbon Metabolism: Lipid Metabolism and Lipidomics, *Molecular Mechanisms in Yeast Carbon Metabolism*, Springer, pp. 169-215.

Polakowski, T., Bastl, R., Stahl, U. and Lang, C. (1999). Enhanced sterol-acyl transferase activity promotes sterol accumulation in *Saccharomyces cerevisiae*. *Applied microbiology and biotechnology* **53,** 30-35.

Porro, D., Vai, M., Vanoni, M., Alberghina, L. and Hatzis, C. (2009). Analysis and modeling of growing budding yeast populations at the single cell level. *Cytometry. Part A : the journal of the International Society for Analytical Cytology* **75,** 114-20.

Powell, C. D., Quain, D. E. and Smart, K. A. (2003). The impact of brewing yeast cell age on fermentation performance, attenuation and flocculation. *FEMS yeast research* **3,** 149-157.

Qin, L., Liu, L., Zeng, A.-P. and Wei, D. (2017). From low-cost substrates to single cell oils synthesized by oleaginous yeasts. *Bioresource technology*.

Rank, G., Casey, G. and Xiao, W. (1988). Gene transfer in industrial *Saccharomyces* yeasts. *Food Biotechnology* **2,** 1-41.

Rappaz, B., Cano, E., Colomb, T., Kühn, J., Depeursinge, C., Simanis, V., Magistretti, P. J. and Marquet, P. (2009). Noninvasive characterization of the fission yeast cell cycle by monitoring dry mass with digital holographic microscopy. *Journal of biomedical optics* **14,** 034049-034049-5.

Raschke, D. and Knorr, D. (2009). Rapid monitoring of cell size, vitality and lipid droplet development in the oleaginous yeast Waltomyces lipofer. *Journal of Microbiological Methods* **79,** 178-183.

Rathore, A. S., Agarwal, H., Sharma, A. K., Pathak, M. and Muthukumar, S. (2015). Continuous Processing for Production of Biopharmaceuticals. *Preparative Biochemistry and Biotechnology* **45,** 836-849.

Ratledge, C. and Wynn, J. P. (2002). The biochemistry and molecular biology of lipid accumulation in oleaginous microorganisms. *Advances in Applied Microbiology***,** 1-51.

Reay, D., Ramshaw, C. and Harvey, A. (2013). *Process Intensification: Engineering for Efficiency, Sustainability and Flexibility*. Elsevier Science.

Rintala, E., Toivari, M., Pitkanen, J. P., Wiebe, M. G., Ruohonen, L. and Penttila, M. (2009). Low oxygen levels as a trigger for enhancement of respiratory metabolism in *Saccharomyces cerevisiae*. *BMC genomics* **10,** 461.

Rodrigues, F., Ludovico, P. and Leão, C. (2006). Sugar metabolism in yeasts: an overview of aerobic and anaerobic glucose catabolism. *Biodiversity and ecophysiology of yeasts***,** 101-121.

Ronneberger, O., Fischer, P. and Brox, T. (2015). U-net: Convolutional networks for biomedical image segmentation. *International Conference on Medical Image Computing and Computer-Assisted Intervention*, pp. 234-241.

Rosano, G. L. and Ceccarelli, E. A. (2014). Recombinant protein expression in *Escherichia coli*: advances and challenges. *Frontiers in microbiology* **5**.

Rosenfeld, E., Beauvoit, B., Blondin, B. and Salmon, J. M. (2003). Oxygen consumption by anaerobic *Saccharomyces cerevisiae* under enological conditions: effect on fermentation kinetics. *Applied and environmental microbiology* **69,** 113-21.

Rosenthal, K., Oehling, V., Dusny, C. and Schmid, A. (2017). Beyond the bulk: disclosing the life of single microbial cells. *FEMS Microbiology Reviews* **41,** 751-780.

Rupes, I. (2002). Checking cell size in yeast. *Trends in genetics : TIG* **18,** 479-85.

Ryall, B., Eydallin, G. and Ferenci, T. (2012). Culture history and population heterogeneity as determinants of bacterial adaptation: the adaptomics of a single environmental transition. *Microbiology and Molecular Biology Reviews* **76,** 597-625.

Saldi, S., Driscoll, D., Kuksin, D. and Chan, L. L.-Y. (2014). Image-based cytometric analysis of fluorescent viability and vitality staining methods for ale and lager fermentation yeast. *JOURNAL OF THE AMERICAN SOCIETY OF BREWING CHEMISTS* **72,** 253-260.

Sandoval-Basurto, E. A., Gosset, G., Bolivar, F. and Ramirez, O. T. (2005). Culture of *Escherichia coli* under dissolved oxygen gradients simulated in a two-compartment scale-down system: metabolic response and production of recombinant protein. *Biotechnology and bioengineering* **89,** 453-63.

Sarris, D. and Papanikolaou, S. (2016). Biotechnological production of ethanol: Biochemistry, processes and technologies. *Engineering in Life Sciences* **16,** 307-329.

Schmoller, K. M. and Skotheim, J. M. (2015). The biosynthetic basis of cell size control. *Trends in cell biology* **25,** 793-802.

Schreiber, F., Littmann, S., Lavik, G., Escrig, S., Meibom, A., Kuypers, M. M. and Ackermann, M. (2016). Phenotypic heterogeneity driven by nutrient limitation promotes growth in fluctuating environments. *Nature microbiology* **1,** 16055.

Serrano-Carreón, L., Galindo, E., Rocha-Valadéz, J., Holguín-Salas, A. and Corkidi, G. (2015). Hydrodynamics, fungal physiology, and morphology, *Filaments in Bioprocesses*, Springer, pp. 55-90.

Shaked, N. T., Satterwhite, L. L., Rinehart, M. T. and Wax, A. (2011). Quantitative analysis of biological cells using digital holographic microscopy, *Holography, research and technologies*, InTech.

Shapiro, H. M. (2003). Practical flow cytometry.

Shcheprova, Z., Baldi, S., Frei, S. B., Gonnet, G. and Barral, Y. (2008). A mechanism for asymmetric segregation of age during yeast budding. *Nature* **454,** 728-734.

Sieck, J. B., Schild, C. and von Hagen, J. (2017). Perfusion Formats and Their Specific Medium Requirements. *Continuous Biomanufacturing: Innovative Technologies and Methods*.

Sijtsma, L. and De Swaaf, M. (2004). Biotechnological production and applications of the ω-3 polyunsaturated fatty acid docosahexaenoic acid. *Applied microbiology and biotechnology* **64,** 146-153.

Silva-Rocha, R. and de Lorenzo, V. (2010). Noise and robustness in prokaryotic regulatory networks. *Annual review of microbiology* **64,** 257-275.

Soifer, I. and Barkai, N. (2014). Systematic identification of cell size regulators in budding yeast. *Molecular systems biology* **10,** 761.

Sommer, C. and Gerlich, D. W. (2013). Machine learning in cell biology–teaching computers to recognize phenotypes. *Journal of cell science* **126,** 5529-5539.

Sonnleitner, B. (2012). Automated measurement and monitoring of bioprocesses: key elements of the M3C strategy, *Measurement, Monitoring, Modelling and Control of Bioprocesses*, Springer, pp. 1-33.

Sonnleitner, B. and Kappeli, O. (1986). Growth of *Saccharomyces cerevisiae* is controlled by its limited respiratory capacity: Formulation and verification of a hypothesis. *Biotechnology and bioengineering* **28,** 927-37.

Specht, E. A., Braselmann, E. and Palmer, A. E. (2017). A Critical and Comparative Review of Fluorescent Tools for Live-Cell Imaging. *Annual review of physiology* **79,** 93-117.

Suhr, H. and Herkommer, A. M. (2015). In situ microscopy using adjustment-free optics. *Journal of biomedical optics* **20,** 116007-116007.

Sweere, A., Janse, L., Luyben, K. and Kossen, N. (1988a). Experimental simulation of oxygen profiles and their influence on baker's yeast production: II. Two-fermentor system. *Biotechnology and bioengineering* **31,** 579-586.

Sweere, A., Mesters, J., Janse, L., Luyben, K. and Kossen, N. (1988b). Experimental simulation of oxygen profiles and their influence on baker's yeast production: I. One-fermentor system. *Biotechnology and bioengineering* **31,** 567-578.

Szczebara, F. M., Chandelier, C., Villeret, C., Masurel, A., Bourot, S., Duport, C., Blanchard, S., Groisillier, A., Testet, E. and Costaglioli, P. (2003). Total biosynthesis of hydrocortisone from a simple carbon source in yeast. *Nature biotechnology* **21,** 143.

Taheri-Araghi, S., Bradde, S., Sauls, J. T., Hill, N. S., Levin, P. A., Paulsson, J., Vergassola, M. and Jun, S. (2015). Cell-size control and homeostasis in bacteria. *Current biology : CB* **25,** 385-91.

Takors, R. (2012). Scale-up of microbial processes: impacts, tools and open questions. *Journal of biotechnology* **160,** 3-9.

Tehlivets, O., Scheuringer, K. and Kohlwein, S. D. (2007). Fatty acid synthesis and elongation in yeast. *Biochimica et Biophysica Acta (BBA)-Molecular and Cell Biology of Lipids* **1771,** 255-270.

Thi, T. Y. D., Sivaloganathan, B. and Obbard, J. P. (2011). Screening of marine microalgae for biodiesel feedstock. *Biomass & Bioenergy* **35,** 2534-2544.

Thomson, K., Bhat, A. and Carvell, J. (2015). Comparison of a new digital imaging technique for yeast cell counting and viability assessments with traditional methods. *Journal of the Institute of Brewing* **121,** 231-237.

Tibayrenc, P., Preziosi-Belloy, L., Roger, J.-M. and Ghommidh, C. (2010). Assessing yeast viability from cell size measurements? *Journal of biotechnology* **149,** 74-80.

Timoumi, A., Bideaux, C., Guillouet, S. E., Allouche, Y., Molina-Jouve, C., Fillaudeau, L. and Gorret, N. (2017). Influence of oxygen availability on the metabolism and morphology of Yarrowia lipolytica: insights into the impact of glucose levels on dimorphism. *Applied microbiology and biotechnology* **101,** 7317-7333.

Tocher, P. D. (2018). Review of the Environmental Impacts of Salmon Farming in Scotland, The Scottish Parliament: City.

Torres, N. P., Ho, B. and Brown, G. W. (2016). High-throughput fluorescence microscopic analysis of protein abundance and localization in budding yeast. *Critical reviews in biochemistry and molecular biology* **51,** 110-119.

Turner, J. J., Ewald, J. C. and Skotheim, J. M. (2012). Cell size control in yeast. *Current Biology* **22,** R350-R359.

Van Nierop, S., Rautenbach, M., Axcell, B. and Cantrell, I. (2006). The impact of microorganisms on barley and malt quality-A review. *JOURNAL-AMERICAN SOCIETY OF BREWING CHEMISTS* **64,** 69.

Van Urk, H., Postma, E., Scheffers, W. A. and Van Dijken, J. P. (1989). Glucose transport in Crabtree-positive and Crabtree-negative yeasts. *Microbiology* **135,** 2399-2406.

Viazzi, S., Lambrechts, T., Schrooten, J., Papantoniou, I. and Aerts, J.-M. (2015). Real-time characterisation of the harvesting process for adherent mesenchymal stem cell cultures based on on-line imaging and model-based monitoring. *Biosystems Engineering* **138,** 104-113.

Vitova, M., Bisova, K., Kawano, S. and Zachleder, V. (2015). Accumulation of energy reserves in algae: from cell cycles to biotechnological applications. *Biotechnology advances* **33,** 1204-1218.

Vojinović, V., Cabral, J. and Fonseca, L. (2006). Real-time bioprocess monitoring: Part I: In situ sensors. *Sensors and Actuators B: Chemical* **114,** 1083-1091.

Warikoo, V., Godawat, R., Brower, K., Jain, S., Cummings, D., Simons, E., Johnson, T., Walther, J., Yu, M., Wright, B., McLarty, J., Karey, K. P., Hwang, C., Zhou, W., Riske, F. and Konstantinov, K. (2012). Integrated continuous production of recombinant therapeutic proteins. *Biotechnology and bioengineering* **109,** 3018-3029.

Wen, Z. Y., Jiang, Y. and Chen, F. (2002). High cell density culture of the diatom *Nitzschia laevis* for eicosapentaenoic acid production: fed-batch development. *Process Biochemistry* **37,** 1447-1453.

Wiedemann, P., Guez, J. S., Wiegemann, H. B., Egner, F., Quintana, J. C., Asanza-Maldonado, D., Filipaki, M., Wilkesman, J., Schwiebert, C. and Cassar, J. P. (2011a). In situ microscopic cytometry enables noninvasive viability assessment of animal cells by measuring entropy states. *Biotechnology and bioengineering* **108,** 2884-2893.

Wiedemann, P., Worf, M., Wiegemann, H. B., Egner, F., Schwiebert, C., Wilkesman, J., Guez, J. S., Quintana, J. C., Assanza, D. and Suhr, H. (2011b). On-line and real time cell counting and viability determination for animal cell process monitoring by in situ microscopy. *BMC proceedings*, pp. P77.

Willis, L. and Huang, K. C. (2017). Sizing up the bacterial cell cycle. *Nature Reviews Microbiology* **15,** 606.

Wittmann, C., Liao, J. C., Lee, S. Y., Nielsen, J. and Stephanopoulos, G. (2016). *Industrial Biotechnology: Products and Processes*. Wiley.

Xiao, Y., Bowen, C. H., Liu, D. and Zhang, F. (2016). Exploiting nongenetic cell-to-cell variation for enhanced biosynthesis. *Nature chemical biology* **12,** 339-344.

Xie, D., Jackson, E. N. and Zhu, Q. (2015). Sustainable source of omega-3 eicosapentaenoic acid from metabolically engineered Yarrowia lipolytica: from fundamental research to commercial production. *Applied microbiology and biotechnology* **99,** 1599-610.

Xu, B., Jahic, M. and Enfors, S. O. (1999). Modeling of Overflow Metabolism in Batch and Fed-Batch Cultures of *Escherichia coli*. *Biotechnology Progress* **15,** 81-90.

Xu, Y., Xie, X., Duan, Y., Wang, L., Cheng, Z. and Cheng, J. (2016). A review of impedance measurements of whole cells. *Biosensors and Bioelectronics* **77,** 824-836.

Xue, C., Zhao, X. and Bai, F. (2010). Effect of the size of yeast flocs and zinc supplementation on continuous ethanol fermentation performance and metabolic flux distribution under very high concentration conditions. *Biotechnology and bioengineering* **105,** 935-944.

Zhang, H., Cui, X., Bi, J., Dai, S. and Ye, H. (2015). Single-cell analysis for bioprocessing. *Engineering in Life Sciences* **15,** 582-592.

Zhu, L. D., Li, Z. H. and Hiltunen, E. (2016). Strategies for Lipid Production Improvement in Microalgae as a Biodiesel Feedstock. *BioMed research international* **2016,** 8792548.

Zimmermann, S., Gretzinger, S., Scheeder, C., Schwab, M. L., Oelmeier, S. A., Osberghaus, A., Gottwald, E. and Hubbuch, J. (2016). High-throughput cell quantification assays for use in cell purification development - enabling technologies for cell production. *Biotechnol J* **11,** 676-86.

Zinser, E., Paltauf, F. and Daum, G. (1993). Sterol composition of yeast organelle membranes and subcellular distribution of enzymes involved in sterol metabolism. *Journal of bacteriology* **175,** 2853-2858.